DEVELOPMENT OF A VOLUMETRIC STRAIN INFLUENCE GROUND IMPROVEMENT PREDICTION MODEL WITH SPECIAL REFERENCE TO IMPACT COMPACTION

ALAN DAVID BERRY

Dissertation submitted in partial fulfilment of the requirements of the degree of

MASTER OF ENGINEERING

in the

FACULTY OF ENGINEERING, BUILT ENVIRONMENT AND INFORMATION TECHNOLOGY

UNIVERSITY OF PRETORIA
PRETORIA

July 2001

ACKNOWLEDGEMENTS

I would like to thank the following people who made this project report possible:

- The directors of Landpac, particularly Charles Davis, who have given me the permission to publish this work, which is largely based on the research I did for the company. The use of the material and time spent is gratefully acknowledged. It has been a privilege to be afforded the opportunity to undertake this research.
- Professor A T Visser and Professor E Rust, my supervisors for their guidance and enthusiasm.
- Mr D Mulville of Mulville & Associates for the loan of the FLAC software.
- Mr H Greyling and Mr E Nkosi for their assistance with much of the field work.
- Permission from the CSIR to publish the references compiled by themselves is also acknowledged.
- Mr G Byrne of Franki Africa for permission to publish some of the dynamic compaction test data from the Mozal Smelter site in Mozambique.
- My mother and late father, for their encouragement to study further.
- Karen, my wife, for her love and support while buried in the books or staring into the computer screen.
- To my Maker, the Giver of all good gifts, for a greater degree of understanding than I had before.

DISSERTATION SUMMARY

DEVELOPMENT OF A VOLUMETRIC STRAIN INFLUENCE GROUND IMPROVEMENT PREDICTION MODEL WITH SPECIAL REFERENCE TO IMPACT COMPACTION

ALAN DAVID BERRY

Supervisor: Professor A T Visser
Co-supervisor: Professor E Rust
Department: Civil Engineering
University: University of Pretoria
Degree: Master of Engineering (Geotechnical Engineering)

Aubrey Berrangé, a South African roads engineer, invented the impact compactor in 1949 with the intention of achieving improved compaction to greater depths than possible with conventional equipment available at the time. The aim of this dissertation is to present a simple prediction model for the profile of improvement in the ground, using surface settlement as the main input parameter. The model is based on the information reviewed, observation of field data and a static numerical analysis. For simplicity sake, no attempt is made to predict the energy requirement to achieve the input value of settlement. The model is then verified on fifteen impact compaction profiles at six different sites. A 2 ton-meter dropping mass compactor was also used in the verification process with reasonable success. In addition, the model was tested against comprehensive testing performed at a dynamic compaction site with very promising results. The method is also shown to give acceptable results for prediction of density increase during a vibratory compaction trial. It is concluded that the improvement in the ground can be estimated with reasonable success if the surface settlement is monitored, providing lateral strains are taken into account.

Keywords: Compaction, Compaction modelling, compaction prediction, impact compaction, dynamic compaction, ground improvement, volumetric strain, plastic deformations

SAMEVATTING VAN VERHANDELING

DIE ONTWIKKELING VAN 'N VERVORMINGSINVLOED GRONDVERBETERING VOORSPELLINGSMODEL MET SPESIALE VERWYSING NA SLAGROLLERS

ALAN DAVID BERRY

Promotor:	Professor A T Visser
Medepromotor	Professor E Rust
Departement:	Siviele Ingeneurswese
Universiteit:	Universiteit van Pretoria
Graad:	Magister in Ingenieurswese (Geotegniese Ingenieurswese)

Aubrey Berrangé, 'n Suid Afrikaanse padingenieur, het die eerste slagroller in 1949 ontwerp. Die bedoeling was om beter kompaksie tot groter dieptes te behaal invergelyking met wat die kompaksie toerusting van daardie tyd moontlik was. Die doel van hierdie verhandeling is om 'n vervormingsinvloed grondverbetering voorspellingsmodel voor te stel, met die oppervlak-versakking as hoof invoer parameter. Die metode is gebaseer op veldmetings asook analitiese berekenige. Geen voorspelling van energie behoeftes word gemaak nie. Die model is op vyftien veskillende grondprofiele op ses verskillende slagroltereine getoets. 'n 2 ton vallenende massa kompakteerder was ook gebruik in die verifierings proses met bevrediginde resultate. Die model is ook op 'n dinamiese kompaksie terein getoets. Daar is gevind dat digtheid vebetering voorspellings verkry uit die model, beveredigend is op onversadigde materiale. Die navorsing wys dat die grondverbetering 'n funksie is van die grondoppervlakte versakking met dien verstande dat laterale vervorming in ag geneem word.

Sleutelwoorde: Kompaksie, kompaksie modelering, kompaksie voorspelling, slagrollers, dinamiese kompaksie, grondverbetering, volumetriese vervorming, plastiese verformings

TABLE OF CONTENTS

LIST OF FIGURES

LIST OF TABLES

LIST OF PHOTOGRAPHS

CHAPTER 1

INTRODUCTION

1.1 BACKGROUND

Impact compaction was invented by Aubrey Berrangé in 1949 in order to address the deep compaction problems experienced by the Cape Roads Department at the time (Paige-Green, 1998). The use of impact compaction has since grown and recently it was used for the construction of the runways at Chep Lap Kok airport in Hong Kong, one of the largest construction projects of the 20th century.

Initial development was undertaken by the CSIR in Pretoria where a 4 sided impact compactor was successfully developed. Berrangé later left the CSIR to continue the commercial development of his ideas, designing both three sided machines and five sided machines shown below.

Plate 1.1: ***A 3 sided impact compactor***

Plate 1.2: ***A 5 sided impact compactor***

On his retirement he sold the patents to the manufacturers of the machines based in Nigel, along with the South African contracting wing he owned. The new company, Landpac, has continued the development and has been largely responsible for funding the research presented here.

1.2 PROBLEM STATEMENT AND STUDY OBJECTIVES

Most methods currently available to predict the improvement in the ground after compaction are either entirely empirical or semi-empirical in nature, or based on laboratory testing. Recently, sophisticated computer based models have been combined with laboratory testing to predict the improvement in the ground with some success.

However, there is currently no simple method of predicting the reduction in the void ratio of the soil after compaction using impact compactors.

Although it is intuitively obvious that the ground improvement is proportional to the surface settlement, none of the literature surveyed made use of this easily measurable parameter to predict the improvement that can be achieved. In addition, little clarity was found in the literature regarding the fundamental mechanisms at work, which result in compaction of the ground.

The purpose of this dissertation is to show that the profile of improvement in the ground after impact compaction is predictable and proportional to the surface settlement of the compacted ground, provided lateral deformation is taken into account. The objective is therefore to measure, model and predict the typical volumetric response of the soil during the impact compaction process.

A need therefore exists for a simple model that can be used with some degree of confidence. The aim of this dissertation is to provide such a model.

1.3 SCOPE OF DISSERTATION

This report firstly reviews the literature for predictive models that can be used or modified for use the address the problem stated. In order to support the hypothesised ground improvement model, a static numerical analysis is undertaken to examine the induced strain profile. To allow a reasonable estimate of the maximum dynamic force for input into the software, the decelerations of the impact compaction masses were measured. The influence of the cohesion and friction angle of the soil in, on the strain profile is also investigated.

Based on the numerical analysis and patterns observed in the field, a prediction model is presented for unsaturated conditions and verified on various sites. This is done for both impact compaction and dynamic compaction. The possible use of the model for conventional compaction is also demonstrated. The effect of layered soils is also briefly discussed.

Based on the findings made during the investigation, areas of further research are also suggested.

1.4 METHODOLOGY

The stated objective was addressed in the following sequence:

- Collect, compile and review the relevant papers and publications
- Determine the range of dynamic forces imparted to firstly, a initially soft soil, and secondly a hard soil [establish the upper and lower bound decelerations]
- Perform numerical analyses
- Develop a volumetric strain influence ground improvement prediction model
- Verify model and discuss shortcomings
- Summarise in report form

1.5 LAYOUT OF THE REPORT

The report is arranged in the following order:

- Chapter 1 introduces the problem and how it will be solved
- Chapter 2 summarised the finding of the literature review.
- Chapter 3 describes how the decelerations were measured and reviews the results
- Chapter 4 details the numerical analysis and the influence of the Mohr Coulomb soil parameters on the strain profile
- Chapter 5 presents the proposed prediction model
- Chapter 6 summarised the verification of the model on various sites and discusses the main issues and difficulties in modelling this complex subject
- Chapter 7 draws conclusions
- References
- Appendices

CHAPTER 2

LITERATURE STUDY

2 INTRODUCTION

The aim of this section of the report is summarise and synergise the most promising ground improvement prediction models found in the literature. Impact compaction literature is first reviewed, followed by those models found in the dynamic compaction and conventional (cylindrical vibrating drum) literature. Lastly, compaction models based on the soil characteristics are covered.

Some useful prediction models were found. Although much work has been done in the field of dynamic compaction (DC), most models found are still semi-empirical in nature. This is probably due to the influence of the water table, compactor geometry, soil parameters and surface settlement being largely ignored. From the DC literature it is concluded that the primary *impact compactor* parameters required for a prediction model are the compactor mass, drop height, contact area and total energy.

The more general compaction literature is mostly concerned with predicting compactor performance over a standard depth, through the use of empirical methods. Some useful models were found.

2.1 PREVIOUS WORK DONE ON IMPACT COMPACTION (IC)

A detailed review of the impact compaction literature was undertaken by the CSIR (Paige-Green, 1998). The author makes the observation that "Impact compaction…results in compaction at depth, with disturbance of the upper portion of the layer". This is the simplest form of prediction, and well known to most users of impact compaction. He also notes that "larger loads and larger contact areas are better for deep compaction". This is one of the main limiting factors of conventional cylindrical compactors in deep compaction: the contact width of the applied line load is difficult to enlarge. In considering the large force imparted by impact compactors Clifford (1978) noted that "principles that hold true for impact

devices hold true for impact rollers, except that, in addition, an impact roller delivers generated momentum due to the rotational effect of the roller mass". In a report investigating this hypothesis, it was found that this was not the case (Heyns, 1998), and that the potential energy of the machines formed the bulk of the imparted energy. In this report typical decelerations were found to be in the order of 100m/s^2 to 200m/s^2 (10 to 20 g's). Clifford rightfully notes in his conclusion that "the paucity of mathematical studies on various aspects on compaction, from generated energy to the soil response limits, show how difficult evaluation is".

In a recent paper, Berry et al (1998) noted that the impact compaction trials undertaken at Kriel revealed a peak in density in the post compaction test pits that were dug, and that this appeared similar to the shape of the Schmertman strain influence diagram (Schmertman, 1970). A trial pit excavation revealed the strain profile shown in Figure 2.1.

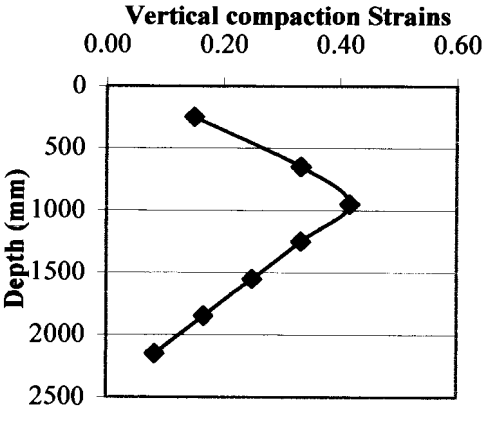

Figure 2.1: Trial indicating variation of strain with depth (Berry et al, 1998)

The above results were obtained by excavating a trial pit to a depth of 2.5m and replacing the soil carefully in 300mm layers. The interface between layers was marked with a chalk layer. After compaction by the 25kJ impact compactor, the pit was carefully excavated and the compression of the layers measured throughout the profile. Details of the measurements are given in Appendix A. Apart from this observation, no mention was found of any prediction model in the IC literature, only descriptive trends.

2.2 AN OVERVIEW OF PREDICTION MODELS USED IN DYNAMIC COMPACTION

In the 1960's a French engineer Louis Menard devised a method of compacting the ground by using a crane to lift a mass weighing a couple of tons to the full lift height of the crane and then releasing it. The nett effect was that the imparted force on impact was effectively 10 to 20 times larger than the static mass due to the inertia force imparted. This compaction technique has since become used world-wide, and much study has been undertaken in order to better understand the technology. The following parameters are typically predicted: patterns of improvement, depth of influence, surface settlement, settlement profile, surface stress, stress profile, residual horizontal stress profile and more recently, the void ratio reduction profile.

2.2.1 Descriptive/observational pattern of improvement

Initially, before the development of any mathematical prediction tools typical patterns of behaviour based on in-situ test results are all that is available to the engineer. Usually these offer little explanation. The most useful of these is given by Lukas (1986) and shown in Figure 2.2.

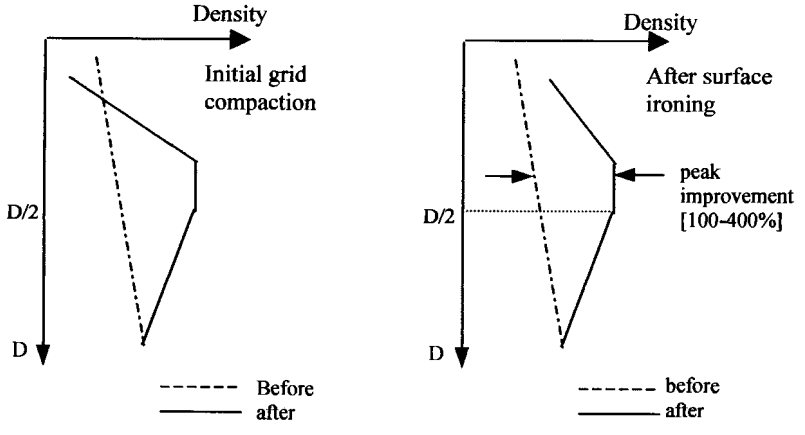

Figure 2.2: Descriptive pattern of DC soil improvement (Lukas, 1986)

This improvement pattern seems to tie in with the observation by Paige-Green, that the surface is loosened, and compaction takes place deeper down.

2.2.2 Predictions of depth of influence

One of the most important questions that needs answering is the depth to which improvement is achieved. To this end Menard et al (1976) suggested the well-known relation

$$d_{max} = \sqrt{W.H} \qquad \text{(Eq. 2.1)}$$

where W=pounder mass (t), H=drop height (m)

and d_{max}=maximum depth of influence

This was revised with experience and Lukas (1976) suggested

$$d_{max} = n\sqrt{W.H} \qquad \text{(Eq. 2.2)}$$

where *n=an empirical coefficient (0.3-0.8 typically)*

The modified Menard equation (Eq. 2.2) is still widely used in the industry, with the factor n=C.δ, where C=the velocity efficiency and δ= the stratagraphic coefficient (Varaksin, 1991). In the same publication Varaksin notes "In any type of unsaturated soil the shock causes a Proctor type compaction." and that "the phenomenon becomes highly complex in saturated or impervious soil". He then gives a formula to predict the increase in pore water pressure under saturated conditions. According to Varaksin, C=0.9 for cable drop and 1.2 for free fall. He also noted that 67% of the energy is dissipated in the Rayleigh surface wave, that this is represented by the δ coefficient. Once the point of liquifaction is reached, a rest period is required for the pore water pressures to dissipate. This rest period is of predictable duration. As impact rollers are generally used in non-saturated conditions, this is not pursued any further, other than to note that the presence of the water table is of great consequence and needs to be considered if present.

A typical energy-depth of influence chart from the use of the above equations is given in Figure 2.3.

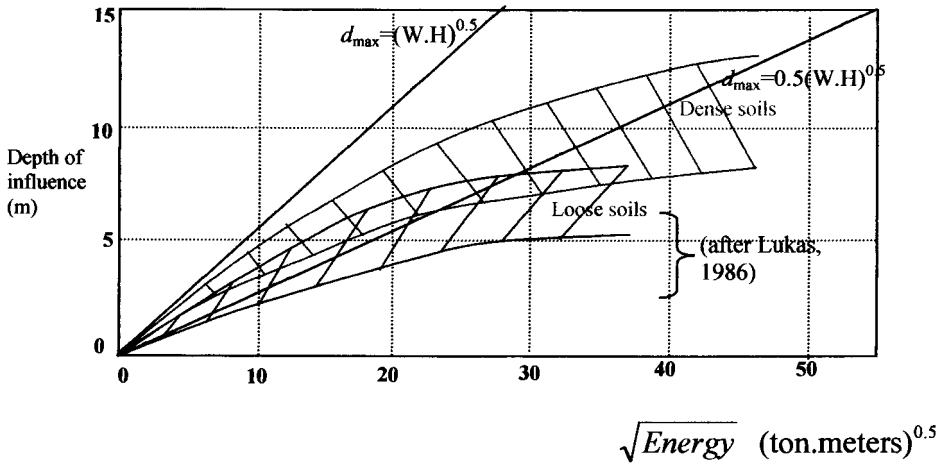

Figure 2.3: Typical energy-depth of influence chart for DC (Slocombe, 1989)

It is interesting to note that the depth of influence is thought to increase for denser materials. Note: "Energy" is defined in DC as ton.meters (t.m), which is not strictly correct as the gravitational constant is omitted.

Scott and Pearce (1976) presented an idealized model of the depth of the compacted zone in an energy dissipation analysis using a elasto-plastic soil model. The paper high-lights the many difficulties in analysing the problem and adopts a one-dimensional approach to obtain an equation for the depth of the compacted zone:

$$h = \frac{m}{\rho_c}\left\{\sqrt{1+\frac{k\rho(V-\mathrm{v})^2}{\sigma_L}}-1\right\} \qquad \text{(Eq. 2.3)}$$

where h=depth of compacted zone, m=mass/unit area

ρ_c=compacted soil density, ρ=initial soil density, V=impact velocity

v=velocity of radiated stress wave, σ_L=elastic stress limit and

$$k = \frac{\rho}{\rho_c - \rho} \qquad \text{(Eq. 2.3a)}$$

From the equation for h it is clear that the compacted density is required to determine the depth of compaction, which is almost self-defeating. The paper does not clearly indicate if the density is constant over the depth h, but the use of and average compacted density (ρ_c) seems to indicate that this is the case. To complicate matters, the velocity of impact and of the radiating stress wave is required, making the model dependent on extensive in-situ measurements.

2.2.3 Predictions of impact displacements/settlement

In a massless soil of constant stiffness k (kPa/mm) the displacement is given by (Sears et al, 1982):

$$y = \frac{1}{2}\left[\frac{2mg}{k} + \sqrt{\left(\frac{2mg}{k}\right)^2 + \frac{8mgh}{k}}\right] \text{, where } \frac{mg}{k} = \text{static displacement} \qquad \text{(Eq. 2.4)}$$

This is an elastic model, however, and would therefore rebound entirely if the theory was correct.

Kwang et al (1990) suggested that the ground improvement is related to the enforced (plastic) settlement curve and that this is uniquely related to the energy input and the pressuremeter limit pressure. The proposed curve is shown in Figure 2.4. The energy intensity characteristic I_s, is a function of only the energy imparted per unit area (E_B) and the pressuremeter limit pressure (P_L). The method indicates a "saturation energy intensity" after which there are limited returns. It fails to clearly describe the influence of moisture however, and gives no guidance as to the distribution of the improvement with depth. The enforced strain, η_{SE}, is defined below as

$$\eta_{SE} = \frac{S_E}{H_t} \text{ , } S_E = \text{enforced settlement , } H_t = \text{thickness requiring treatment} \qquad \text{(Eq. 2.4a)}$$

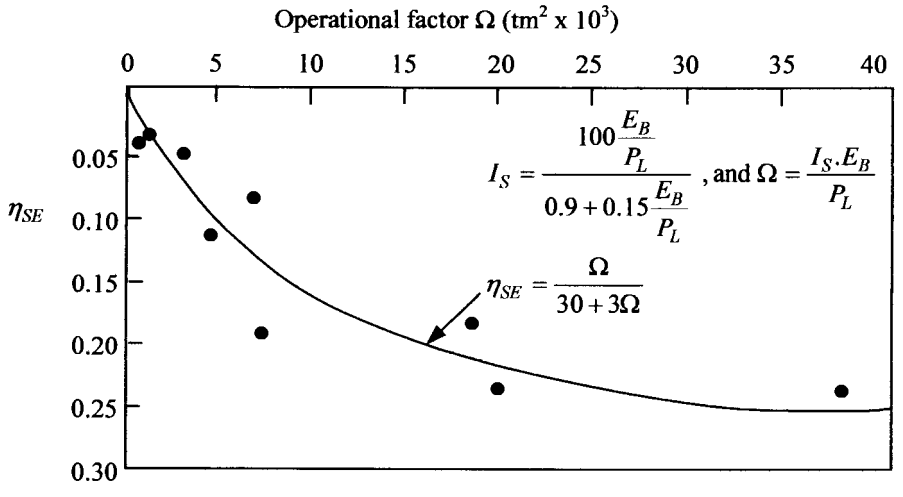

Figure 2.4: Unique enforced strain diagram (Kwang et al, 1990)

The selection of the depth requiring treatment, H_T, is left to the engineer, and leaves the method open to overestimation of this parameter.

It is nevertheless a step forward as it demonstrates that there is a predictable level of energy input after which there is little gain in the ground improvement. It confirms that the ground improvement is a function of the enforced surface settlement. The critical parameters required by the method are the input energy (Σmgh) and the limit pressure of the soil.

Davies et al (1995) proposed a useful elastodynamic prediction of the surface displacement, velocity and acceleration on and after a load impacts the ground. Good agreement was obtained between predicted and measured data over the first wavelength of displacement. The displacement equation used is as follows:

$$z = V_o.e^{\left(-\varpi_n.D.t\right)}.\sin\left(\varpi_d.t\right)/\varpi_d \qquad \text{Eq. 2.5}$$

not given in the paper are the velocity and acceleration equations :

$$v = V_o.e^{-\varpi_n.D.t}.\left[Cos(\varpi_d.t) - D.\frac{\varpi_n}{\varpi_d}.Sin(\varpi_d.t)\right] \qquad \text{Eq. 2.5a}$$

$$a = V_o.e^{-\varpi_n.D.t}.\left[Sin(\varpi_d.t)\left(\frac{\varpi_n^2.D^2}{\varpi_d}\right) - 2\varpi_n.D.Cos(\varpi_d.t)\right] \qquad \text{Eq. 2.5b}$$

where z = displacement, v = velocity, a = acceleration, t = time
D = damping ratio, ϖ_n = undamped natural frequency
ϖ_d = damped natural frequency, V_o = impact velocity

The above equations were used to estimate the displacement, velocity and accelerations of the Landpac 10kJ, 15kJ and 25kJ impact compactors. The results of the calculations are given in Appendix B, and are of a sensible order of magnitude for the parameters used. The method is best suited to prediction of Falling Weight Deflectometer (FWD) deflections where the materials behave fairly elastically.

2.2.4 Prediction of settlement profile

Wallays (1983) suggested a method to predict the settlement at various depths below the compacted surface, i.e a settlement profile. The potential energy from the drop of the mass is equated to the work done by the vertical stress induced in

the soil, plus the work done in moving the soil mass by the residual settlement. The derivation results in equations for a layered soil, predicting the surface stress, the surface settlement and the settlement profile:

$$\therefore \sigma_{max} = \frac{1}{B^2}\sqrt{\frac{\eta.G.H}{A}}\left[\sqrt{1+\left(\frac{F}{2\sqrt{\eta.G.H.A}}\right)^2}-\frac{F}{2\sqrt{\eta.G.H.A}}\right] \quad \text{(Eq 2.6}$$

$$s_{max} = \sigma_{max}.B^2.A \quad \text{(Eq 2.6a)}$$

$$s_z = \sigma_{max}.B^2.\left[\sum_{i=j+1}^{n}\frac{1}{E_i}\left(\frac{1}{B+z_{i-1}}-\frac{1}{B+z_i}\right)+\frac{1}{E_j}\left(\frac{1}{B+z}-\frac{1}{B+z_j}\right)\right] \quad \text{(Eq. 2.6b)}$$

where σ_{max} = maximum contact stress, B=load diameter, E_i=stiffness of layer i, z_i=top of layer i, s_{max}=maximum settlement, A & F are influence factors, s_z=settlement at depth z, the efficiency factor $\eta=\eta_w.\eta_i.h_d$, where η_w = mass efficiency (typically=2/3), η_i= impact efficiency (typically=1/3) and η_d= heave loss factor (typically = 2/3)

The method does not specifically predict improvement, but may well be used or extended to obtain more measurable parameters such as density or void ratio. It does not clearly indicate the effect of the water table or the effect of Poisson's ratio (lateral strains). Material properties are dealt with indirectly through the stiffness used in the equations. Results are given in charts showing the measured settlement compared to the predicted settlement. The efficiency factors are presumably obtained empirically.

2.2.5 Predictions of impact stresses

Intuitively, the contact stress has a large influence on the ground improvement. Estimates of this were of the first to be made, as this could then readily be input into a stress distribution formula. Jessberger and Beine (1981) proposed laboratory testing with an accelerometer attached to a falling mass to determine the relationship between the decelerations and the impact velocity. The constant of proportionality, α, was then used in the equation:

$$\sigma_{0,dyn} = \alpha \frac{m}{A}\sqrt{2gh} \qquad \text{(Eq. 2.7)}$$

where $\sigma_{0,dyn}$ =dynamic contact stress, *m=mass, A=base area of rammer, h=drop ht, g=9.81m/s²*

This shows that the contact stress is proportional to the impact momentum, since the impact velocity, $v = \sqrt{2.g.h}$, for a constant base area. Mayne (1983) proposed a slightly different form of equation, based on the integral of the area under measurements of the impact deceleration-time graph:

$$\sigma_z = \frac{V_s\sqrt{WHB}}{4(B)^2} \qquad \text{(Eq. 2.8)}$$

where *Vs=shear wave velocity, H=drop ht, B=contact dia., W=mass (t)*

The formula Mayne gives for the deceleration ratio (a/g), gives values close to what has been measured by Heyns (1998) on the tube axles of impact compaction plant (this is demonstrated in chapter 3):

$$\frac{a_{\max}}{g} = V_s\sqrt{\frac{HB}{W}} \qquad \text{(Eq. 2.9)}$$

where a_{max}=maximum acceleration of pounder, g=9.81m/s²

Lewis (1957) proposed an equation that related the contact stress to the impact energy:

$$p = \sqrt{\frac{1}{2}.mv^2.\frac{k_s}{A}} \qquad \text{(Eq. 2.10)}$$

where *m=mass,* v=*impact velocity, g=9.81m/s², A=base area, k_s= spring constant*

Therefore, to maintain a constant impact pressure the energy (½mv²) must be proportional to the square root of the base area (for a square base, proportional to the side dimension B). i.e it is difficult to keep the contact stresses down as the energy levels are raised as the compactor dimensions are generally fixed.

The critical parameters for determining contact stress are therefore the mass, the pounder base area, the drop height and the soil stiffness. The deceleration, impact velocity, energy and momentum are related to these parameters.

2.2.6 Predictions of dynamic stress profile

The proponents of the above contact stress predictions usually assumed some form of distribution of stress with depth to give a dynamic stress profile estimate. Jessberger and Beine (1981) proposed the following stress distribution based on Frolich's 1934 equation:

$$\frac{\sigma_{z,dyn}}{\sigma_{0,dyn}} = 1 - \left(\frac{z}{\sqrt{z^2 + r^2}} \right)^{v} \qquad \text{with } 7 < v < 15 \qquad \text{(Eq. 2.11)}$$

$\sigma_{o,dyn}$=contact stress (from equation 2.6), $\sigma_{z,dyn}$=stress at depth z, r=contact radius

Similarly, Mayne (1983) proposed the dynamic stress distribution:

$$\sigma_z = \frac{V_s \sqrt{WHB}}{4(B+z)^2}, \textit{variables defined in equation Eq 2.7 above} \qquad \text{(Eq. 2.12)}$$

The authors assume that having this information allows the likely compaction to then be evaluated. No guidance was found on how to convert the applied dynamic stress into effective compaction. It seems that it is assumed that the higher the stress and the deeper the stress profile, the better the compaction.

2.2.7 Prediction of residual stress profile

A method commonly used to predict the increase in horizontal stresses against retaining structures by compaction plant (Norvais Ferriera, 1983) shows the residual horizontal stresses after compaction (Figure 2.5). This method is usually used for the prediction of the increase in lateral stresses against retaining structures, but may also be used in compaction away from structures (Duncan et al, 1986).

The peak in the residual lateral stress diagram is a function of the assumed active and passive pressure lines and the applied dynamic stress profile.

This means that the larger the applied stress and plate/pounder size, the deeper the peak residual horizontal strain. As the method was aimed mainly at the prediction of residual stresses, no attempt was made to use the method for prediction of the compaction profile.

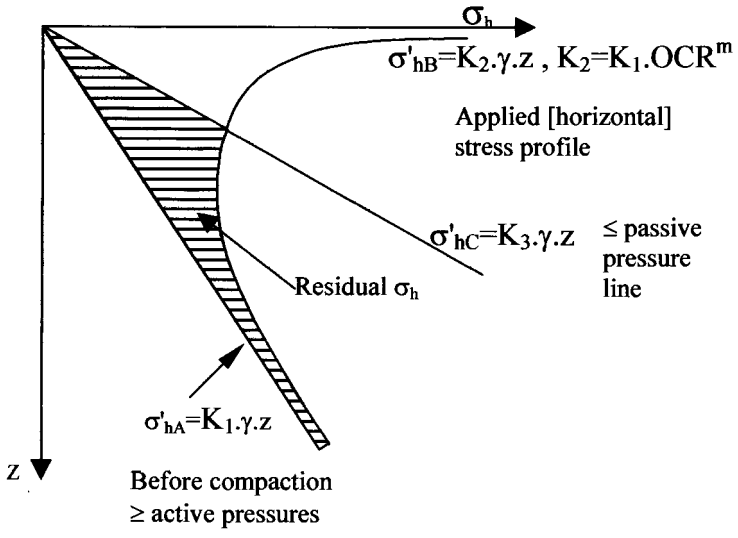

Figure 2.5: Predicted residual horizontal stresses after compaction (Novais Ferriera, 1983)

It is notable that the predicted profile appears to correspond to that found by Berry et al (Figure 2.2).

2.2.8 Prediction of void ratio reduction

Oshima et al (1997) proposed a model that predicts the degree of compaction achieved in terms of the relative density, D_r, based on model testing in sand. They showed that the improvement could be predicted in terms of the total momentum of the pounder:

$$Z = a_z + b_z \log(mvN)$$
$$R = a_R + b_R \log(mvN) \qquad \text{(Eq. 2.13)}$$

where Z=the vertical depth of improvement, R=radial improvement ,mvN=ram momentum, and a & b are empirical constants from laboratory testing.

The method was specifically aimed at dynamic compaction, and if used for the much lower energy/momentum levels of impact compactors, results in negative answers from below 15 passes of a 25kJ machine. With a different format of equation, the model may give better results. A notable omission from the model is the pounder base area. Empirical constants are available for changes in D_r of 40%, 20% and 10% respectively. This enables the bottom half of the profile of improvement to be drawn, including the depth of influence. The model does not predict the entire improvement profile, as the improvement immediately below the pounder is not evaluated.

A similar model was postulated by Poran et al (1992), based on total energy rather than momentum. The model equations are:

$$\frac{b}{D} = j + k\log\left(\frac{N.W.H}{A.b}\right) \qquad \text{(Eq.2.14)}$$

$$\frac{a}{D} = l + m\log\left(\frac{N.W.H}{A.b}\right) \qquad \text{(Eq.2.14a)}$$

where W=mass of pounder, A=base area,
j,k,l &m are empirical constants, H=drop height

The equations must be solved iteratively. The model does not incorporate the effect of the water table (testing was on dry sand), and specific correlation coefficients must be obtained relevant to the conditions under consideration.

Charles' solution (1978) for cohesive materials gives the lowest depth of influence predictions (see Figure 2.6), consistent with the known difficulty of compacting clayey materials. The behaviour is contrary to the other methods, as the depth of influence decreases with increasing pounder dimension (A_p=B^2):

$$D = 0.4\sqrt{\frac{E_d B}{A_p.c_u}} \qquad \text{(Eq.2.15)}$$

where E_d=energy, A_p=compactor base area, B=pounder width, and
c_u=undrained shear strength

2.2.9 Computer simulation based on the wave equation-profile of improvement prediction (Black box solution)

In a paper presented to the American Society of Civil Engineers, Chow et al (1992), gave the most comprehensive (and complicated) predictive model found in the literature surveyed. This method predicts the reduction in the void ratio as measured by the relative density D_r as well as the surface settlement (Figure 2.6).

Central to the method is a software program that solves partial differential equations of a non-linear (spring and dashpot) soil model that takes plastic behaviour of the soil into account.

Good correlation was found between predicted and measured parameters. It is again noteworthy that a peak appears in the improvement profile is also predicted by this model.

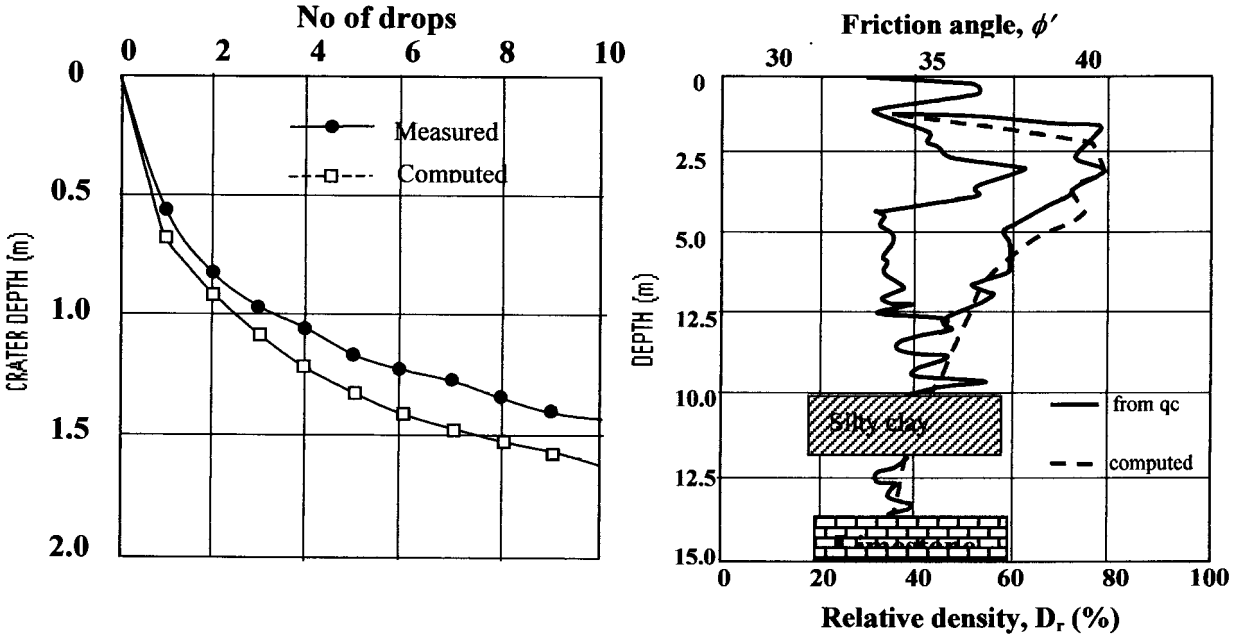

Figure 2.6 : Wave equation modelling of soil improvement (Chow et al, 1992)

The model could well be used to predict the behaviour of impact compactors, but has the following drawbacks:

- The modelling is complex: it requires a computer program to solve the wave equation model. This means that no understanding of the patterns of behaviour can be obtained without the use of the software. [i.e a black box solution].
- Laboratory testing is required to determine the "phenomenological" soil model.
- The spring and damping constants (k_s & c_s) have to be measured in the laboratory
- The soil springs behave in an elastic-perfectly plastic manner
- ϕ' is estimated from empirical equations [$\phi'=28+15.D_r$ (Meyerhof, 1976)]
- The ratio of vertical to horizontal stresses is estimated from empirical equations (the analysis is sensitive to this)-i.e the model is sensitive to the value of Poisson's ratio used.
- Clarity on the effect of the water table was not given
- The "measured" value of the relative density, Dr, was based on Dutch Cone point resistance values, q_c,and not block samples-i.e entirely empirical answers were obtained

The method is able to predict both the settlement and the reduction in void ratio as measured by the relative density [D_r], and then, using Meyerhof's empirical equation, an estimate of the increase in friction angle is made.

The same authors (Chow et al, 2000) performed a parametric study using the model developed and suggested the following equation to predict the crater depth for dynamic compactors:

$$d_c = \frac{E_B}{31.2 + 0.39E_B} - 0.125 \qquad \text{(Eq. 2.16)}$$

where d_c=crater depth (m) and E_B=input energy (ton.meters)

The authors then go on to give an estimate of the depth of improvement based on the energy input (E_B in ton.meters):

$$d_{max} = \frac{E_B}{5 + 0.075E_B} \qquad \text{(Eq. 2.17)}$$

These equations are valid for pounder base areas of between $3m^2$ and $4m^2$, and initial SPT penetration resistance of 1-15 blows/300mm.

This is the most comprehensive compaction modelling reviewed thus far.

Using the above equations for a 25kJ impact compactor yields a depth of influence of 3.7m and a crater depth of 0.62m, at 20 passes/blows (at one point). This is clearly an overestimation and the model is thus only applicable to the dynamic compactors for which it was developed.

Figure 2.7 shows a comparison of the various depths of improvement predicted by the models reviewed. The sensitivity of the Menard type equations to the empirical coefficient (n in Eq.2.2) is clearly shown.

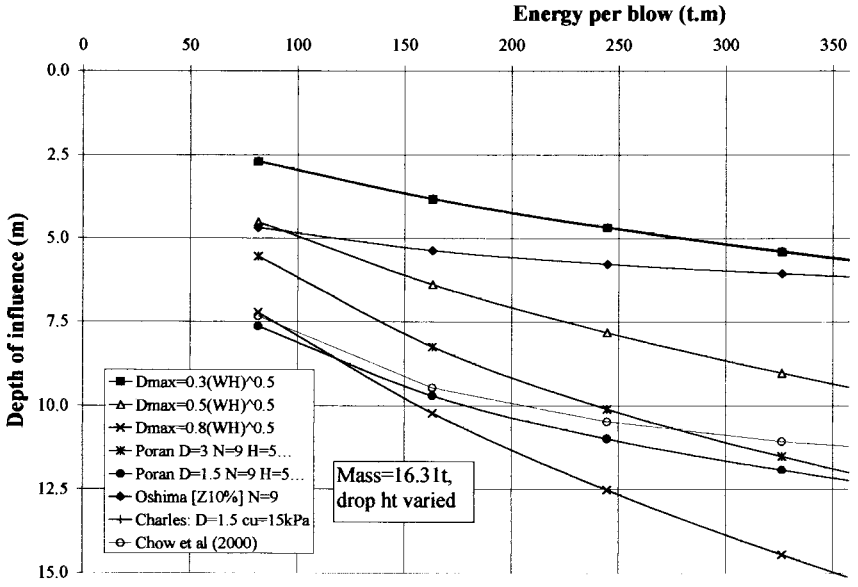

Figure 2.7 : Comparison of various prediction models – DC depth of influence

The figure shows a wide scatter in the predictions using the various models. This may be a result of the water table depth and the compactor contact area often not being considered. Also few of the models differentiate between soil types in their formulation. Only the model by Chow (2000) takes the soil consistency prior to compaction into account.

2.3 AN OVERVIEW OF PREDICTION MODELS USED IN CONVENTIONAL COMPACTION

2.3.1 INTRODUCTION

This section has been sub-divided into three parts. Firstly, the most common type of prediction model (that which assists the engineer to evaluate the likely success of the compaction equipment on a soil layer of standard/known thickness) is discussed. Then, models that take elasto-plasticity into account are looked at. Thirdly, some models that allow the achievable compaction, based on the soils characteristics, are reviewed. Lastly, appropriate, pertinent comments by experts in the field of compaction are given.

2.3.2 PREDICTIONS OF COMPACTOR PERFORMANCE

Biarez (1980) noted that an increase in density of the soil requires permanent deformation, which implies the yield stress is exceeded. Assuming an elastic perfectly plastic soil model (ϕ=0), this means that a pressure p=π.c (i.e 3 x cohesion) is required to compact the soil. He suggested that the bearing capacity formula be used as the permanent deformation reference stress:

$$q = \frac{1}{2}\gamma.B.N\gamma + c.N_c \qquad \text{Eq. 2.18}$$

with B= load contact width, γ=unit mass of soil, c=effective cohesion and N_c and N_γ are the bearing capacity factors.

The contact pressure and imprint width can be evaluated from Hertz's elastic formula:

$$p = \sqrt{\frac{Mg}{L.d}}.\frac{1}{2\sqrt{2}}.\sqrt{\frac{E}{1-v^2}} \qquad \text{Eq. 2.18a}$$

$$B = 2\sqrt{2}.\sqrt{\frac{Mg.d}{L}}.\sqrt{\frac{1-v^2}{E}} \qquad \text{Eq. 2.18b}$$

where B=compactor width (cm), Mg=mass (kg), L=contact length (cm), E =elastic stiffness (units not given), v=Poisson's ratio, d=diameter (cm)

Biarez further suggested that the layer thickness be restricted by the vertical stress at the bottom of the layer and that this thickness be calculated from:

$$z = 0.3\sqrt{Mg} \quad \text{with } Mg \text{ in kg, z in cm} \qquad \text{Eq. 2.18c}$$

Inherent in this thinking is the assumption that the compaction is proportional to the contact stress (assumed to be 8 bar in Eq. 2.18), it's magnitude, and the contact area. The above equation yields a 31cm layer thickness for an 11000kg roller.

Yoo and Selig (1979) proposed the use of a coefficient of compaction (fc) for the evaluation of vibratory roller performance and amount of compaction.

The performance prediction model is based on a dynamic analytical model as shown in Figure 2.8, the output of which is the transmitted dynamic force Ft.

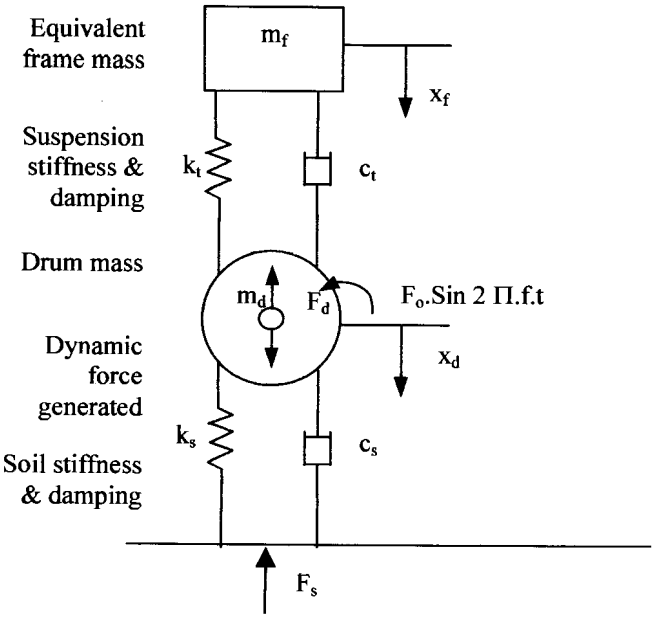

Figure 2.8: Dynamic analytical vibratory compaction model (Yoo & Selig, 1979)

An important finding of this work was that although the generated force can theoretically be increased with increasing vibration frequency (within the limits of the mechanical strength of the machine), the transmitted force reaches a maximum value and then decreases (Figure 2.9).

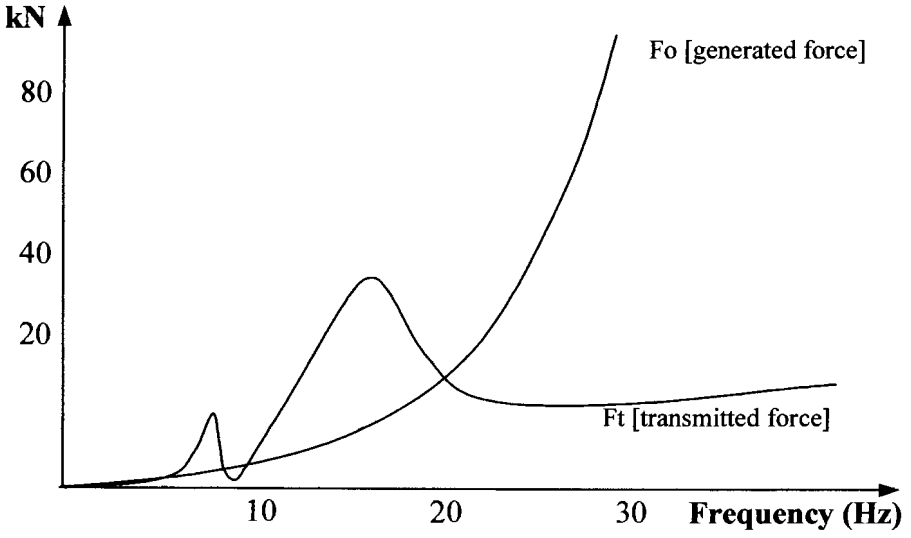

Figure 2.9: Dynamic forces in vibratory compaction (Yoo & Selig, 1979)

The authors conclude that the "possibility of developing relationships between roller motions and the amount of compaction" exists. They note that the main roller characteristic appears to be the drum displacement during vibration.

At the International Conference on Compaction the following year in Paris Yoo (1980) noted that the dimensionless coefficient of compaction f_c is given by the expression:

$$f_c\left(\frac{W}{B}\right) = f_s\left(\frac{W}{B}\right) + f_d\left(\frac{f.A}{s}\right) \qquad \text{(Eq.2.19)}$$

where W=mass (kN), B=contact length (m), A=occilation magnitude (m), s=travel speed (m/s) and f= vibration frequency (Hz), f_s=static coefficient, f_d=group dynamic coefficient

This coefficient of compaction "relates roller mass, roller width, number of roller passes, and compacted layer thickness to the roller compactive effort per unit volume". Values of f_d are obtained from field tests and f_s from compaction tests without vibration. The value of A is calculated from the model given in Figure 2.8. The paper concludes that the amount of compaction is a function the two components on the right hand side of equation 2.19: the first representing the static linear load (SSL) and the second a group dynamic parameter (f.A/s). From these parameters a conventional compactor's performance can be evaluated.

The French (LCPC, 1986) now classify compactors according to the product of the static linear load and the theoretical amplitude:

$$\frac{M1}{L}.\sqrt{AO} \qquad (2.20)$$

"where *M1*=total mass fitting over the generator of a cylinder (kg), *L*=cylinder length in cm [*M1/L=SSL*] and *AO*=theoretical amplitude = 1000 *m.e / MO*, where *m.e*=moment of the eccentric stage of the shaft of unbalance, *MO* is the mass of the vibrating part attached to the shaft of unbalance".

Compactors are then grouped from V1 to V5 types, according to this product. A V1 compactor is for shallow compaction and a V5 compactor for deep compaction (Dunn, 2000). The grouping takes into account the average achievable density throughout a layer as well as the average density of the bottom 8cm of the layer, as shown in Figure 2.10.

pdm = average dry volume mass on the whole thickness of the compacted layer

pdfc = average dry volume mass over the bottom 8cm of the compacted layer

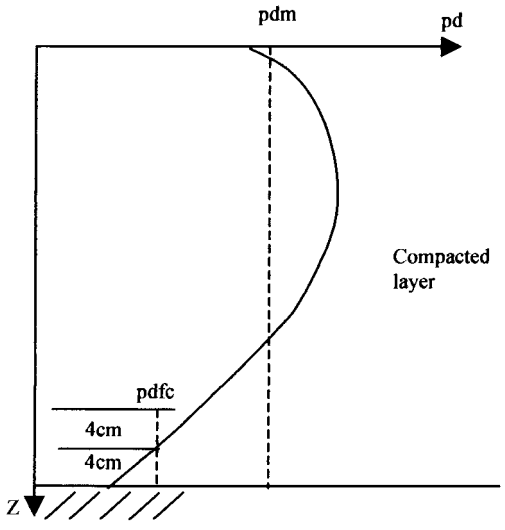

Figure 2.10 : Definitions used in French compaction literature (LCPC, 1986)

The prediction is therefore one of the ability of the compactor to achieve minimum values of pdm and pdfc. It is also clear that a peak in the density profile occurs below the surface, after which the density drops off quite rapidly.

It is interesting to note that the shape of the density profile depicted in Figure 2.10 is one that appears in many of the results given in the literature. None of the literature reviewed discusses the mechanisms that cause this typical profile.

With the advent of continuous compaction control (CCC), some sophisticated models are becoming available. Recent work by Adam and Kopf (2000), incorporates complex predictions that allow both conventional oscillatory and horizontally adjusted *VARIO* rollers to be evaluated. The authors use the substructure method to evaluate the dynamic soil-structure interaction, whereby the various components are evaluated separately while ensuring compatibility is satisfied. The soil substructure is modelled as a translational cone as shown in Figure 2.11.

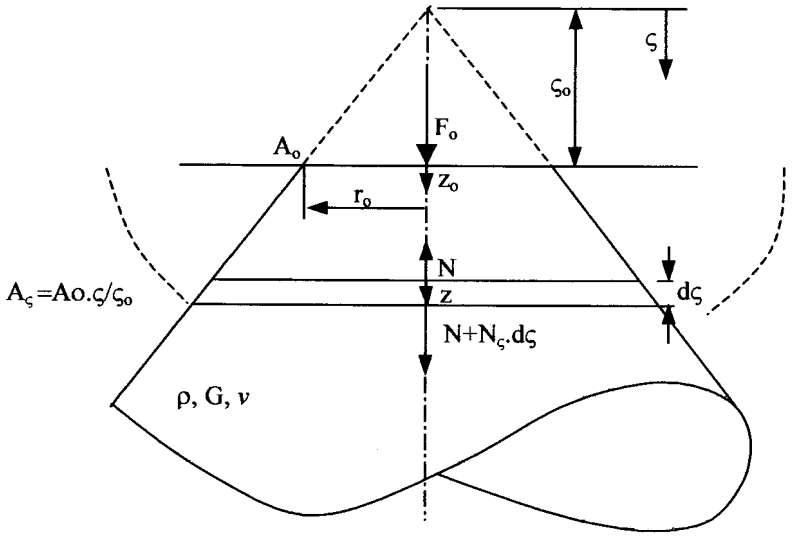

Figure 2.11 : Soil substructure as a translational cone (Adam and Kopf, 2000)

Horizontal motions can be accounted for in a similar fashion. Dynamic equilibrium is achieved using the wave equation. The model gives equations for the spring and dashpot coefficients, *K* and *C*. Non-cohesive soils are modelled separately from cohesive soils. In doing so, the authors note that the Poisson;s ratio for non cohesive soils is typically between 0.25 and 0.35, while for cohesive soils, it increases from 0.33 to 0.5. In the contact zone "elastic behaviour is no longer sufficient to describe the behaviour of soil correctly". Compaction is said to take place in a "plastic zone" that is "embedded within the contact area". Total displacement consists of both elastic and plastic parts, z_o and z_p.

A new parameter is introduced called the plasticity parameter, ε, defined by:

$$\varepsilon = \frac{k^p}{K + k^p} \qquad \text{Eq. 2.21}$$

The plasticity parameter ε, varies from 0 to 1 as the soil varies from entirely plastic to perfectly elastic in behaviour (Figure 2.12). The parameter ε, is a new plasticity parameter derived from the ratio of elastic to total strains:

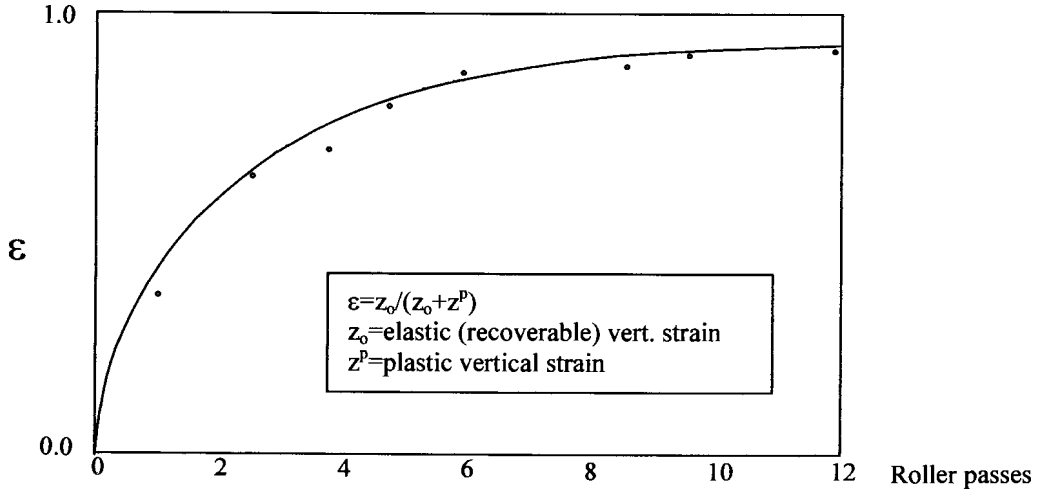

Figure 2.12 : Variation of plasticity parameter ε with roller passes

The result of the model is the ability to predict continuous compaction control parameters (OMEGA, CMV and RMV). Although these parameters are indicators of compaction, the soil improvement profile is not predicted.

Hussein & Selig (1980) predict the performance of a compactor and give equations for the towed force, the compactive effort, the compactive effort per unit volume, the rate of compaction and finally, the power required. The prediction uses the coefficient of compaction, f_c, described above:

$$H = d.f_c.W.S \qquad \text{Eq. 2.20}$$

where d=units conversion factor (HP/(N.km/hr)=3.8×10^{-4}, W=mass (N), S=speed (km/hr), H=power required (horsepower)

Again, due to the nature of conventional compaction, thin layers are invariably used, which results in the assumption that the density is approximately constant throughout the layer. The above model therefore predicts the power required to achieve a constant average density through the layer being considered.

2.3.3 COMPACTION MODELS

2.3.3.1 *Stress based models*

Spangler and Handy (1982) noted that compaction must avoid dilation of the soil and thus the mean normal effective stress (p) must increase without allowing the maximum effective shearing stress (q) to exceed the line indicated by the K_f line (Figure 2.13). i.e if the apex of the Mohr circle is below the K_f line, behaviour is perfectly elastic.

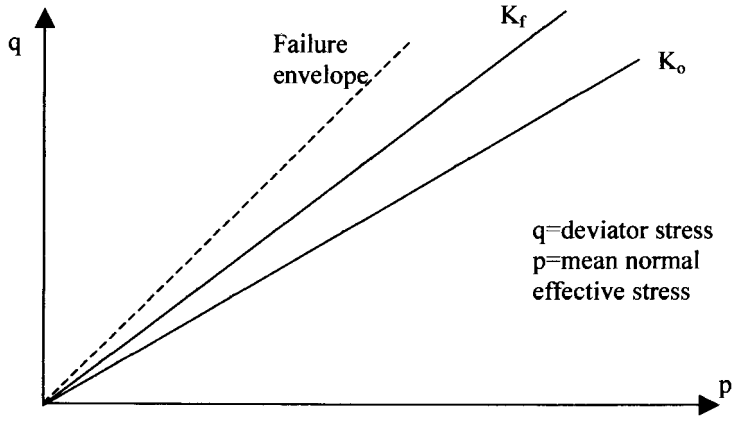

Figure 2.13 : Mohr Coulomb lines indicating elastic or plastic behaviour (Spangler & Handy, 1982)

They note that "during the initial stages of compaction, soil will start at or above the critical void ratio, so the Kf and Ko lines will coincide, and the maximum allowable q will be low. … but on successive passes, the Kf line will be higher and shearing stresses tolerated without dilatancy." They continue to state that one of the main problems with compaction is that the lateral stresses dissipate more rapidly with depth than the vertical stresses do.

A stiff base assists in ensuring that the vertical and horizontal stress difference is reduced. This allows compaction zones to form at the top and bottom of the layer, as shown in Figure 2.14.

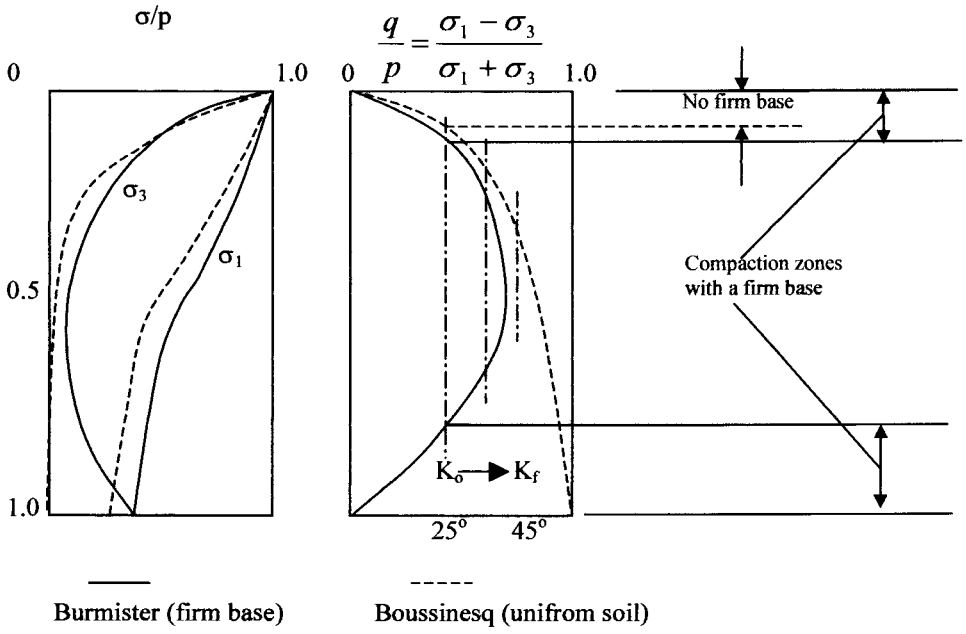

Figure 2.14: Compaction mechanism according to Spangler & Handy (1982)

With successive passes, this theory suggests that the compaction works it's way to the center, with the bottom compacted zone effectively becoming part of the "firm base" after each pass. It is noteworthy that if there is no firm base then compaction only takes place from the top down, according to this model. The material is thus assumed to behave plasticly only if the Mohr Coulomb failure criteria is satisfied (i.e perfectly elastic behaviour inside the yield surface).

2.3.3.2 *Strain based models*

Ullah and Selig (1980) assumed that the volumetric strain equals the vertical strain (zero horizontal strains) and suggested the following equation for predicting the density increase under a vibratory plate compactor on a 152mm layer:

$$\gamma = (1+\varepsilon)\left[\frac{\gamma_f}{1+\varepsilon_f}\right] \qquad \text{Eq. 2.21}$$

where γ = density of soil after any pass (kg/m^3), ε = soil strain after any pass, γ_f = soil density after 16 passes (kg/m^3), ε_f = soil strain after 16 passes

This confirms the intuitive observation that the degree of densification is proportional to the surface settlement. The predicted density is the average measured over the layer thickness. Hence the authors assume that the strain is evenly distributed throughout the layer.

The relationship between settlement and density was confirmed by Forssblad (1980b) when investigating the compaction meter for improved compaction control. The data from his paper is re-plotted with the x axis on a natural scale instead of a log scale, in Figure 2.15.

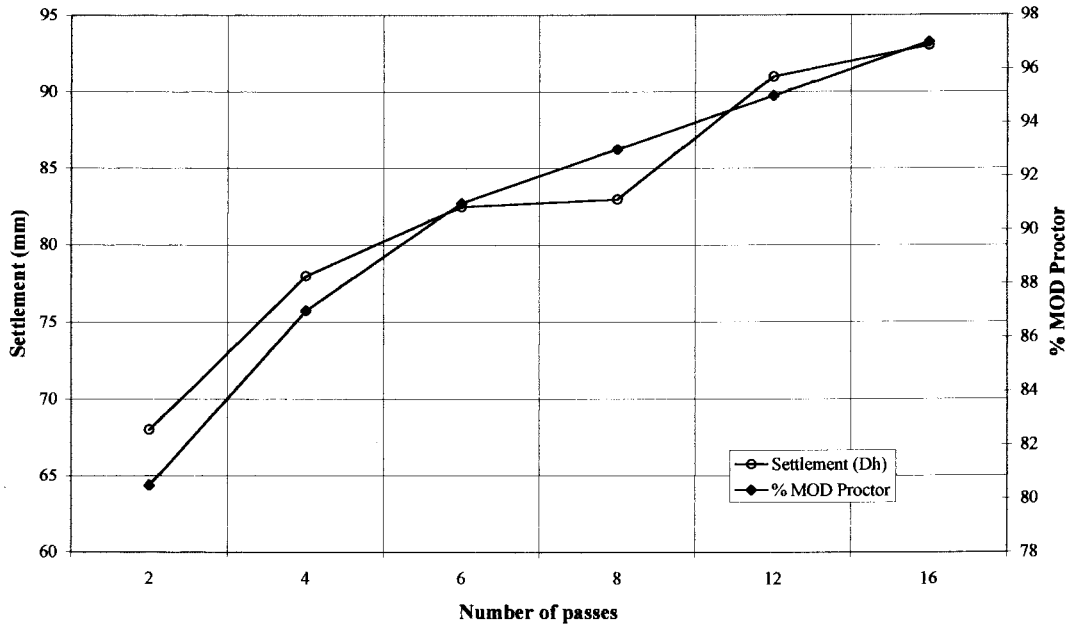

Figure 2.15: Relationship between surface settlement and density (Forssblad, 1980b)

A clear correlation between settlement and the compaction meter value is also seen in Figure 2.16:

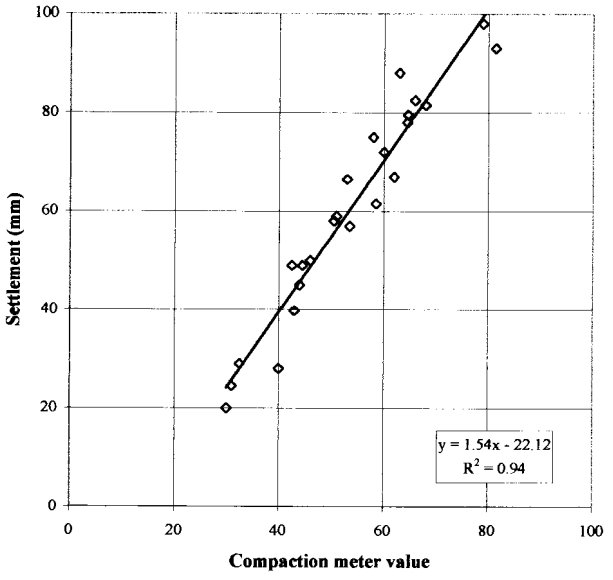

Figure 2.16: Relationship between surface settlement and compaction meter values (Forssblad, 1980b)

The implication of Figure 2.15 is that reliable and accurate measurement of the surface settlement (permanent/plastic strain) is just as good as fitting compaction meters to the compaction equipment. It is interesting to note that both impact compaction contractors and dynamic compaction contractors use settlement as an indicator of when compaction should cease.

2.3.3.3 *Work done based models*

Lytton (1999) has proposed a model that relates the dry density of a soil to the volumetric water content, θ, and the soil suction pressure. The equation is of the well known form:

$$\gamma_d = \frac{G_s.\gamma_w}{1+\theta\left(1+a.|h|^m\right)} \qquad \text{Eq. 2.22}$$

where γ_d=dry density (kg/m^3), h=soil suction head (m), a & m are constants

G_s=soil unit mass (kg/m^3), γ_w=unit mass of water (kg/m^3)

An equation relating the cumulative plastic strain to the cumulative dissipated strain energy is also given:

$$\varepsilon^p = \theta_a.e^{-\left[\frac{\rho}{N.\Delta E}\right]^\beta} \qquad \text{Eq. 2.23}$$

where θa=volumetric air content, ρ = a scale factor, β= logarithmic rate of work hardening

The shape of the curve given by equation 2.23 is similar to that given by Adam and Kopf in Figure 2.12 above. There appears to be consensus, therefore that the magnitude of plastic strain decreases with increasing compactive effort.

2.3.3.4 *Hysteresis and cyclic loading models*

Yandel (1971) proposed a mechano-lattice analogy to predict the permanent deformation and the development of residual stresses in road materials. The prediction was aimed mainly at the post construction evaluation of roads. The model takes the hysteresis into account by using different loading and unloading moduli, as shown in Figure 2.17:

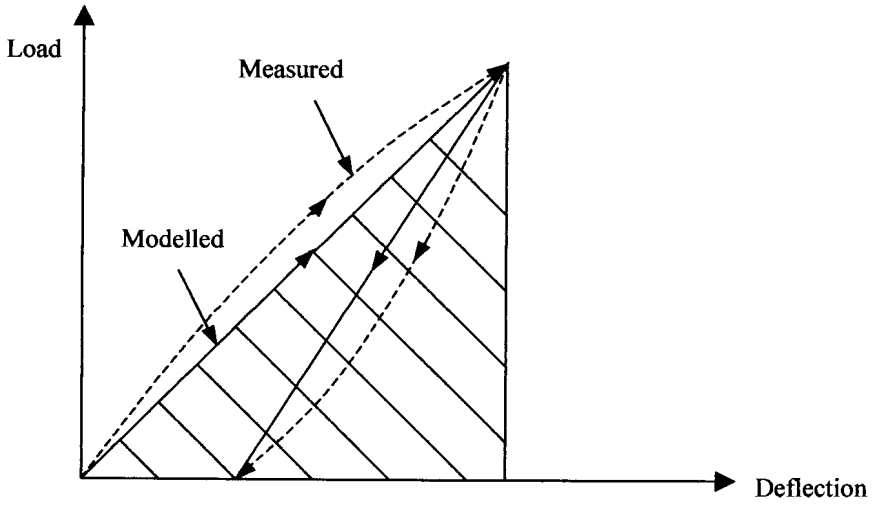

Figure 2.17 : Modeling of hysteresis (Yandell, 1971)

This is then incorporated into either a plane strain or three dimensional mechano-lattice grid to perform the calculations. In addition to permanent deformations, the model allows prediction of residual horizontal stresses, as shown for a thin asphalt layer rolled with a pneumatic tyre in Figure 2-18.

The presence of these residual horizontal stresses cannot occur without the presence of residual horizontal strains. The vertical residual stresses are almost zero.

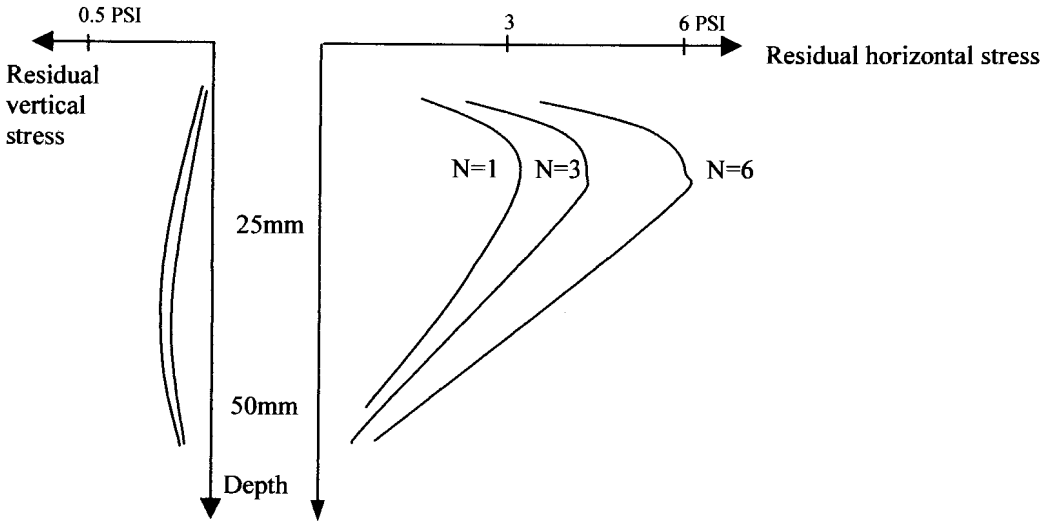

Figure 2-18 : Residual horisontal stresses from mechano-lattice model (Yandell, 1971)

Sawicki and Swidzinski (1990) developed a finite element method that predicts compaction beneath repeated wheel loads. The model is solved numerically by calculating the maximum strains in the subsoil, from which the second invariant of strain amplitude deviator is calculated:

$$J = \frac{1}{3}\left[\left(E_x - E_y\right)^2 + E_x.E_y\right] + E_{xy}^2 \qquad \text{Eq. 2.23}$$

where E_x, E_y and E_{xy} are components of the maximum strain tensor in MPa, corresponding to the maximum load, P.

The compaction , Φ, is given by the constitutive equation:

$$\frac{d\Phi}{dN} = D_1.J.e^{-D_2.\Phi} \qquad \text{Eq. 2.24}$$

where D_1 and D_2 are obtained in the lab, N=number of load repetitions

The settlement is then calculated from:

$$S = \frac{n_0}{1-n_0}\int \Phi.dy \qquad \text{Eq. 2.25}$$

where n_0=initial porosity

Sawicki and Swidzinski (1989) describe a common compaction curve (Figure 2.19) which in their opinion play "a fundamental role in the mechanics of granular materials subject to cyclic loadings, as one of the basic characteristics of granular soils".

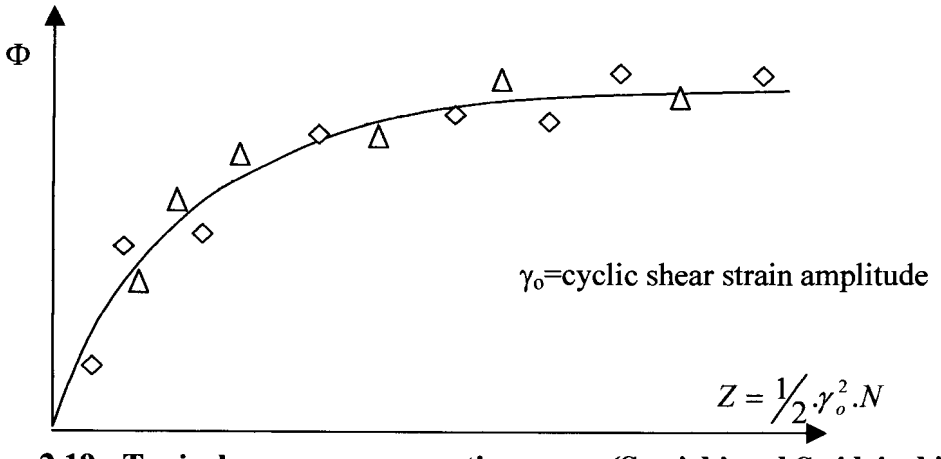

Figure 2.19 : Typical common compaction curve (Sawicki and Swidzinski (1989)

The compaction Φ, is a measure of the irreversible porosity decrease. There is some similarity between Figure 2.19 and the enforced strain diagram proposed by Kwang et al (1990) (Figure 2.4).

Intergration of the distribution of J with depth then leads to the formula,

$$\Phi = C_1.\ln(1 + C_2 J.N) \qquad \text{Eq. 2.26}$$

(where C_1 & C_2 are laboratory determined constants, N=No. of loading cycles) from which "the irreversible volume changes can be computed".

The paper does not show a distribution of the compaction Φ with depth, for vertical cyclic loading, so no indication of the predicted distribution of compaction with depth could be extracted.

A cyclic loading model based on Cam Clay theory, has been presented by Muir Wood (1991). The author notes that simple models do not allow for energy dissipation for states that fall within the yield surface. A "Bubble" model is suggested as one of the solutions to the problem, whereby sub-yield surfaces

within the ultimate failure surface are used. The modelling is complex and no global patterns of improvement in the ground can be easily gleaned from the theory.

2.3.3.5 *Semi-empirical models*

Marr and Christian (1981) give a semi empirical prediction of the settlement of structures based on the accumulated volumetric strains 'on a system" using the following equation:

$$\varepsilon_{vc} = 3.6\left(\frac{\tau_{cy}}{\sigma_{no}}\right)^{3} 2.5^{\log N} \qquad \text{Eq.2.27}$$

where τ_{cy}=cyclic shear stress (kPa), σ_{no}=mean consolidation normal stress (kPa) and N = number of cycles

The predicted versus measured settlements show good agreement. No distribution of the cumulative volumetric strains with depth is given.

O'Riordan (1991) also noted that the surface behaviour (settlement) of silos and circular storage tanks can typically be estimated from:

$$\delta_t = \delta_i 1.5^{\log N}$$

Eq 2.28

where δ_i = initial settlement (mm), N=number of filling/emptying cycles

Some reasonable estimates of cyclic surface settlement therefore appear possible, but none of the predictions discuss the distribution of the strains below the surface.

The models discussed below are not compaction models in the sense that the predictions are of post-construction deformations in road pavements. They are never-the-less reviewed as they show methods that could be adopted for use in compaction modelling.

Wolff and Visser (1994) noted that "permanent deformation takes place with every load repetition, although traffic loading normally induces stresses far below the failure stress of the material defined by the Mohr-Coulomb failure envelope".

In view of this fact, a model was proposed based on extensive measured data from Heavy Vehicle Simulator (HVS) testing that more realistically predicted the pavement deformation at a large number of load repetitions. The model relates the bulk stress θ, at the centre of the layer being considered, to the expected deformation of the layer. The deformation of a specific layer was found to be represented well by an equation of the following form:

$$y = (m.x + a)(1 - e^{-bx}) \qquad \text{Eq. 2.29}$$

where x is the number of load repetitions, y=permanent strain in the layer and a,m, and b are regression constants

The model allows the average strain in a particular layer to be estimated based on the average bulk stress level at the centre of the layer. A summation of the plastic vertical strains predicted for each of the pavement layers then gives the surface deformation.

Lotfi et al (1988) proposed a model whereby the permanent strain at the top of the subgrade of a road could be calculated at any stage of the cyclic loading cycle. The loading modulus E_{lo} is assumed to stiffen continuously according to the equation:

$$E_{lo} = \frac{Mr}{1 + \mu.N^{\alpha}}$$

where $\mu = \frac{ab}{\varepsilon_r}$ and $\alpha = 1 - b$, ε_r = resilient vertical strain (a and b are two new material parameters) Eq. 2.30

The resilient (rebound) modulus, M_r, is assumed to remain constant throughout.

The stiffening model is shown in Figure 2.20:

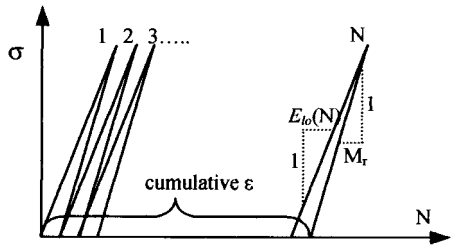

Figure 2.20 : Calculation of cumulative plastic strains at top of subgrade (Lotfi et al, 1988)

The model was found to provide good estimations of subgrade rutting. Charts are given that show the influence of compaction on the anticipated deformation of the pavement. The model is semi-empirical as the constants are obtained from test data. No distribution of the vertical strains with depth is given.

2.3.4 PREDICTION OF ACHIEVABLE COMPACTION BASED ON SOIL CHARACTERISTICS

The models found in this category generally make the assumption that density is achieved by using sufficiently thin layers and adequate energy per unit volume. The models are based on the standard soil classification tests.

Wang and Huang (1984) presented a model that predicts the maximum dry density and optimum moisture content of a soil based on the grading (D_{10}), fineness modulus (FM), plastic limit and uniformity coefficient (U) of the material. The equations are as follows:

Maximim dry density model: [R^2=0.954]

$$\frac{\gamma_{d\max}}{\gamma_{bulk}}.100 = 45.6 - 1.28\overline{FM}.\log(D_{10}) - 4.4.10^{-2}\overline{FM}.\overline{PL} + 1.43.\overline{FM} \qquad \text{Eq. 2.31}$$

Optimum moisture content model: [R^2=0.886]

$$w_{opt}.100 = 2.614 + 12.7\overline{PL} - 95\overline{FM}^2 - 88.1\log^2 U \qquad \text{Eq. 2.32}$$

The authors also give equations for estimating the 90% relative bulk density.

Semmelink and Visser (1995) proposed the use of a similar model that uses the standard classification test information such as the grading and plasticity data, as well as two new tests, the Shakedown Bulk Density (SBD) and Weighted Fractional Density test (WFD). Their model allows the prediction of the optimum compaction moisture content as well as the maximum dry density achievable over a spectrum of moisture contents, as shown in Figure 2.21.

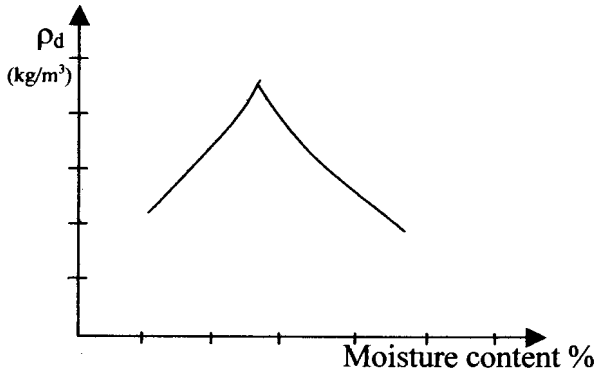

Figure 2.21 : Typical output from Semmelink and Visser (1994) model

The authors conclude that "nearly all design parameters required for road building materials could be obtained from the grading after compaction, LL, LS, SBD, SF (or WFD)". The model is designed to indicate what is achievable with a particular material and therefore does not predict any distribution of compaction through a layer compacted. The SBD and WFD tests may prove useful in a predictive model for compaction, though, as the tests can be used to give the minimum and maximum void ratios of compacted materials. The regression models could also prove useful.

2.3.5 OBSERVATIONS BY EXPERTS

Forssblad (1980a) noted: "When the degree of compaction is successively increased the soil is getting more and more solid and elastic, and, as already said, the theories of Boussinesq can be used with good results, to calculate for example the compaction effect of a pneumatic-tyred roller. Also at vibratory compaction the stress distribution, at least approximately, can be calculated according to the theories of Boussinesq. The reason that the dynamic stresses can be calculated according to the same rules as the static is that the impulse times at vibratory

compaction, around 0.01 to 0.02 seconds, are of such a comparatively low magnitude that the distribution of the dynamic loads is rather similar to the distribution of the corresponding static loads".

Selig (1980) made the following remarks at the same conference: "compaction is the process of producing strains. More specifically, it's the process of producing volumetric compression. Therefore measurement of strain will indicate the amount of compaction. The percent change in density from compaction is equal to the percent volumetric strain which is the sum of the three principal strains". Prof. Selig also noted that the compaction strain measured using induction coil strain measurements showed most of the strains in vibratory compaction were vertical.

2.4 CONCLUSIONS

Little information was found in the impact compaction literature that could assist in a prediction model for ground improvement using impact compaction plant. This is probably due, apart from the complexity of the problem, to impact compaction only being used in a few countries throughout the world to date. This is changing however, and research is currently underway locally, in Australia, and in China.

The dynamic compaction literature survey produced some useful models, although the bulk of the work has ignored the contact area of the rammer, which is a critically important parameter. The work of Chow (1992) indicates that the use of the wave equation and a phenomological model give good results for computer based solutions using finite element analysis. A parametric study of the variables by the same authors (Chow et al 2000) resulted in settlement and depth of improvement prediction equations based on the energy input. Unfortunately the paper does not assist in the understanding of the mechanisms at work, other than to note that the wave-equation is suitable for the modelling of the compactor-soil interaction. The work of Wallays (1983) and Poran and Rodriguez (1992) appear to be the most promising in terms of assisting in the understanding of the mechanisms at work.

Most of the modelling surveyed did not clearly differentiate between saturated and unsaturated conditions.

The literature covering conventional compaction only predicted compactor performance over a limited depth layer, assuming a constant density throughout the layer thickness.

This is probably due to much of the research being undertaken by manufacturers, who are mostly concerned with productivity. This is no doubt also the driving force behind the amount of work that has gone into the development of compaction meters that is installed in many of these compactors today.

The recent theoretical approach proposed by Lytton et al (1999), relating the dissipated strain energy is promising, but full details are not currently available.

The work done by Sawicki and Swidzinski (1990) and Yandell (1971) on cyclic loading and hysteresis effects, although being computer based and thus tend to be black box solutions, could be used to evaluate general patterns that could simplify the understanding of the compaction process.

The model given by Spangler and Handy in Figure 2.12 is believed by the author to be the opposite of what actually happens in practice. The high stresses in the top layer do not generally lead to compaction, but dilation and decompaction. This has been observed in much the test data surveyed in this study. It is therefore of utmost importance to correlate the theory with observation of field behaviour.

Consensus was found in the proposed models, that the incremental increase in compaction decreases with increasing compactive effort. A negative exponential form of equation was commonly used to model this effect. The strong correlation between surface settlement and compaction achieved was confirmed in the review.

None of the literature surveyed was found to contain a prediction model based on surface settlement. The patterns observed in the field test data for both impact and dynamic compaction were similar to that noted by Lukas (Figure 2.2).

The model proposed in this dissertation attempts to offer some explanation for these patterns and a simple means of estimating the void ratio reduction possible.

CHAPTER 3

COMPACTOR FORCE MEASUREMENTS

3.1 INTRODUCTION

In order to estimate the applied pressure in the numerical analysis (undertaken in Chapter 4) the typical range of decelerations of the masses of the impact compactor drums during the compaction process is required. From the deceleration measurements maximum and minimum strains and the depth of influence of the compactors can be estimated (Chapter 4). Knowledge of the input force is also useful for comparison with other compaction plant.

3.2 PREVIOUS WORK

As mentioned in section 2.1, Heyns (1998) undertook a detailed analysis of the three sided and five sided impact compactors using a MATLAB model to estimated the energy imparted to the soil. This was backed up by accelerometer testing on one site. Good agreement was achieved between the estimated and measured accelerations in this study. The results showed a deceleration of the three-sided compactor of 186 m/s^2 (19 g's) on hard ground.

Heyns showed that the imparted force increases with the speed at which the compactors are towed (Figure 3.1).

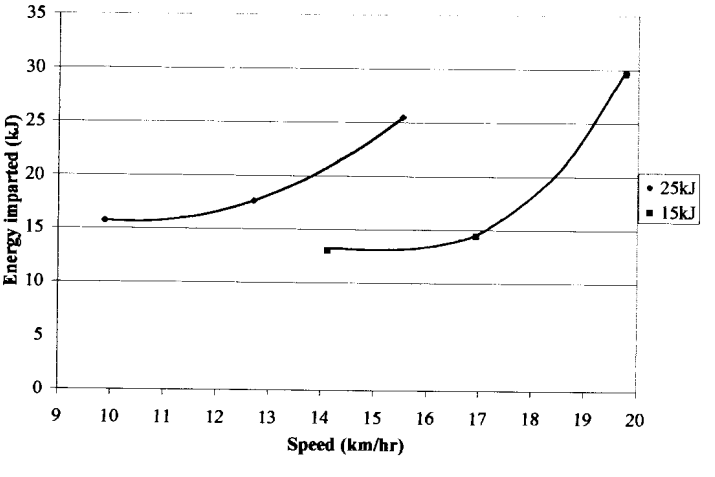

Figure 3.1 : Variation of imparted energy with towing speed (Heyns, 1998)

In his overview in the report Heyns noted that "this work is based on a multi-body dynamics approach, (which) entails that the system be modelled in terms of rigid bodies, connected to one another by means of arbitary non-linear springs and dampers, as well as constraints such as common points, or light rigid rods." He goes on to say that "the system response is found by Runge-Kutta time domain integration of system equations of motion under the influence of time-varying state dependant external variables." He verified the model by comparing simulated responses with measured accelerometer readings. For the parameters assumed in the MATLAB model, it was found that the machines must be towed at about 12 to 17km/hr to achieve the rated energy levels. The 14km/h recommended by the manufacturers is in the middle of this theoretical range.

3.3 AIM OF THE CURRENT TESTING

The objective of this additional testing was to ascertain the *range* of decelerations that are likely over the range of soil stiffnesses encountered. This is necessary as the decelerations are higher in a stiffer soil and lower in a soft soil. From this information, a typical average impact force can be estimated for use in a numerical analysis.

3.4 EQUIPMENT USED

The three standard Landpac impact compactors were used, namely the 10kJ, 15kJ and 25kJ machines. A PCB 353B14 shear accelerometer capable of measuring up to 1000g's was used. The data was collected via a Quatech 16 bit DAQP-16 A/D card with 16 channels capable of measuring up to 100kHz.

Measurement was typically done at 5kHz-10kHz to ensure sufficient definition in the result as the peaks were expected to be quite steep. The data and calibration sheet of the accelerometer and A/D card are given in Appendix C.

3.5 SITE SELECTION

Two sites were selected in the Nigel (South Africa) area close to NCS Engineering, were the machines are manufactured. The first site was chosen due to the presence of a shallow ferricrete layer (at about 600mm below ground level), which represents a very hard subgrade. The site was already well compacted by testing of the impact compactors. The second site was located about two kilometres from the first on very soft, loose hillwash material, with the ferricrete nodules only appearing at 1.6m and becoming hardpan at a depth of about 2.4m. Figure 3.2 shows the site positions.

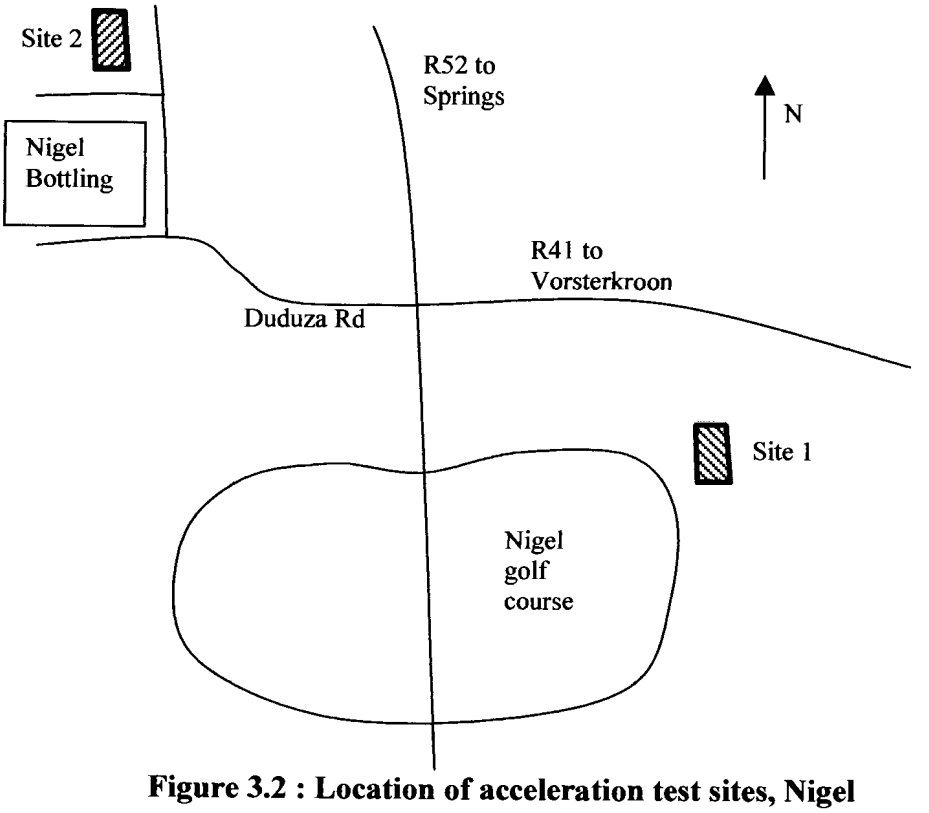

Figure 3.2 : Location of acceleration test sites, Nigel

3.6 ESTIMATION OF ACCELERATIONS USING MAYNE (1983)

In order to estimate the magnitudes of the decelerations of the machines, the method proposed by Mayne (1983) for dynamic compaction was used. The results, shown in Figure 3.3, seem quite reasonable and appeared to confirm the values predicted and measured by Heyns (1998).

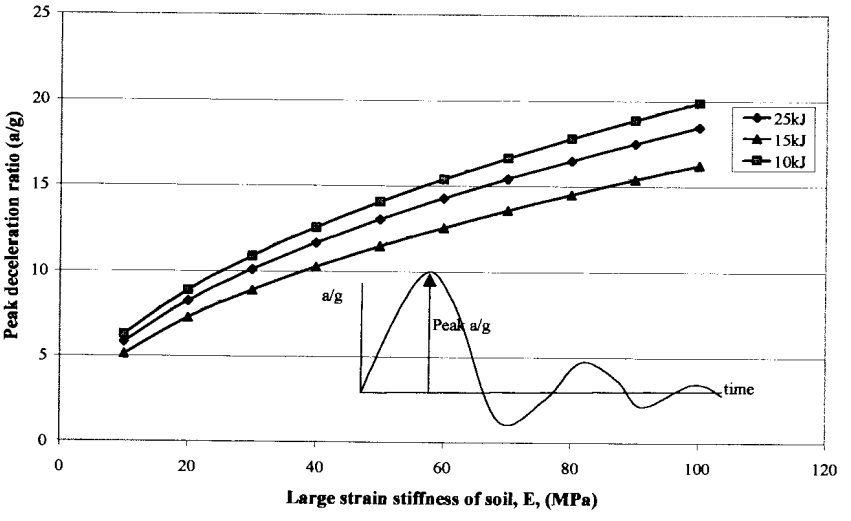

Figure 3.3 : Estimation of decelerations of impact compactors (Mayne, 1983)

The PCB accelerometer available was capable of measuring up to 1000g's to an accuracy of 0.1g. Although the instrument was being used at the bottom of the scale, the results were deemed sufficiently accurate for the purposes of the study.

3.7 PRESENTATION OF TEST RESULTS

Table 3.1 shows typical deceleration ratios measured.

Table 3.1 : Measured deceleration ratios (a/g)

	Soft ground (10-15MPa)	Hard ground (±75MPa)
10kJ	6.9	10.2
15kJ	5.2	14.2
25kJ	5.4	17.4

The pattern of decelerations measured on soft ground conforms to that predicted in Figure 3.3. The 10kJ impact compactor values appear low and do not conform to the predictions using Mayne's method. This may be due a slower speed than required.

The deceleration of the 10kJ is higher that the 15kJ machine due to it's lighter mass. Examination of Maynes formula will clarify this behaviour.

Measurements taken when the machines moved at low speed, or when slowing down for corners, showed a decrease in the impact force, as expected.

Typical deceleration plots are given in Appendix E.

3.8 CONCLUSIONS

The testing confirmed the magnitude of the decelerations predicted by Heyns (1998), as well as the occurrence of higher decelerations on stiffer ground. The range of accelerations found varied from just above 5g's to 19g's. An average value of 10g's is therefore reasonable for use in a numerical model.

CHAPTER 4

VOLUMETRIC STRAINS UNDER A IMPACT COMPACTOR

4.1 INTRODUCTION

This chapter investigates the profile of volumetric strain produced by a single blow of an impact compactor. The volumetric strain profile is reviewed rather than the orthogonal components, as it seems logical that to produce permanent volume changes in the soil, a relationship must exist between the volumetric strain profile and the void ratio reduction profile.

From this perspective, some logical conclusions are hoped to be found regarding the patterns of improvement that can be expected under a compactive load.

4.2 AIMS OF THE ANALYSIS

The aim of the modelling was to determine the approximate distribution of volumetric strain under an impact compactors' imprint. The influence of using various soil models is also briefly investigated in order to answer the basic geotechnical questions:

- How does the profile of volumetric strains vary under a loaded area using various soil models?
- How variable is the volumetric strain profile?
- Do all these variations need to be built into a model?
- Can the patterns be represented in a simple manner?

The effect of dynamics was approximated by using a load approximately equal to the peak dynamic load as measured in the previous chapter (i.e using a deceleration ratio of about 10. It is hoped that this simplification will shed some light on the approximate nature of the volumetric strains that can be expected, thus providing a point of departure for the development of a prediction model for compaction using impact compactors.

4.3 MODELLING METHODOLOGY AND LIMITATIONS

The effects of layering and that of the water table are not included in order to keep the analysis simple. These effects must be taken into account in a more detailed study. Not including the water table in the analysis is a reasonable simplification, as impact compaction is not generally undertaken under saturated conditions.

The soil was analysed using a perfectly elastic constitutive model (i.e no failure possible) as well as an elastic-plastic model with a Mohr-Coulomb failure criteria, for comparative purposes.

Figure 4.1 shows the essential differences in the stress – strain curves of various soil models:

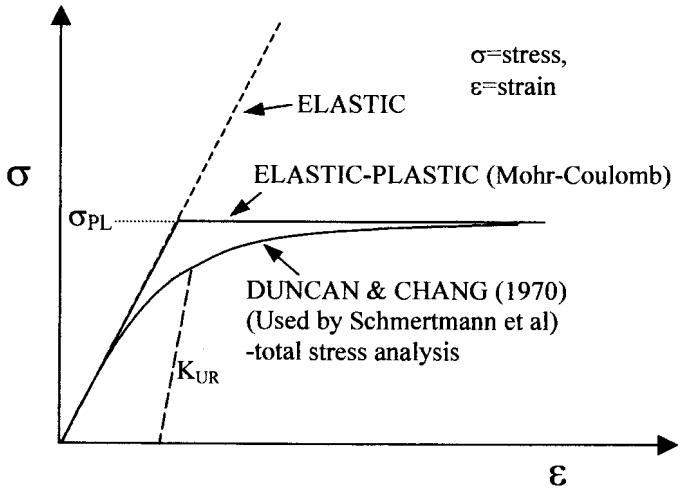

Figure 4.1 : Comparison of soil models

Both non-linear models allow the cumulative plastic strain to be evaluated with the aid of an unload-reload modulus within the failure surface. The total strain can therefore be partitioned into both elastic and plastic components. An important difference between the Duncan and Chang model and the Mohr Coulomb model is that plastic strains only occur after the plastic limit (σ_{PL}) is reached in the latter model. This will tend to mean that plastic strains tend to occur only in the vacinity of the compactive load. The hyperbolic form of the Duncan and Chang model, (more realistically) allows plastic strains to occur at

loads below the plastic limit. None of the above models take the effects of hysteresis into account and are therefore not entirely appropriate for modelling compaction directly. Although the software used in the analysis did not have the Duncan and Chang model, an initial indication of the approximate distributions of strain can be evaluated from both the elastic and Mohr-Coulomb models.

Furthermore, all of the above analyses were static analyses, and it must be noted that the dynamic stress profile is probably slightly deeper. This was highlighted by Hansbo (1979), who noted that the dynamic strain profile is more hyperbolic in nature than the static strain profile, as shown in Figure 4.2.

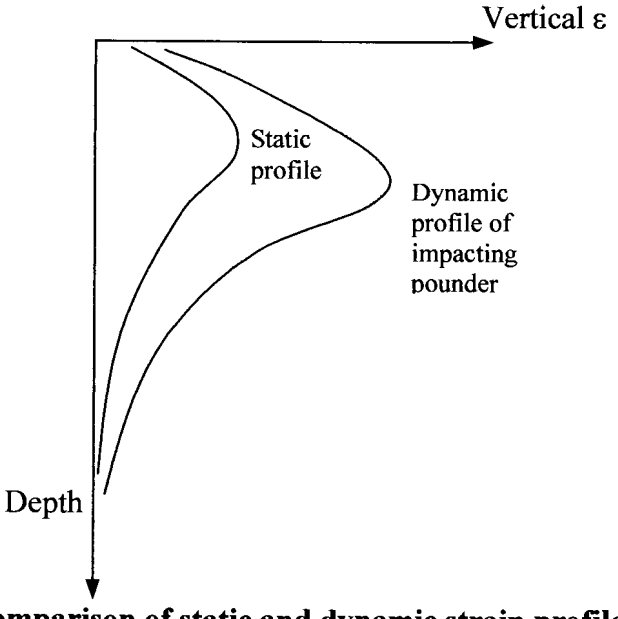

Figure 4.2 : Comparison of static and dynamic strain profiles (Hansbo, 1979)

The magnitudes of the stiffness used in the analysis are typical of those found in un-compacted ground, but due to the comparative nature of the analysis the exact value is not of primary importance. A subgrade stiffness of 25 MPa was used in most of the analyses.

Measurement of average plan area of the three sided impact compactor's indent based on a 40mm penetration of the curved surface yields an approximately square area of 900mm x 900mm. Using this area, the load imprint was modelled with an equivalent circular area of radius 0.5m.

4.4 ELASTIC ANALYSIS OF THE VOLUMETRIC STRAIN PROFILE

According to the generalized Hooke's law the unit volumetric strain ε_{vol} is given (Gear and Timoshenko, 1984): (for axi-symmetric loading):

$$\varepsilon_{vol} = \frac{\Delta V}{V} = (1+\varepsilon_z)(1+\varepsilon_\theta)(1+\varepsilon_r) - 1 \qquad \text{Eq. 4.1}$$

which for small strain becomes :

$$\varepsilon_{vol} \approx \varepsilon_z + \varepsilon_\theta + \varepsilon_r = \varepsilon_z + 2\varepsilon_r \qquad \text{Eq. 4.2}$$

The volumetric strain can also be written in terms of stress as follows for the three dimensional case:

$$\varepsilon_{vol} = \frac{1-2v}{E}(\sigma_1 + \sigma_2 + \sigma_3) = \frac{1-2v}{E}\theta \qquad \text{Eq. 4.3}$$

The volumetric strain and bulk stress, θ are invariants (independent of axis orientation). The above equations show that they are a measure of the change in a fundamental soil property, the volumetric strain and hence also related to void ratio changes. Equation 4.2 shows that the volumetric strain is independent of shearing strains. This may be an indication that the normal strains are more important in the compaction process than shear strains. Similarly, equation 4.3 shows the volumetric strain is proportional only to the normal stresses (no shear stresses in the equation) for small strains.

Equation 4.3 also highlights the significant effect of Poisson's ratio on the elastic volume change in a soil. The use of v=0.5 for saturated materials yields no volume change. Table 4.1 demonstrates the *relative* volume change in an elastic material for a constant bulk stress and stiffness, with Poisson's ratio varied. The volumetric strain for a Poisson's ratio of 0.25 is used as the reference point - using equation 4.3 above:

Table 4.1 : Effect of Poisson's ratio on volume change (elastic material)

v	(1-2v)	Relative volume change
0.25	0.5	100%
0.30	0.4	80%
0.35	0.3	60%
0.40	0.2	40%
0.45	0.1	20%

The conclusion drawn from the above table is that Poisson's ratio is very significant in soil volume changes.

Figure 4.4 shows a summary of the various strains using elastic equations (Huang, 1993) under the centre of a flexible plate, loaded to 10g's (by a 25kJ impact compactor).

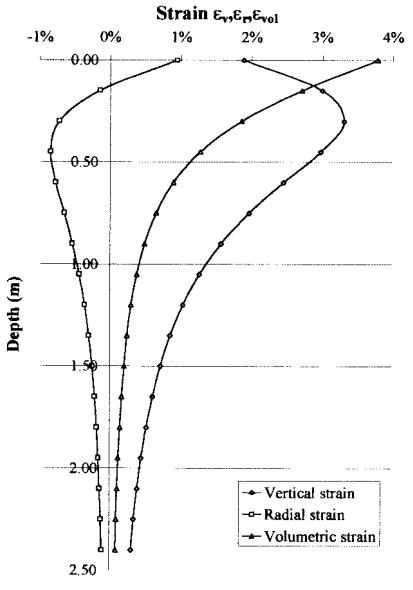

Figure 4.3 : Elastic volumetric strains under a flexible plate (ν=0.3)

Figure 4.3 shows that the volumetric strain profile is similar in shape to the profile of vertical stress according to elastic theory, and does *not* have a peak like the vertical strain profile.

An elastic *FLAC* analysis was also undertaken to check the distribution of volumetric strains beneath the contact area, using a rigid rather than flexible plate. This is shown in Figure 4.4, where it can be seen that the distribution is fairly similar throughout, except near the edge of the loaded area, where higher volumetric strains occur close to the contact surface. Something that should be investigated further is that the ratio of the vertical to horizontal strains according to the above equations is not constant (and equal to Poisson's ratio).

The reduction in volumetric strain is also less rapid that given by the flexible equation above.

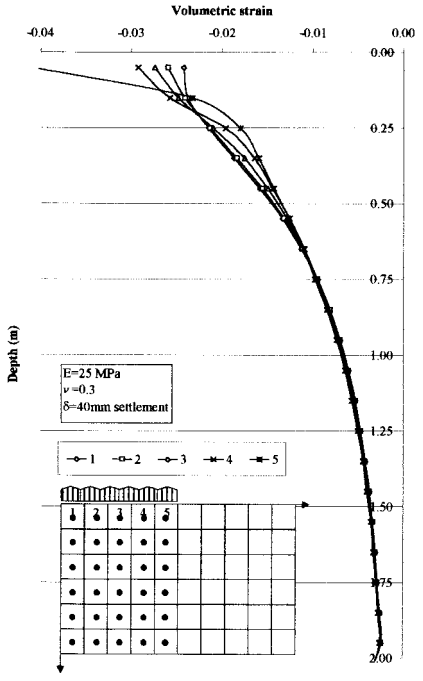

Figure 4.4 : Elastic volumetric strains under a rigid circular plate (a/g=10)

According to elastic theory, all of the volumetric strain shown above returns to zero on removal of the load. This is clearly not what happens in reality, as a proportion of the strains are permanent, resulting in compaction of the soil.

The effect of elasto-plastic soil models on the strain profile is investigated below.

4.5 ELASTIC-PLASTIC STRAINS

The *FLAC* [Fast Lagrangian Analysis of Continua] finite difference software (Version 2.7) (Starfield and Cundel, 1988) was used in the further analysis. The software allows the Mohr-Coulomb constitutive model to be used in addition to standard elastic analysis.

The software also uses the equations of motion in conjunction with local damping to ensure equilibrium is achieved. The pseudo-static analysis should therefore be reasonably realistic.

The analysis therefore has a dynamic basis, although the dynamic module was not utilised (or available) in the analyses performed.

The aim of this analysis was to assess the profile of volumetric strain and compare this with that found in the elastic analysis.

The FLAC finite difference grid is shown in Figure 4.5. For ease of calculation of strains, a uniform grid of 100mm x 100mm was used. The load was applied by applying slowly applying a fixed surface settlement to the grid over the plate of radius (0.5m.) and ensuring that the force was of the correct order of magnitude.

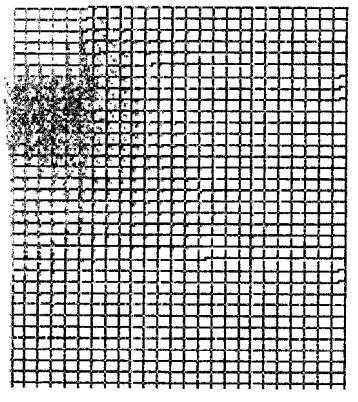

Figure 4.5 : FLAC grid and velocity vectors

To assess the effect of changes in the Mohr Coulomb parameters on the strain profile, the values given in Table 4.2 were used. The parameters that were varied are shown in bold letters. Details not presented below are attached in Appendix G.

Table 4.2 : Mohr-Coulomb model parameters (ν=0.3)

Analysis	E (MPa)	G (MPa)	K (MPa)	c' (kPa)	ϕ'	δ (mm)
MC1	25	9.62	20.83	1	***25***	40
MC2	25	9.62	20.83	1	***30***	40
MC3	25	9.62	20.83	1	***35***	40
MC4	25	9.62	20.83	***5***	25	40
MC5	25	9.62	20.83	***10***	25	40

The vertical, horizontal and volumetric strains were calculated over a depth of 2m below the contact area, for each of the five grid zones [numbered 1 to 5] adjacent the axis of symmetry beneath the loaded area.

The manner in which the total volumetric strains (sum of elastic and plastic strains) varies underneath the rigid loaded area is shown in Figure 4.6.

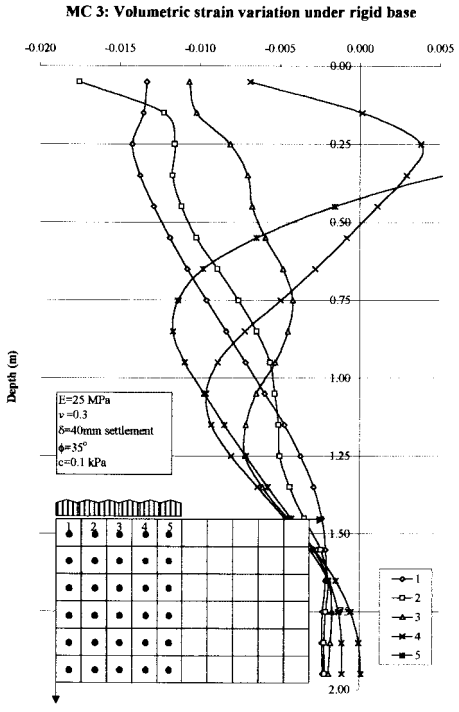

Figure 4.6 : Elastic-plastic volumetric strains under a rigid plate

It is immediately apparent that volumetric strains vary from the centre of the load to the edge quite significantly. Near the axis of symmetry the volumetric profile is similar to the elastic volumetric strain profile, but nearer the edges a reduction occurs due to dilation and a reduction in lateral frictional restraint. The behaviour is complex. It seems reasonable however, to use an average value of volumetric strain to evaluate patterns of behaviour, as the impact imprints vary in position, resulting in an averaged nett volumetric change after a number of passes. Soil testing will also tend to evaluate averages.

Figure 4.7 shows the average volumetric strain for all of the analyses listed in Table 4.1.

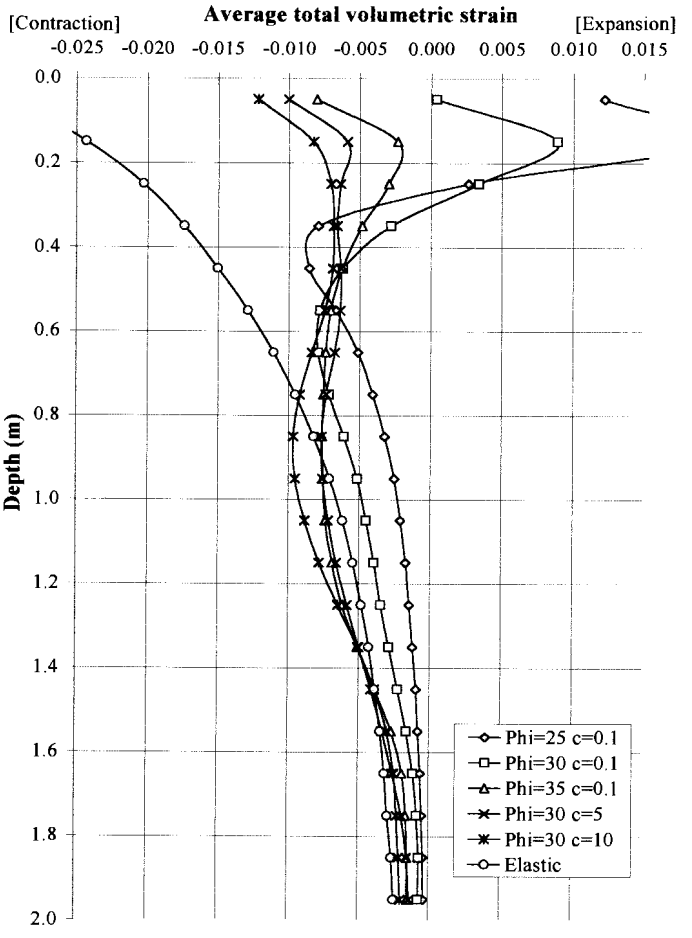

Figure 4.7 : Elastic-plastic volumetric strain variation with soil parameters

For comparison, the elastic volumetric strain is also shown. From the above analyses, the following patterns are evident:

- The "elastic" analysis over-estimates the surface volume changes
- The Mohr-Coulomb analyses show reduced strains just below the load due to plastic behaviour and dilation. This results in a peak in the volumetric strain profile below the surface and very often an "S" shaped profile. [This looks remarkably similar to the diagram on the left of Figure 2.2 in Chapter 2].
- The weaker materials exhibited a greater tendency to dilate just below the loaded area
- The stronger materials (high cohesion and friction angles) showed a deeper peak in the total strain profile.

The use of an appropriate model is therefore essential.

Notwithstanding the limitations in the modelling undertaken, an estimate of the approximate volumetric strain distribution under the application of a single load has been obtained. It would appear reasonable that under the application of repeated loading the shape of the above profiles would be accentuated, with peaks becoming more pronounced.

In summary, the volumetric strain profile has been evaluated using both elastic and elasto-plastic soil models and some patterns of behaviour highlighted, although the behaviour is complex. The soil strength parameters were found to significantly effect the volumetric strain profile, but in what appears to be a predictable manner. In order to simplify the currently proposed model, a single profile of improvement is currently proposed that is believed to simulate average behaviour, but refinements are certainly possible.

4.6 CONCLUSIONS

Significant differences are found when comparing the vertical, horizontal and volumetric strains when using different soil models. An elastic analysis shows little variation in the volumetric strains from the centre to the edge of the loaded area, while a Mohr-Coulomb model indicates a tendency for the soil to dilate towards the edge of the loaded area near the surface.

As the behaviour under the loaded area is complex it is therefore proposed that the average behaviour under a rigid plate can be represented in a manner similar to that of Figures 4.7 and 4.9, where an "S" shape is apparent. The depth of influence is in the order of 2 to 3 times the compactor diameter in the above analyses. A simplified model simulating this behaviour is constructed in the next chapter.

CHAPTER 5

DEVELOPMENT OF A A VOLUMETRIC STRAIN INFLUENCE GROUND IMPROVEMENT PREDICTION MODEL

5.1 INTRODUCTION

This chapter proposes a volumetric strain influence ground improvement prediction model based on the results of numerical analysis, observation of field data and the literature surveyed. The basic hypothesis on which the model is based is given first. Then the model development is overviewed, showing the initial improvement profile hypothesis and the revision that followed. Simplifying assumptions and limitations are high-lighted. Verification of the proposed model is done in Chapter 6.

The main input into the model is the compactor contact dimensions and the surface settlement achieved after compaction. No attempt is made to predict the compaction energy requirements.

5.2 BASIC HYPOTHESIS

From field observations of the typical improvements during the substantial trials undertaken by Africon Engineering for Landpac (Africon, 1998), some patterns of behaviour became apparent (Berry et al, 1998) as discussed in Chapter 2 (Figure 2.1). Subsequent observation of much of the field data seemed to confirm that there is often a peak in the improvement obtained and that this peak appeared to be similar to the Schmertman (1970) vertical strain influence diagram used in the calculation of foundation settlement.

The initial model development therefore focused on using the profile of vertical strain, rather than volumetric strain, as the vertical strain profile has a pronounced peak, which Schmertman simulated with a triangular distribution.

The use of the volumetric strain in the proposed model was a subsequent development, outlined later in the Chapter. None of the compaction models reviewed in chapter 2 specifically discussed a peak in the improvement profile, or the use of surface settlement as an input parameter into the modelling. However, the patterns observed by Lukas (1986) and summarised in Figure 2.2 were confirmed in this study and support the hypothesis of the model proposed here.

The basic hypothesis is as follows:
It is proposed that the plastic volumetric strain profile produced during the compaction process is proportional to the total volumetric strain profile produced by the compactive load. For simplicity sake, it is proposed that this proportion (β) is constant with depth as shown in Figure 5.1.

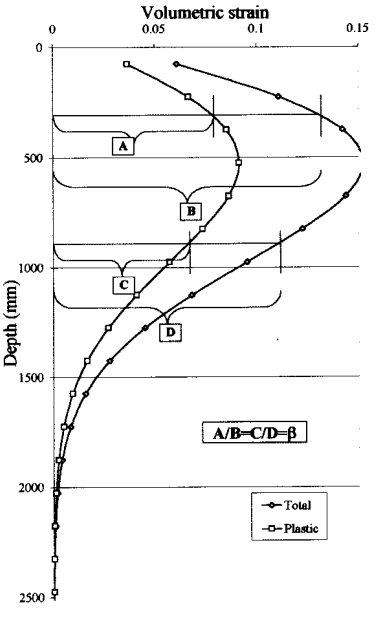

Figure 5.1 : Hypothesised relationship between total and plastic strains

As the surface settlement is the integral of the plastic vertical strain over the depth of influence of the load, it is proposed that this cumulative strain can be re-distributed over the depth of influence of the load, in proportion to the magnitude of the volumetric strain at the depth in question. Provided an estimate of the plastic lateral strains is made, the plastic volumetric strain can be calculated.

Rigid adherence to a single volumetric strain profile pattern is not intended, as the profile is affected by many factors. However, for the initial model development a single profile of volumetric strain is proposed for simplicity sake.

The central hypothesis is therefore that the surface settlement can be re-distributed with depth according to the likely distribution of volumetric strain, which will vary depending on soil parameters. Making allowance for lateral strains allows the volumetric changes in the soil to be estimated.

Layered soils are therefore not excluded from the above hypothesis, as it is proposed that only shape the volumetric strain profile would change, and the back-analysis adjusted accordingly. This further hypothesis is not tested in this study for brevity and simplicity sake, but warrants further investigation.

The above hypothesis has the limitation that the water table is not within the depth of influence of the compactive load. As most impact compaction takes place under unsaturated conditions, the omission of the water table from the model is justified.

To develop and verify the proposed model, however, further simplifying assumptions and limitations have been made as detailed below.

5.3 INITIAL MODEL DEVELOPMENT

Initially the void ratio reduction profile after impact compaction was thought to be proportional to the *vertical* strain distribution below the compactive load.

In the initial development of the prediction model the following simplifying assumptions were made:

- The void ratio reduction profile is proportional to the vertical strain profile, which has a similar shape to the Schmertman strain influence diagram.

- A homogeneous soil is considered, with no layering (i.e a semi-infinite uniform half space)
- The effect of variations in the permanent volumetric strain profile due to changes in friction angle and cohesion are ignored and an average profile assumed representative.
- The magnitude of the surface settlement is either measured in a field trial or estimated (i.e surface settlement is not predicted but used as input into the model).
- The settlement measured at the end of a field trial on granular material is all plastic. (i.e there is no creep recovery).
- Swelling due to wetting up of the soil is ignored.

For ease of calculation, the Rayleigh distribution (Broch, 1980) was used instead of the vertical strain influence factor distribution as proposed by Schmertman (1970). The difference between the two distributions is shown in Figure 5.2. The use of a continuous distribution has obvious benefits in terms of calculations to be made, but is also more realistic. [It can certainly be used as a revision to the triangular strain influence diagram in Schmertman settlement calculations].

The Rayleigh distribution has two useful properties: Firstly, the depth of the peak is at $z=\sigma$ in meters. Secondly, the depth of influence is at $z=3.5\sigma$. The shape of the distribution can therefore be adjusted in a simple manner. According to Schmertman (1970), the maximum vertical strains occur at a depth of between B/2 and B below the foundation/load, depending on the length/width (L/B) ratio of the loaded area (B is the smaller load dimension). As an impact compactor makes a series of impacts in the longitudinal direction and successive passes reinforce this effect, a peak somewhere between B/2 (square load) and B (long load) seems reasonable as a first start to the modelling. The proposed improvement profile was therefore modelled with the depth of the peak vertical strain between 0.67B and 0.8B [B=0.9m in the case of an impact compactor].

Using the Rayleigh distribution results in the depth of influence ranging from about 2m to 2.5m, which ties in with both numerical analyses and field observations. The use of the Rayleigh distribution therefore seems justified.

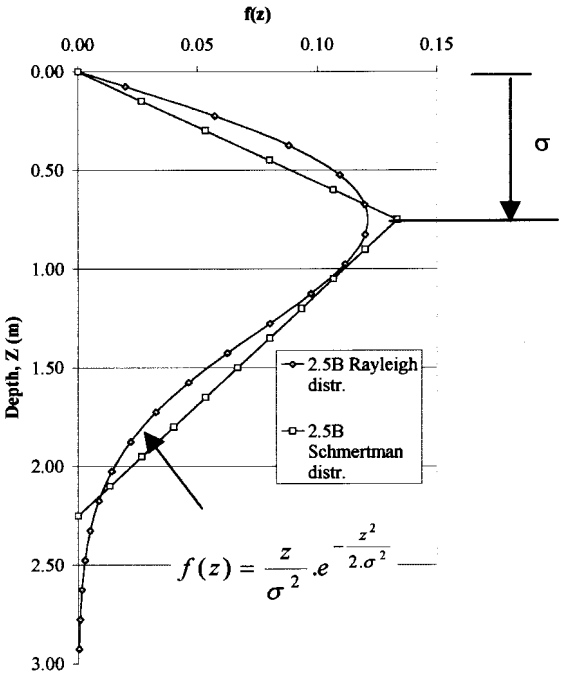

Figure 5.2: Comparison of Rayleigh and Schmertmann distributions of vertical strains

Surface settlement can be conveniently represented by a negative exponential curve as shown in Figure 5.3.

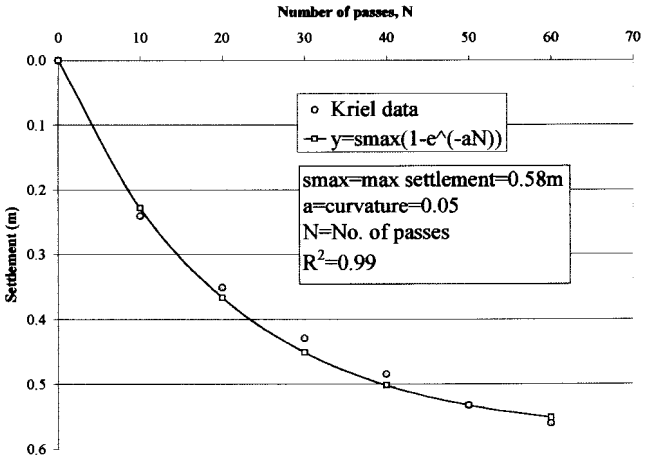

Figure 5.3 : Settlement approximation using a negative exponential curve

The rate of volume change with depth it is argued, is directly proportional to the rate of surface settlement. It is further proposed, that the variation of plastic volumetric strain with depth be simulated by a Rayleigh distribution. The resulting hypothesised three-dimensional surface is given in Figure 5.4.

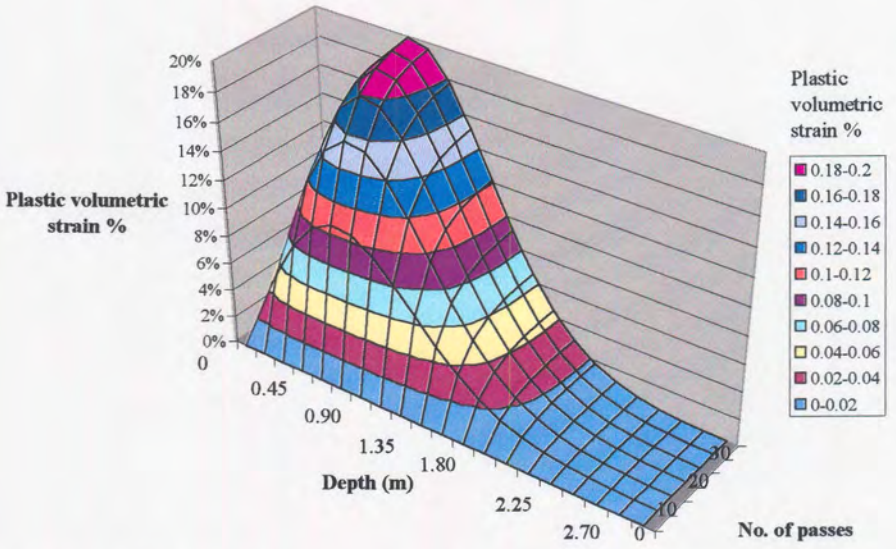

Figure 5.4 : Initial model proposed : Variation of permanent volumetric strain with number of compactor passes

5.4 REVISED MODEL

Calculations based on the above model consistently overestimated the void ratio reduction profile (discussed further in Chapter 6) and this lead to the conclusion that the volumetric strain rather than the vertical strain should be considered as the indicator of the improvement profile. Both vertical, horizontal and tangential strains occur below the compactive load, the sum of which gives the net volumetric strain. In the same manner than permanent vertical strains are produced, permanent lateral and tangential strains result during compaction, and hence permanent volumetric strains are produced. In order to take this into account the method proposed by Gere and Timoshenko (1984) is proposed: Consider a unit volume of soil under uniaxial loading (Figure 5.5).

The initial volume $V_o = a.b.c$

The final volume after compressive strain ε is $Vf = a.b.c\ (1+\varepsilon)(1-v\varepsilon)(1-v\varepsilon)$, So the change in volume is given by $\Delta V = Vf - V_o = a.b.c\ (1+\varepsilon)(1-v\varepsilon)(1-v\varepsilon) - a.b.c$

Which becomes $\Delta V = a.b.c\ (1-2v).\varepsilon$, ignoring higher order terms

So, $\Delta V/V_o = \varepsilon\ (1-2v)$ = unit elastic volumetric strain

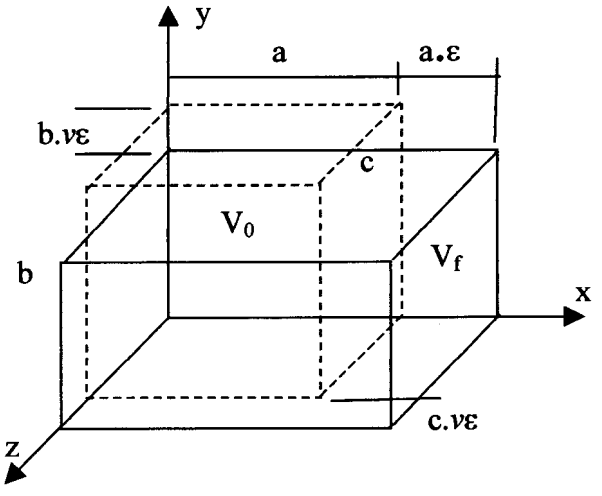

Figure 5.5: Volumetric strain under uniaxial loading

In compaction a proportion of this unit volumetric strain is non-recoverable, and to take this into account, it is proposed that the above formula is modified as follows: $\Delta V/V_o = \varepsilon\ (1-2v_{pl})$, where $v_{pl} = \alpha.v$ and $0 < \alpha < 1.0$ (v=Poisson's ratio, v_{pl} is the operative Poisson's ratio, and α = plastic proportion). It is proposed that initially, during the compaction process, α=1 and as compaction proceeds, approaches a value of about 0.4 for impact compaction, where full surface coverage is standard, and 0.7 for dynamic compaction where compaction is usually done on in grid.

The value of v_{pl} is obtained from back-calculation of field densities from the surface settlements. If the elastic Poisson's ratio, v, is known, α can then be estimated. The back-calculation process is discussed in Chapter 6. The above simplified analysis provides a method of estimating volume change from the vertical strain, if the operative Poisson's ratio is known.

The numerical analysis confirmed that this behaviour is complex and to simplify an average volumetric strain profile is proposed for use in the prediction model. Examples of these patterns of behaviour will be given in chapter 6. A modification to the Rayleigh distribution is proposed to take into account the average volumetric behaviour under an impacting load.

This modified distribution is shown in Figure 5.6 after it has been normalised (i.e the area under the curve made a unit magnitude).

The modification is achieved in a spreadsheet by assuming the peak at the surface is some proportion of the lower peak, say 1.1 times larger.

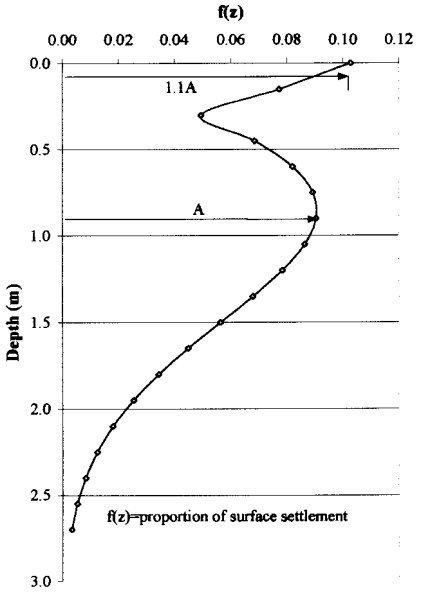

Figure 5.6 : Modified volumetric strain influence distribution

Due to the many simplifications, the exact magnitude of the surface strains is not of primary importance provided the average shape of the volumetric profile is approximated. The hypothesised variation of the permanent volumetric strain profile with increasing number of passes is shown in Figure 5.7.

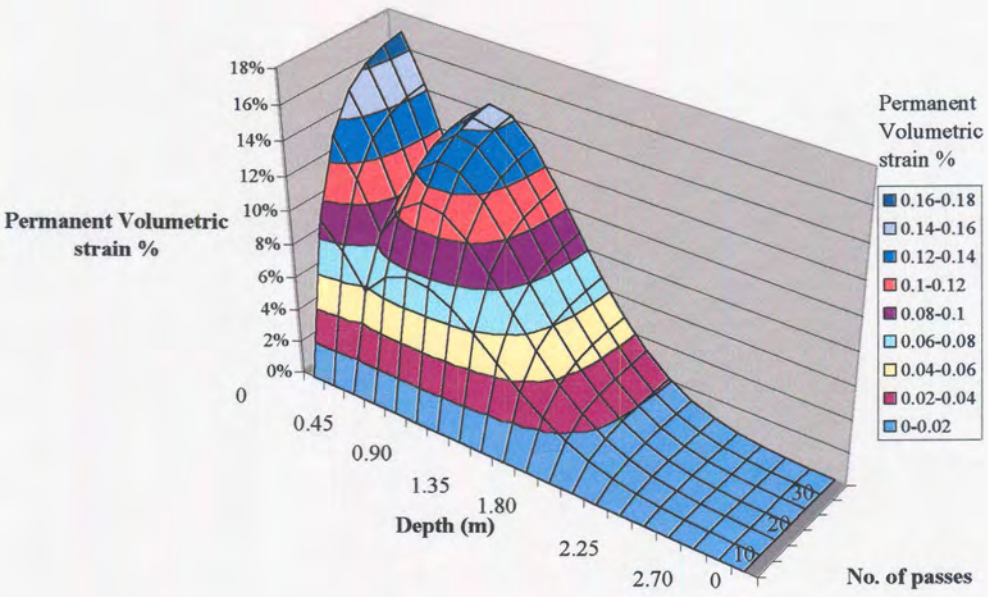

Figure 5.6 : Modified volumetric strain prediction model to take large surface strains into account

The noteworthy aspects of the proposed model are:

- The depth of influence of the compaction load is approximately three times the contact diameter of the loaded area. [Schmertmann (1970) proposed 2B for a square load and 4B for a long load for his settlement model]. Hansbo (1979) also noted that the dynamic strain profile is deeper than the static profile. (Hence a depth of influence profile >2B is justifiable)
- Two peaks appear in the model to simulate the average volumetric behaviour under the compactive load, which is assumed to best represent the profile most likely to be measured in verification testing
- The use of energy as the input parameter is avoided, by using surface settlement. This is both a strength and a weakness. The use of surface settlement bypasses the complication of addressing the different compactive efforts required by differing materials of differing moisture content, structure and grading. This is also a drawback, as most contractors are most interested in the effort required to achieve a specific level of improvement.
- Lateral strains must be taken into account, as will be shown in Chapter 6.

- The principles of volume change are the most important aspect of the proposed model-the exact volumetric distribution needs further detailed dynamic analysis. However, the simplified profile suggested has been found to yield satisfactory results.

An accurate knowledge of the volumetric behaviour near the surface is perhaps not necessary for structural foundations, as the footings are usually placed some depth below the surface. A more detailed knowledge may, however, be warranted for road pavements.

5.5 CONCLUSIONS

A simplified volumetric strain influence ground improvement prediction model is proposed. The main input into the model is the surface settlement, the compactor geometry and the operative Poisson's ratio. A distribution of the permanent volumetric strains with depth is suggested, from which void ratio reduction profile for unsaturated conditions can be estimated.

CHAPTER 6

MODEL VERIFICATION AND DISCUSSION

6.1 INTRODUCTION

In the previous chapter a simplified model for predicting the improvement in the ground based on the profile of volumetric strain, was put forward. The aim of this chapter is to verify the proposed model, discuss some of the shortfalls and suggest some areas for further research.

The calculation procedure is first explained, before verification of the model on fifteen impact compaction soil profiles on six different sites. Reasonable agreement with measured values was found once permanent lateral strains had been taken into account. The model was then checked against the results on a dynamic compaction site, and good correlation found. The effect of lateral strains was found to be more significant on dynamic compaction sites. It is thought that this is due to the relatively large compaction grid spacing.

The use of surface settlement to predict the improvement in a layer compacted with a conventional vibratory compactor is also demonstrated. This confirms that surface settlement can be used to estimate the ground improvement, if the distribution of the permanent strains is known even when simplifying assumptions about the distribution are made.

Confirmation of the patterns of behaviour noted by Lukas (Figure 2.2) and modelled here is also offered via the presentation of various other results. (cone penetrometer results, stiffness measurements etc).

After some discussion, conclusions are drawn and recommendations made regarding the various areas that warrant further investigation. The effect of compaction with the water table present within the depth of influence of the compactor is also hypothesised.

6.2 CALCULATION PROCEDURE

The calculation procedure is outlined below:

Step 1: The surface settlement is either estimated from past experience or obtained from a field trial at the site in question (the latter is preferable)

Step 2: The soil profile is divided into about 20 layers over the depth of influence (DI) of the compactor, assumed to be approximately 3B for an impact compactor, where B is the lessor compactor contact dimension. This is dependant on the energy and drop height of the compactor, as well as the type of materials being compacted. A depth of between 3B and 4B is provisionally recommended for dynamic compactors in the unsaturated conditions commonly found in South Africa.

Step 3: An appropriate volumetric strain influence distribution is selected for the back-calculation process. The modified Rayleigh distribution is suggested as the default, but this need not rigidly be adhered to. The depth of influence can be adjusted by changing the depth of the peak (σ) in the Rayleigh distribution as $DI=3.5\sigma$. From field measurements with impact compactors this depth appears to be between 0.6m and 0.9m (i.e 0.67-1.0B). A provisional value of 0.75B is recommended. This gives a depth of influence of $DI=3.5(0.75B)=3.5(0.75x0.9)=2.363m$ for current model impact compactors. For dynamic compactors the diameter typically varies from 1.4m to 2.4m. Repeating the above exercise and assuming the peak is at 1.0B due to the larger dynamic forces, the calculated depth of influence is between 4.9m and 8.4m. This corresponds well with field measurements in the Gauteng region using this equipment.

Step 4: The settlement that originated in each layer is then back-calculated from $\Delta H=f(z).\delta$, where ΔH is the settlement of the layer, z is the depth to the centre of the layer, and δ is the total measured (or estimated) surface settlement, f(z) is the normalised ordinate of the modified Rayleigh distribution at depth z

Step 5: The vertical strain in the layer is given by $\varepsilon_v=\Delta H/H$, where H is the layer thickness

Step 6: Using an appropriate value of v_{pl}, calculate the permanent volumetric strain from the vertical strain, $\varepsilon_{vol}=(1-2v_{pl}).\varepsilon_v = \Delta V/V_o$, where ΔV is the change in volume and V_o is the initial volume ($V_o=1+e_o$, where e_o is the initial void ratio obtained from pre-compaction testing). Typical values of v_{pl} for impact compaction range from 0.1 to 0.3, with the higher value yielding a conservative estimate of the improvement possible. A value of 0.2 at the end of the compaction process is provisionally recommended. As this is obtained from back-calculation from field data, the model is semi-empirical in nature.

Step 7: The change in volume is obtained from $\Delta V=(1+e_o).(1-2v_{pl}).\varepsilon_v$

Step 8: The final density is given by $\rho=Gs/(V_o-\Delta V)$, where Gs is the relative density of the soil=2650kg/m^3 (typically).

Step 9: Lastly, the void ratio reduction is calculated using the measured initial and predicted final densities. This is done to highlight the changes in the improvement profile before and after compaction, with a view to identifying patterns. This last step is not necessary for routine calculation.

6.3 VERIFICATION ON IMPACT COMPACTION SITES

A list of the impact compacted sites where the model was verified is given in Table 6.1. On all of these sites the primary means of verification was by the measurement of void ratios before and after compaction. The method of void ratio determination is indicated in the table.

Table 6.1 : Impact compaction sites used in model verification

Site No.	Name	Reference	No. of profiles	Void ratio from:
1	Thubelethle, Kriel	Landpac, 1991	4	Sand replacement
2	Thubelethle, Kriel	Africon, 1998	2	Sand replacement
3	Highveld Steel	Clegg, 1969	1	Block samples
4	Middleburg	Barrett & Wrench, 1984	2	Block samples
5	Villa Lisa	Solesbury & Walker (1991)	2	Oedometer
6	Serowe-Orapa	Pinard, 1988	4	
		Total	15	

All calculations for the figures presented are attached in Appendix H.

6.3.1 Site No. 1 – Thubelethle Township, Kriel (1991)

Extensive trials were undertaken at the Thubelethle township in 1991, prior to the construction of the township road network. Testing was supervised by Messrs Schwartz and Tromp consulting engineers. Sand replacement density testing both before and after impact compaction enabled the construction of the void ratio reduction profiles given in Figures 6.1 to 6.4. The back-calculated void ratio reduction assuming one-dimensional strains generally over-estimates the reduction in the void ratio. The model was therefore revised as discussed in chapter 5, assuming that permanent lateral strains are the cause of the overestimation of improvements possible.

The effect of lateral strains is demonstrated by showing two values the operative Poisson's ratio (ν_{pl}). In most cases ν_{pl} ranged from 0.075 to 0.175 at the end of the compaction process (60 passes of the 25kJ impact compactor used). The importance of the permanent lateral strains is highlighted, as a one-dimensional assumption tends to overestimate the volume changes by 15%-35%.

In the 1991 Kriel results, the sampling showed a single peak in the profile. It may be that in fine-grained uniformly graded sands such as those at Kriel, the volumetric strain profile may be better modelled using the initial volumetric strain influence diagram proposed in Figure 5.2 (i.e with a pure Rayleigh distribution). Figure 6.4 indicates that surface dilation may even have occurred.

As the back-calculated void ratio reduction profile yields a consistent value of the operative Poisson's ratio, indicates that prediction using the proposed model appears feasible.

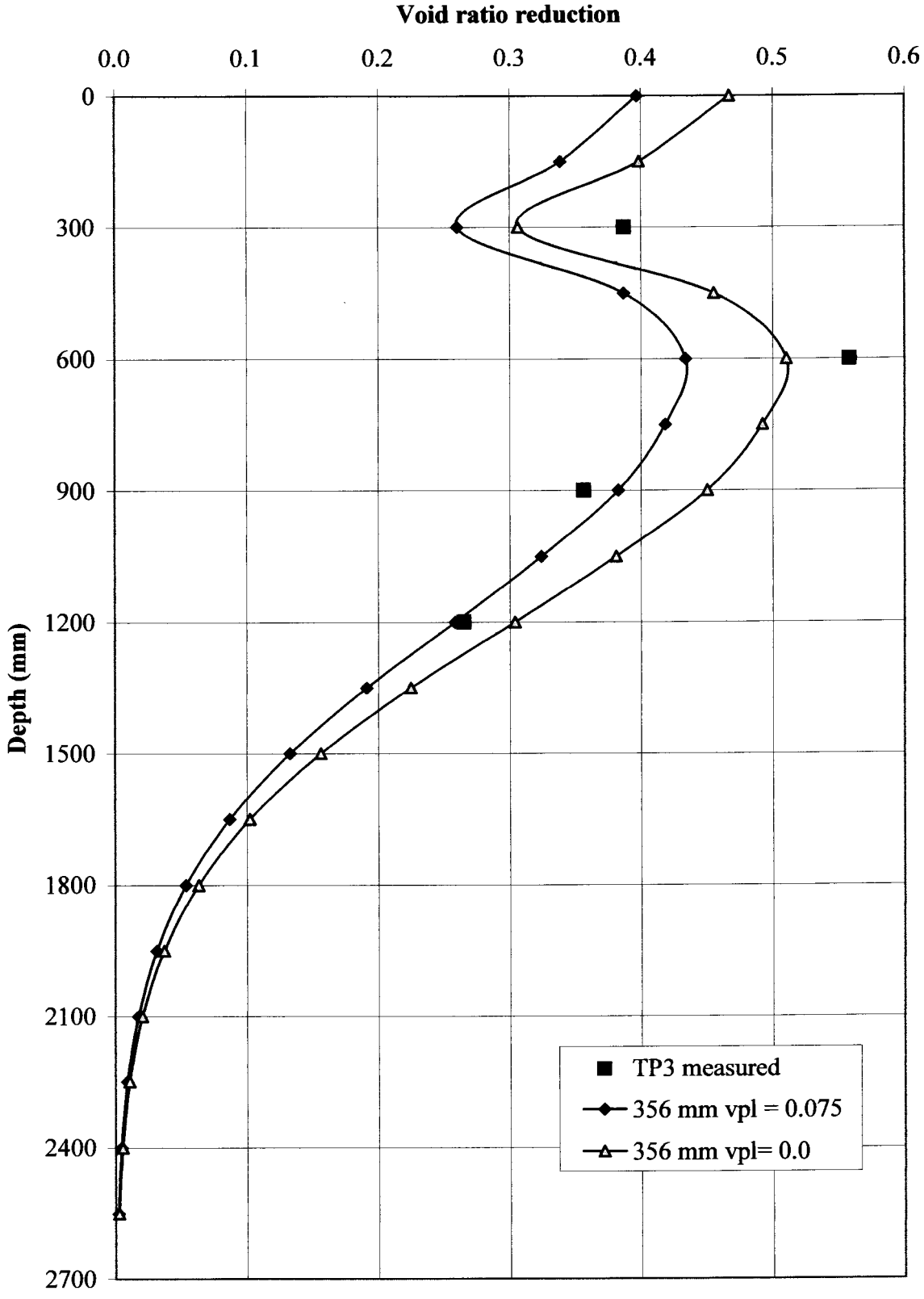

Figure 6.1 : Model verification - TP3 - Kriel, 1991

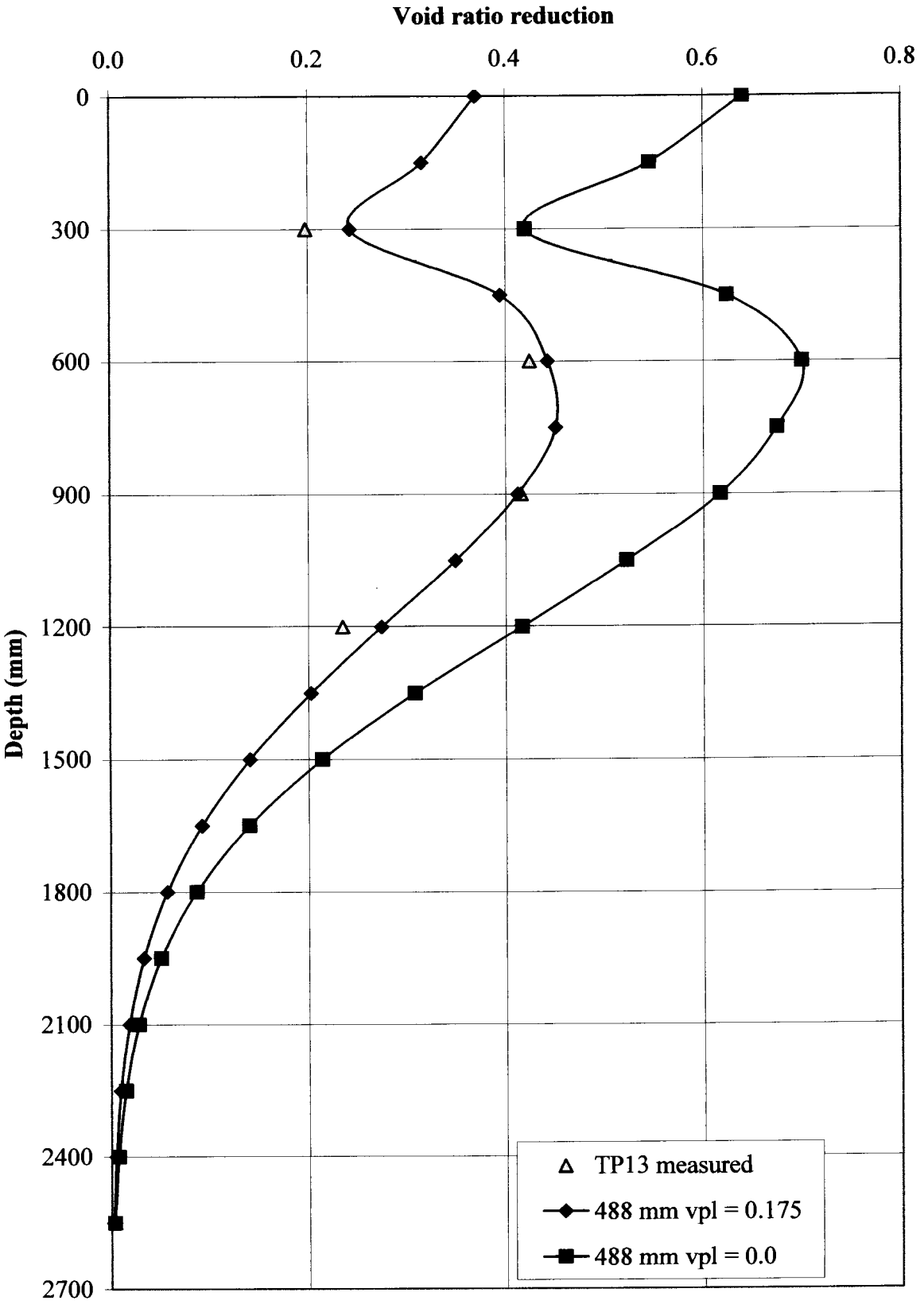

Figure 6.2 : Model verification -TP13 - Kriel, 1991

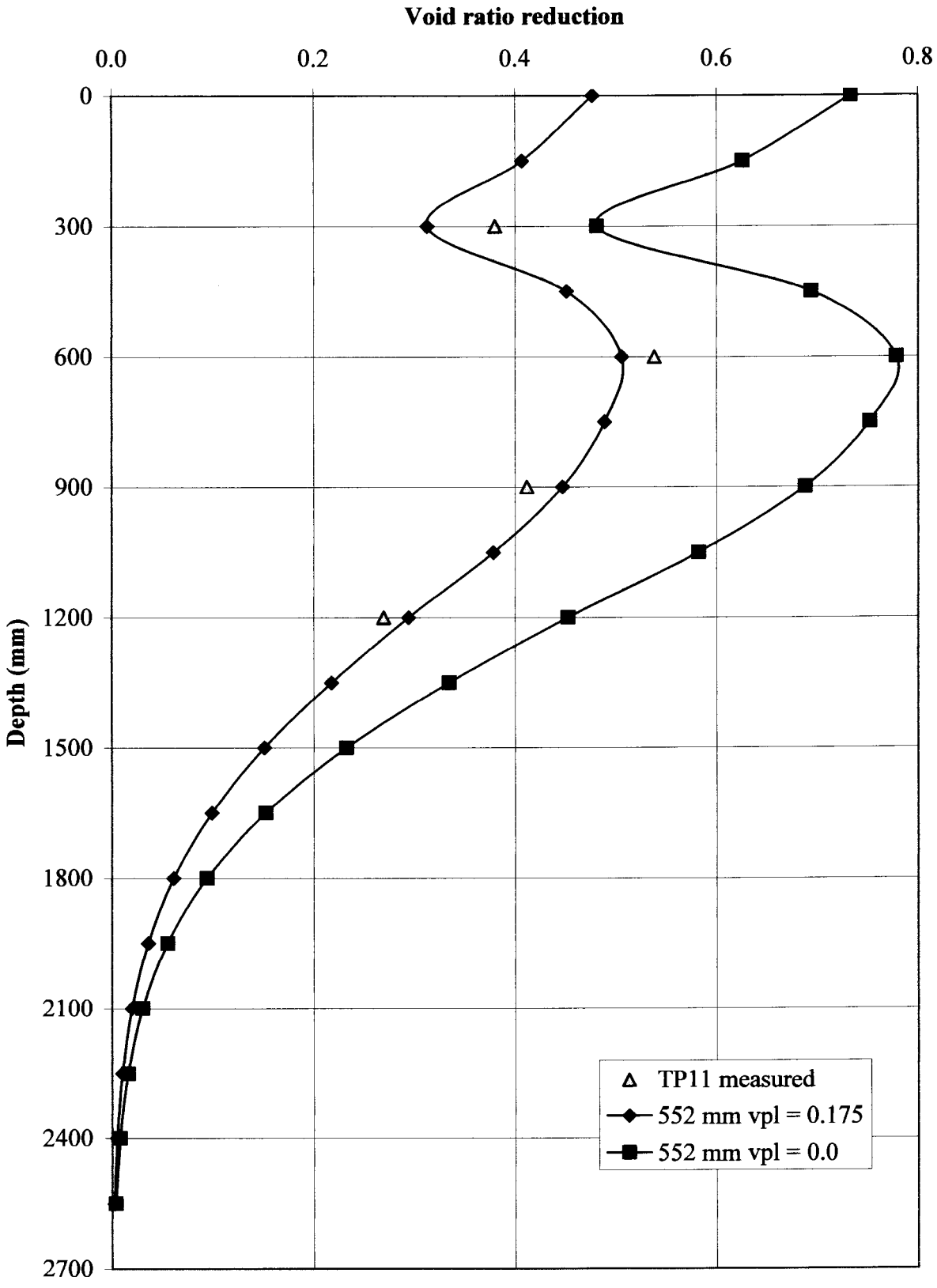

Figure 6.3 : Model verification - TP11 - Kriel, 1991

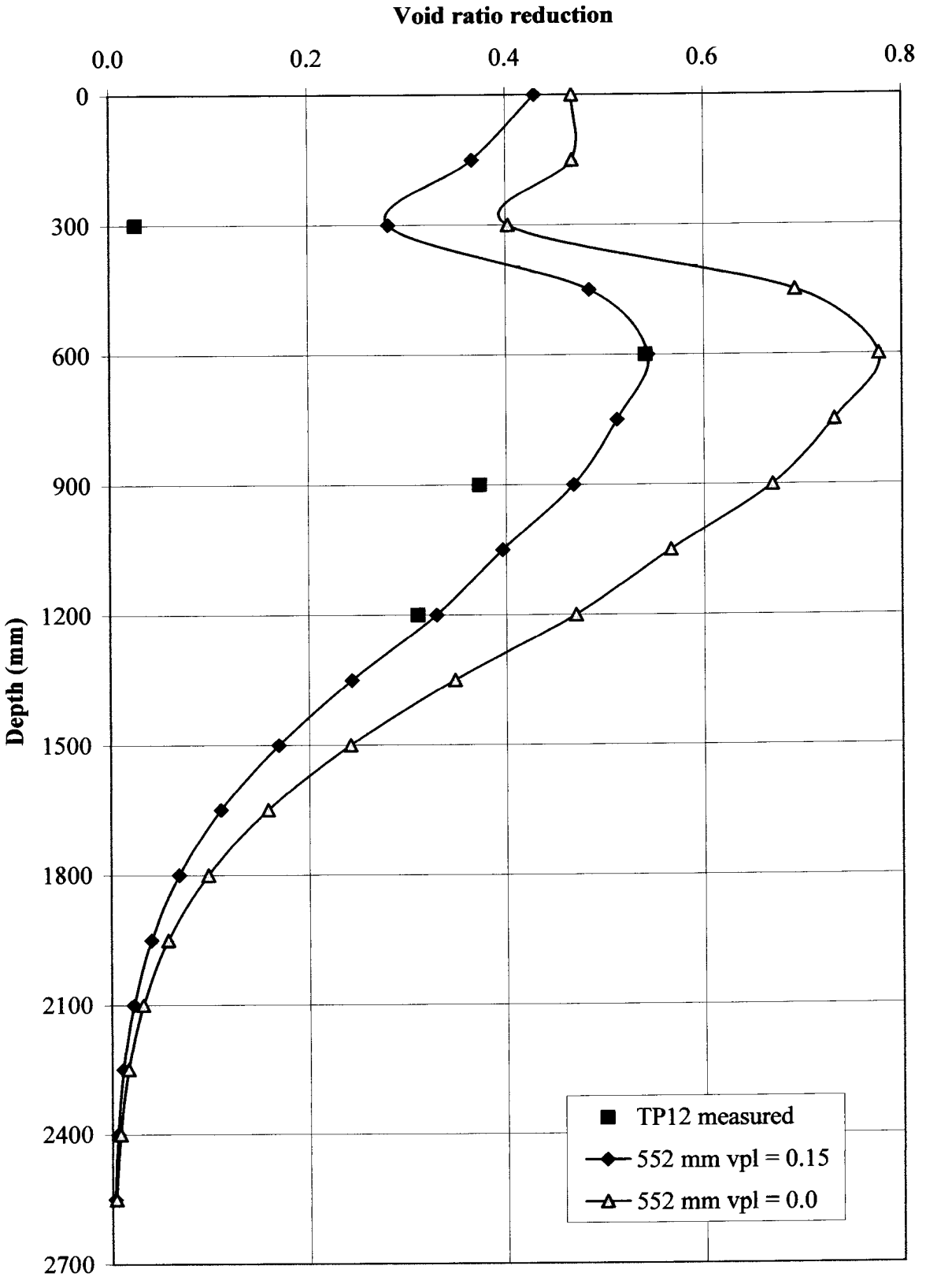

Figure 6.4 : Model verification - TP12 - Kriel, 1991

6.3.2 *Site No. 2 – Thubelethle Township, Kriel (1997)*

As part of an extensive research programme, Africon Engineering conducted further extensive trials for Landpac close to where the original 1991 trails were undertaken. The site was selected due to the fairly uniform conditions to allow comparison of the various models of impact compactors, using a conventional 11 ton vibratory compactor as a yardstick. A discussion of this trial has been presented by Berry (1998) and Strydom (1999).

Figures 6.5 shows the estimated void ratio reduction profile assuming an operative Poisson's ratio of 0.25. The surface settlement was typically 560mm in this trial, after 60 passes of a 25kJ Landpac impact compactor. The model underestimates the compaction below 1.5m at this site.

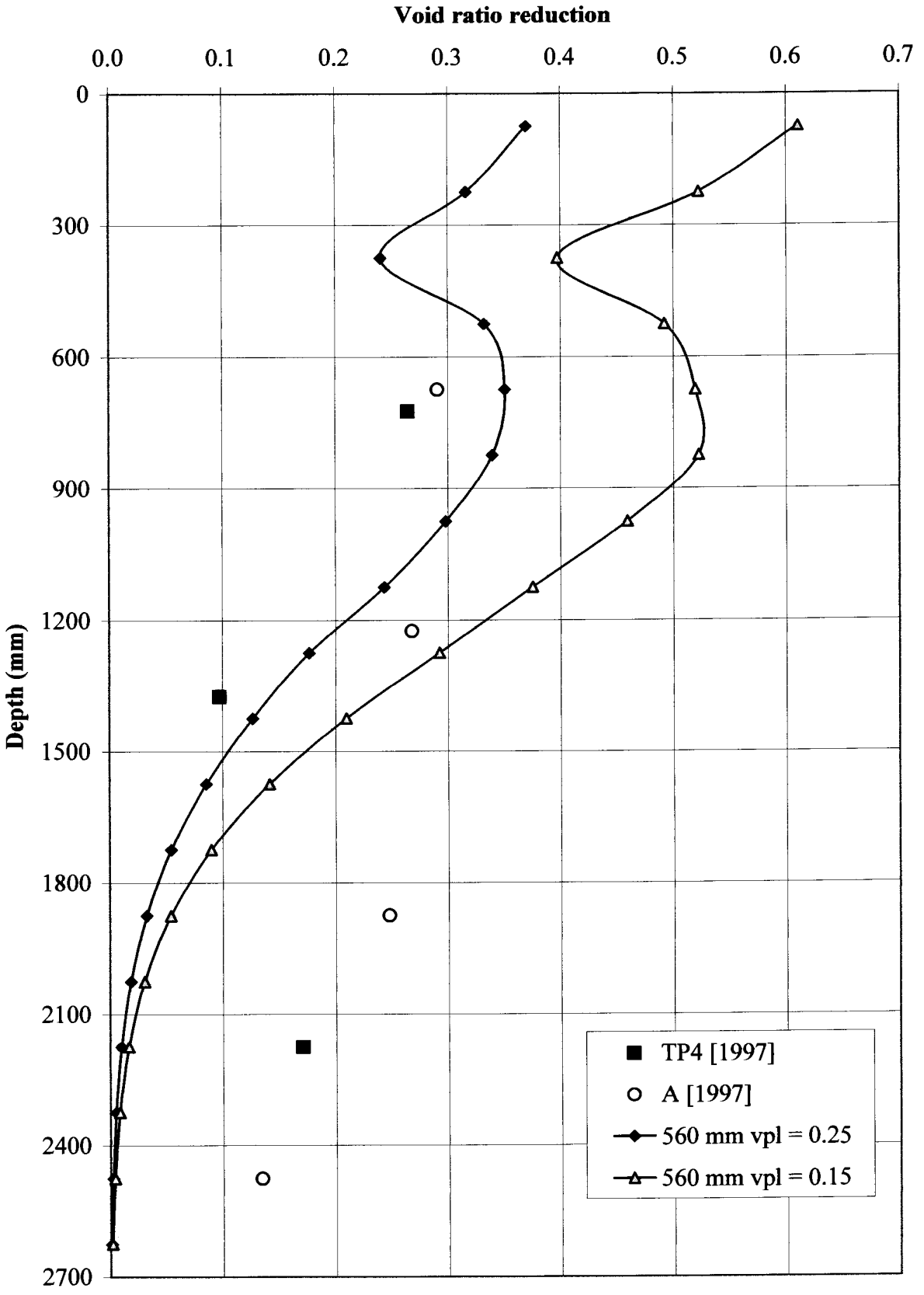

Figure 6.5 : Model verification - Kriel, 1997

6.3.3 *Site No. 3 – Highveld steel, Clegg (1969)*

The soil test results after impact compaction at this site are taken from a paper by Clegg et al (1969).

The measured void ratio reduction and the predicted values are given in Figure 6.6. Good correlation of actual and predicted data is found.

A notable correlation exists between vertical pressure transducer measurements at the site (Figure 6.7) and the predicted improvement profile given in Figure 6.6. The interesting feature of this measurement is the higher pressure at a depth of 0.95m. Theory would suggest that the pressure cannot be higher at a lower depth (a peak, theoretically only occurs in the vertical strain diagram, not the vertical stress diagram). The measurements indicate that under dynamic loading conditions this may not be the case. This behaviour warrants further investigation and analysis.

The vertical strain variation with depth was also measured by means of settlement plates. These strain are shown in Figure 6.8, where a double peak can be seen, as found in the numerical analysis in chapter 4. The magnitudes of the strains may be somewhat exaggerated as the material was placed in a trench and even though lightly re-compacted, it is likely that the soil in the trench was softer than the in-situ condition.

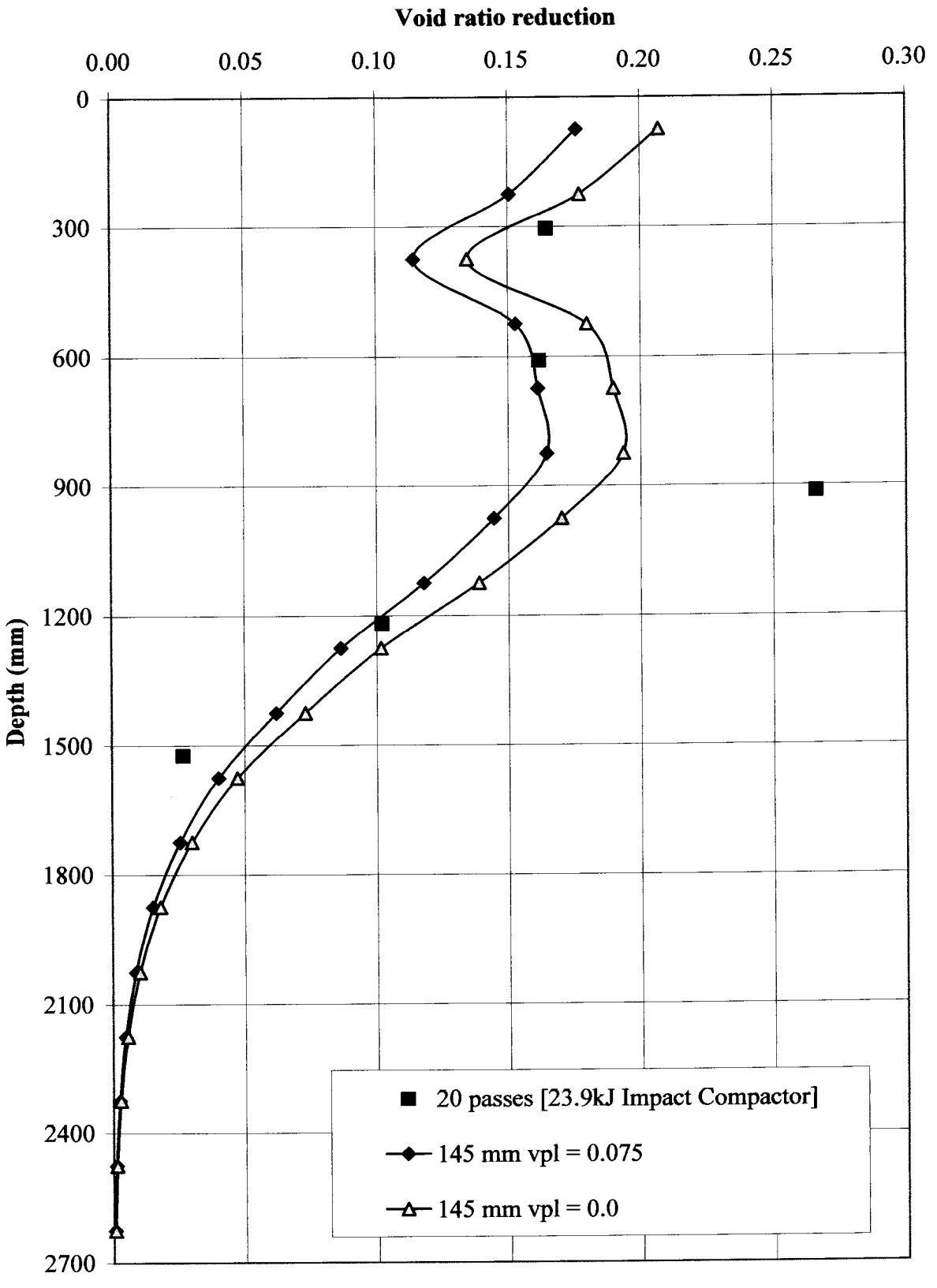

Figure 6.6 : Model verification - Highveld Steel, 1969

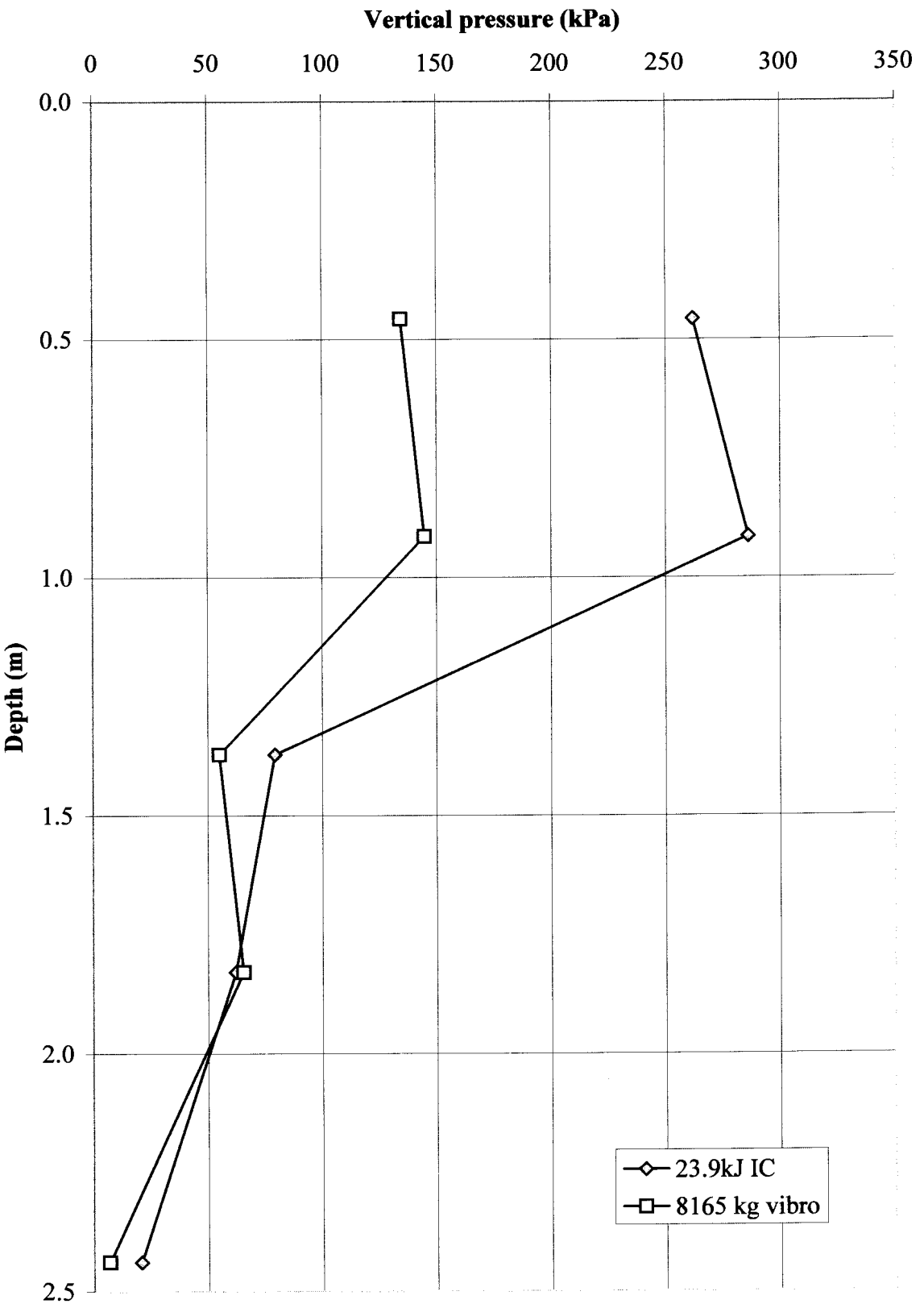

Figure 6.7 : Highveld Steel trial, 1969 : Pressure transducer measurements

(data after Clegg et al, 1969)

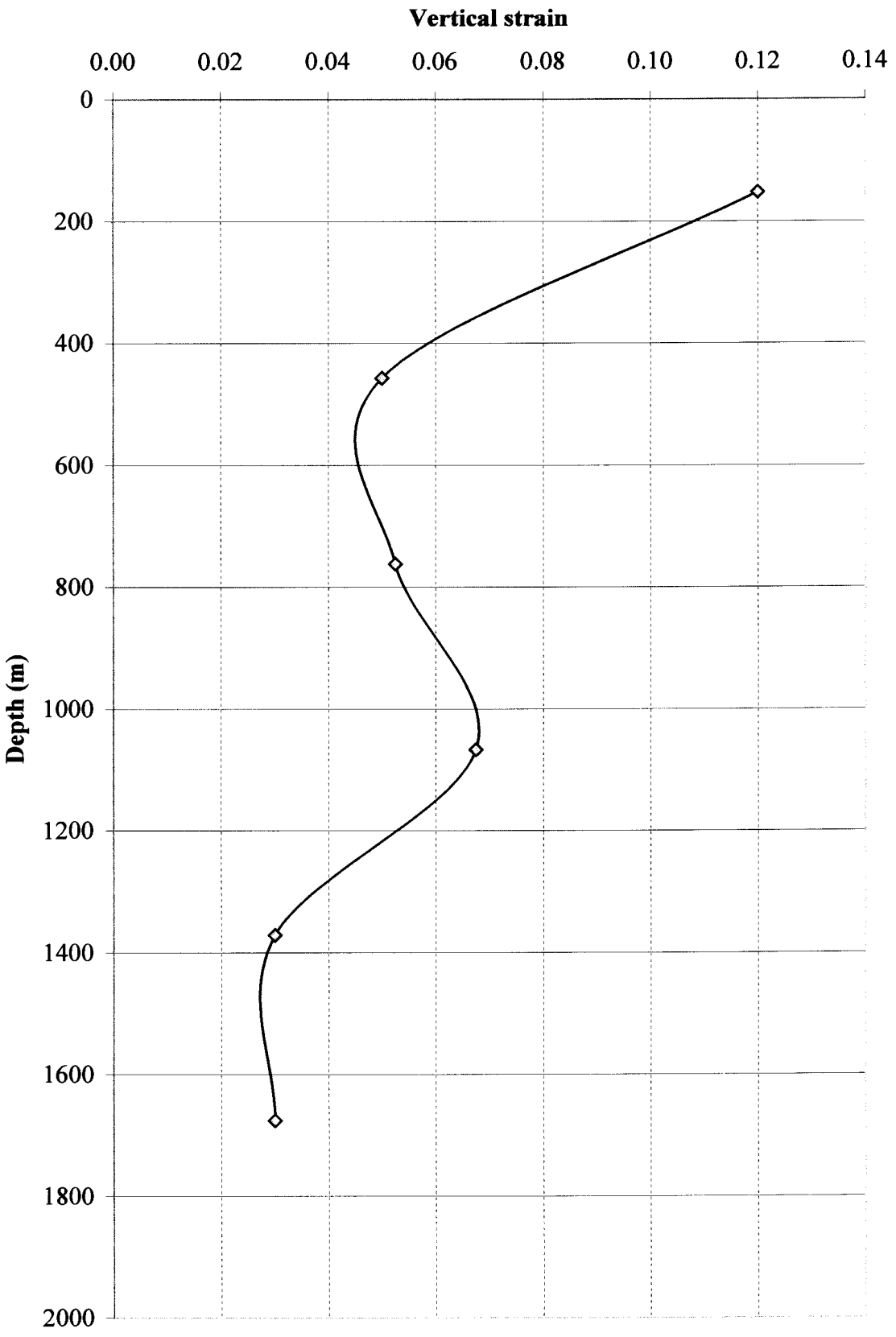

Figure 6.8 Highveld steel trial, Witbank 1969: Strain from settlement plates

(data recalculated from Clegg et al, 1969)

6.3.4 Site No. 4 – Middleburg, Barrett & Wrench (1984)

The results of impact compaction trials at Middleburg reported by Barrett & Wrench in 1984 showed little improvement in the silty materials compacted. Back analysis of the 87mm settlement at 20 passes and 112mm at 50 passes is shown in Figure 6.9. An operative Poisson's ratio of 0.3 was required to correlate the poor improvement achieved at 20 passes. The use of a higher operative Poisson's ratio may be required for clays and silts, where it is know that the elastic Poisson's ratio is about 0.4. At 50 passes the operative Poisson's ratio required to fit the data was about 0.1, indicating that strain hardening may have been taking place to some extent. The paper noted that settlements of up to 300mm occurred in certain areas. The model can be used to plot contours of improvement for different levels of settlement – the 200mm settlement contour is shown to demonstrate the predicted void ratio reduction .

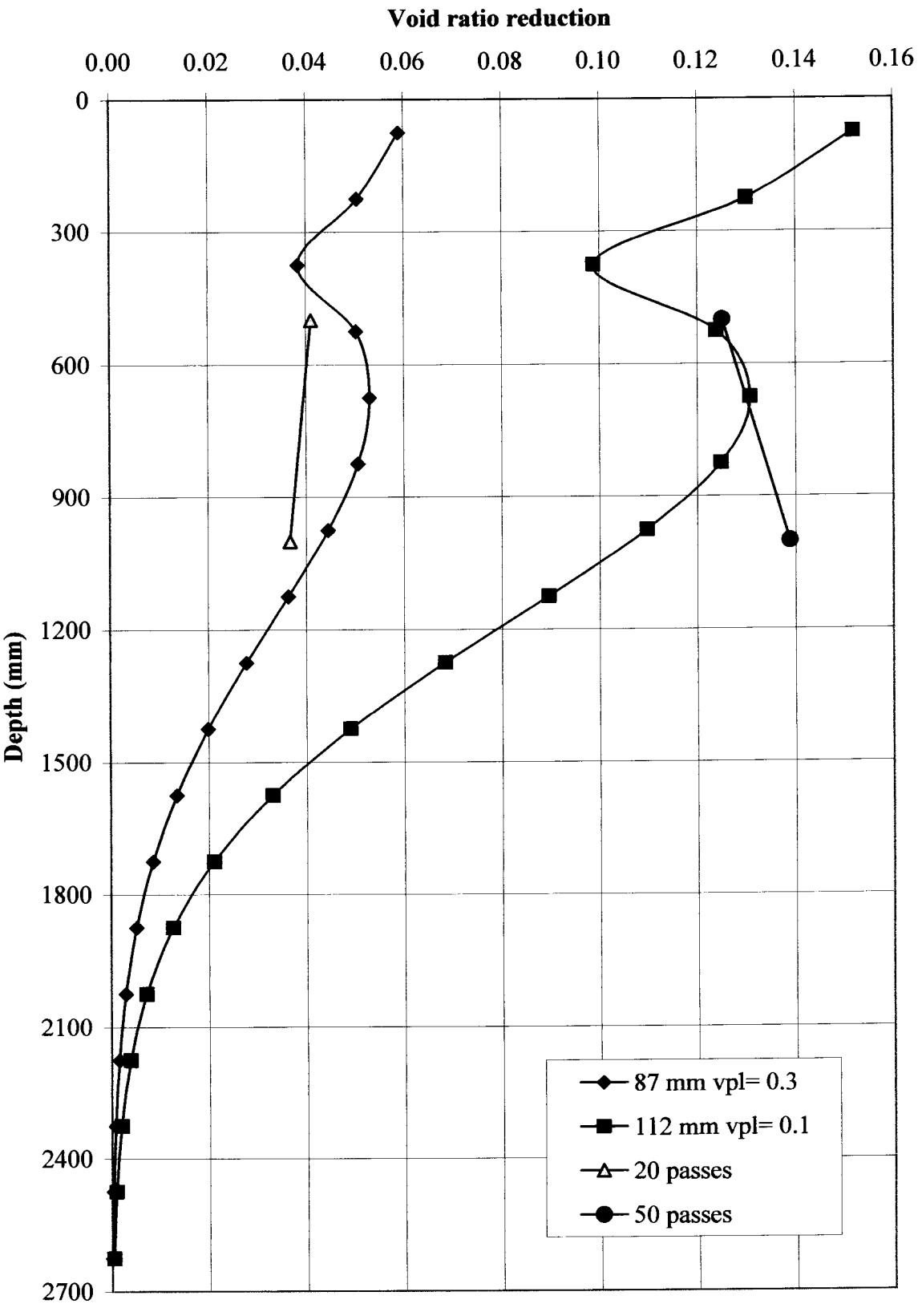

Figure 6.9 : Model verification - Barrett & Wrench trial, 1984

6.3.5 *Site No. 5 – Villa Lisa, Solesbury & Walker (1991)*

Figure 6.10 shows the predicted and measured void ratio reductions at Villa Lisa. Good correlation is found between the model and the measured results. There seems to be a tendency for the operative Poisson's ratio to decrease with increasing number of passes.

Although the theory does not support a distribution with a single peak below the surface (i.e similar to the Rayleigh distribution), much of the measured data seems to indicate a surface loosening, which would practically support such a distribution. The advice given after impact compaction is to finish off with a conventional compactor to rectify the common problem of surface loosening.

A simple Rayleigh distribution analysis is shown in Figure 6.11 for comparison purposes. The model fits well, but higher values of the operative Poisson's ratio are required to fit the data. It is suspected that finer grained and materials may require higher values of the operative Poisson's ratio to fit the data.

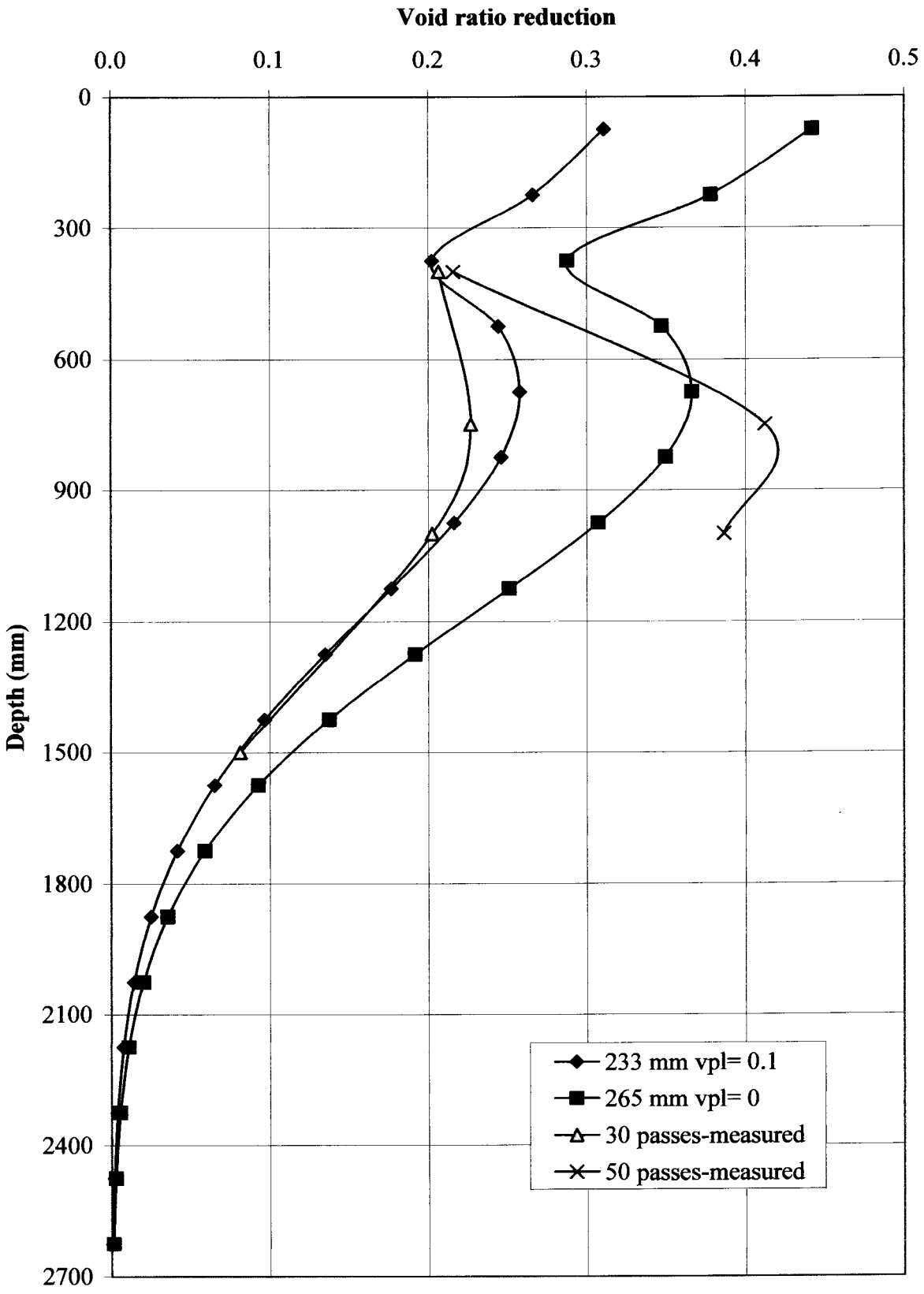

Figure 6.10 : Model verification - Villa Lisa, 1991

(data after Solesbury Walker, 1991)

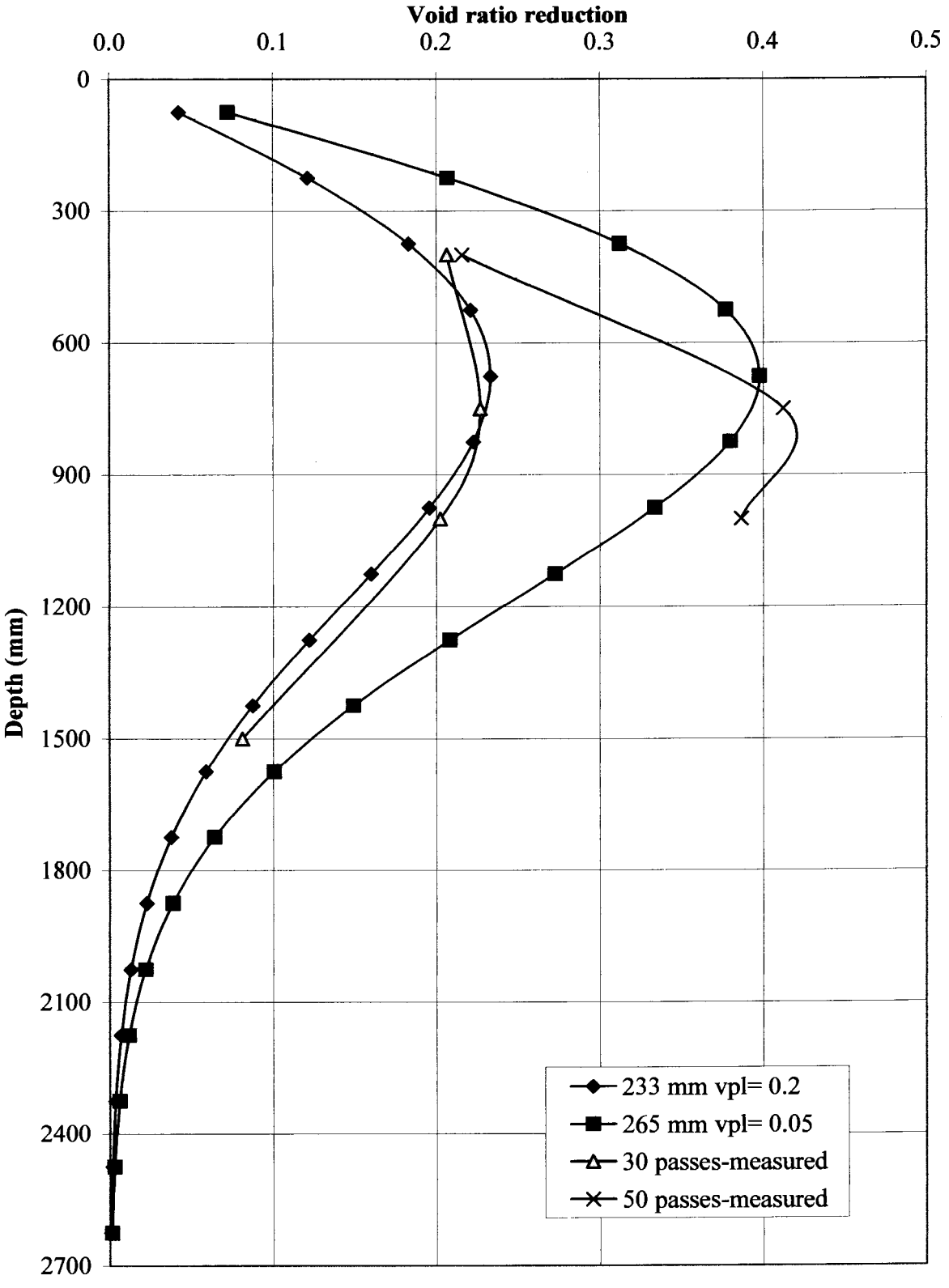

Figure 6.11 : Model verification - Villa Lisa, 1991 [Unmodified Rayleigh volumetric strain distribution]

6.3.6 Site No. 6 – Serowe-Orapa (1991)

Significant trials have also been undertaken in Botswana using mainly three sided 25kJ Landpac impact compactors. The model was checked against tests performed during the construction of the road between Serowe and Orapa, as presented by Pinard (1988).

Back-calculation of void ratios from the settlements recorded are shown in Figure 6.12, using the proposed volumetric strain influence distribution. The model underestimates the densities in the upper part of profile and gives better correlation lower down in the profile. This indicates that the assumed strain influence distribution over the upper portion is not accurate for the conditions at the site. A profile that more closely follows the elastic volumetric strain profiles appears more applicable here. Figure 6.13 shows the effect of modifying the assumed distribution so that the surface strains are twice that of the lower peak, and the depth of the lower peak is rased from the recommended 0.75B to 0.6B. This results is a depth of influence of 2.1m maximum and a volumetric strain influence distribution that more closely follows the shape of the elastic volumetric strain distribution. The result is a much better correlation in the back-calculated data. Further work is clearly warranted to investigate the variation of the volumetric strain profile with different materials, especially over the upper portion of the profile.

Some examples where the modified Rayleigh distribution is used to estimate the void ratio reduction achieved at a dynamic compaction site, where extensive testing was undertaken, are given next. This is done to illustrate that the principal mechanism of improvement is similar, no matter what kind of compactor is used: surface settlement is a good indicator of the improvements achieved, and can be used to estimate the void ratio reductions achieved.

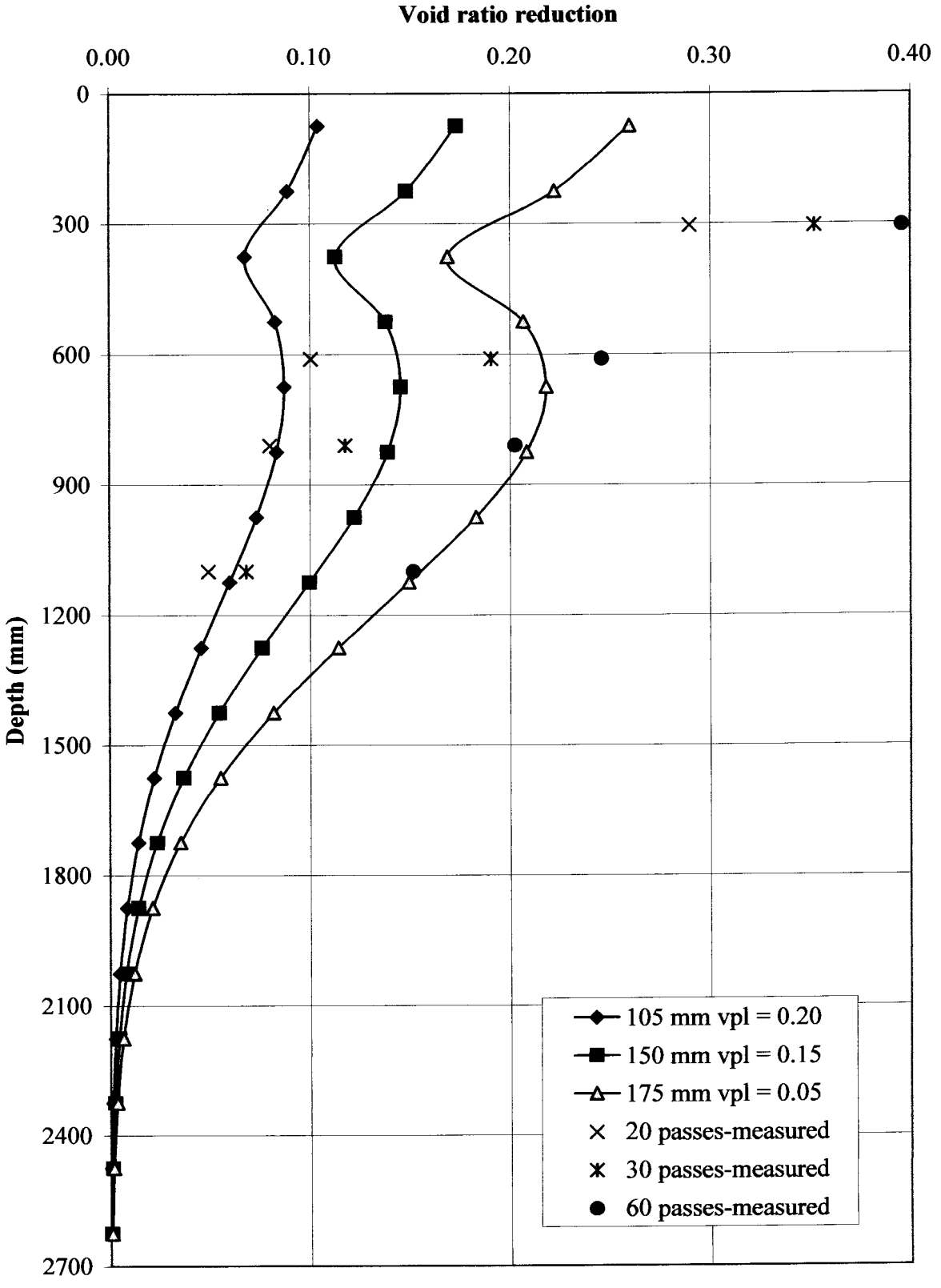

Figure 6.12 : Model verification - Serowe-Orapa, 1988

(data after Pinard, 1988)

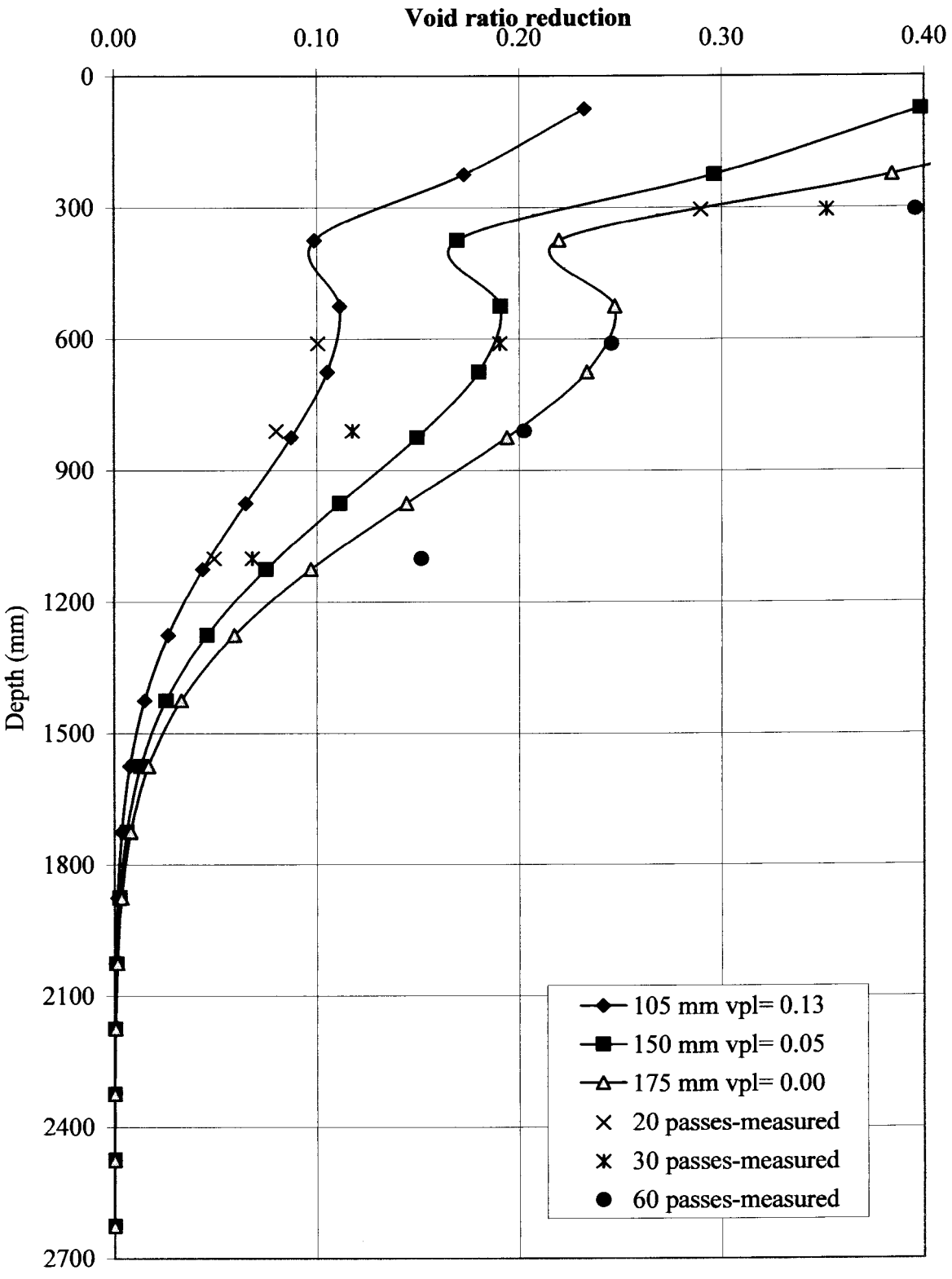

Figure 6.13 : Model verification - Serowe-Orapa, 1988 [Effect of a change in assumed volumetric strain influence distribution]

(data after Pinard, 1988

6.4 VERIFICATION ON DYNAMIC COMPACTION SITES

From the extensive dynamic compaction literature surveyed in the compilation of chapter 2, the patterns of improvement found for impact compactors appeared applicable to dynamic compaction as well. A few additional profiles are also given where the patterns of improvement are confirmed.

Table 6.2 : Dynamic compaction sites used in model verification

Site No.	Name	Reference	No. of profiles	Void ratio from:
7	Nefti, Utah	Rollins, 1998	6	Sand replacement

6.4.1 SITE No. 7 – Rollins (1998).

Extensive work at a site in Utah was undertaken by Rollins to determine whether there is a optimum moisture content for dynamic compaction. Void ratio and moisture content measurements were made throughout the soil profiles, before and after compaction. The use of the data was therefore ideal, especially as the surface settlements were also monitored.

Figures 6.14 to 6.19 show the measured and back-calculated void ratio reduction profiles as the moisture content was increased (to well in excess of optimum for cell 6). It is interesting to note that the operative Poisson's ratio also tended to increase with increasing moisture content. (It is well known that under saturated conditions (undrained behaviour), soil is incompressible and an elastic Poisson's ratio of 0.5 is applicable). [$\varepsilon_{vol}=(1-2\nu)\varepsilon_{vert}=(1-2x0.5)\varepsilon_{vert}=0$]

The modelling showed that for the higher energy levels of a dynamic compactor, a slightly deeper peak in the Rayleigh distribution is applicable (1.0xB compared to 0.67xB for impact compaction). Calculation of the modified distribution is given in Appendix H29, along with the calculations for all the Figures shown in this chapter.

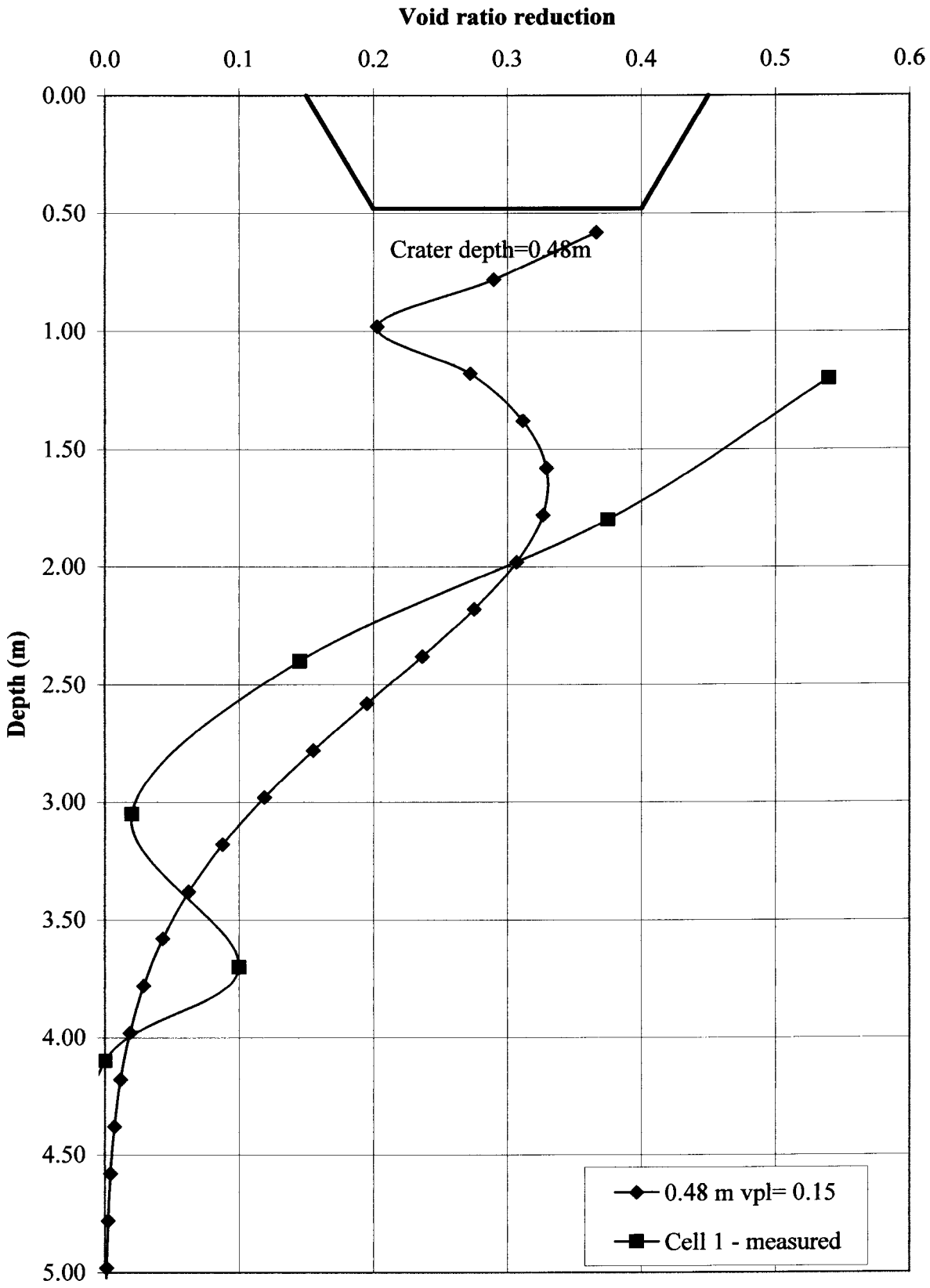

Figure 6.14 : Model verification [DC] - Cell1, Nefti, 1998

data after Rollins, 1998

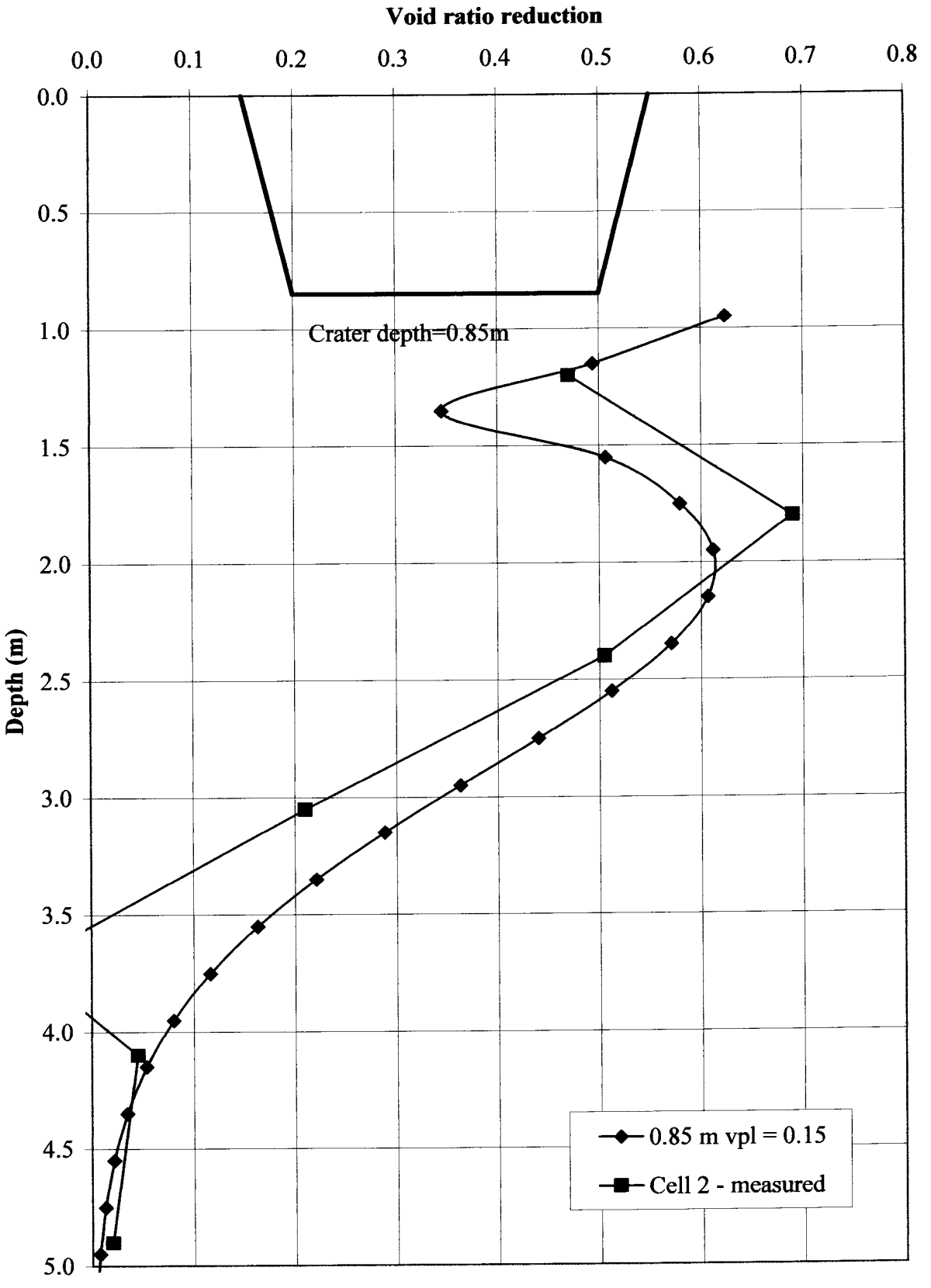

Figure 6.15 : Model verification [DC] - Cell2, Nefti, 1998

data after Rollins, 1998

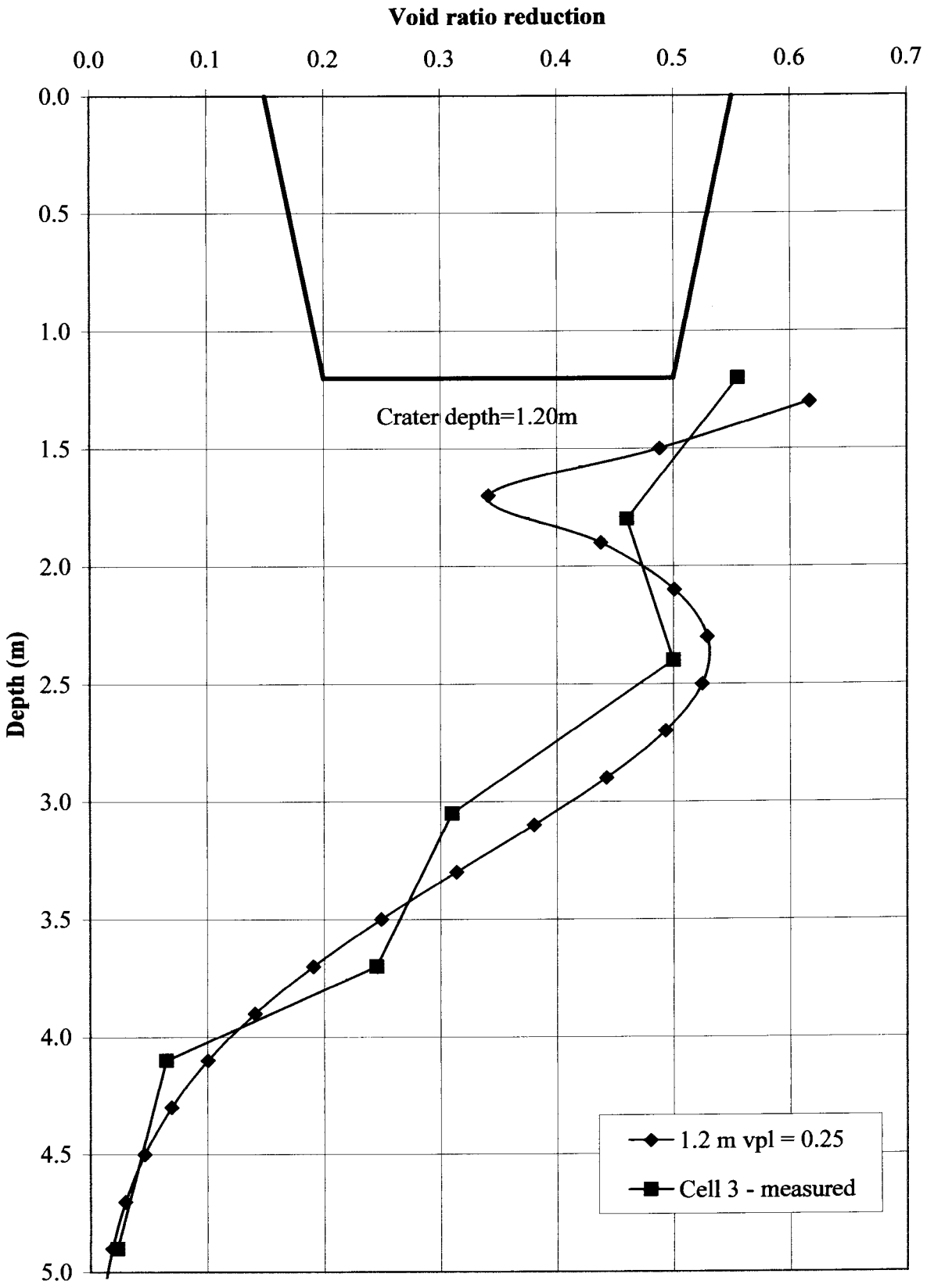

Figure 6.16 : Model verification [DC] - Cell3, Nefti, 1998

data after Rollins, 1998

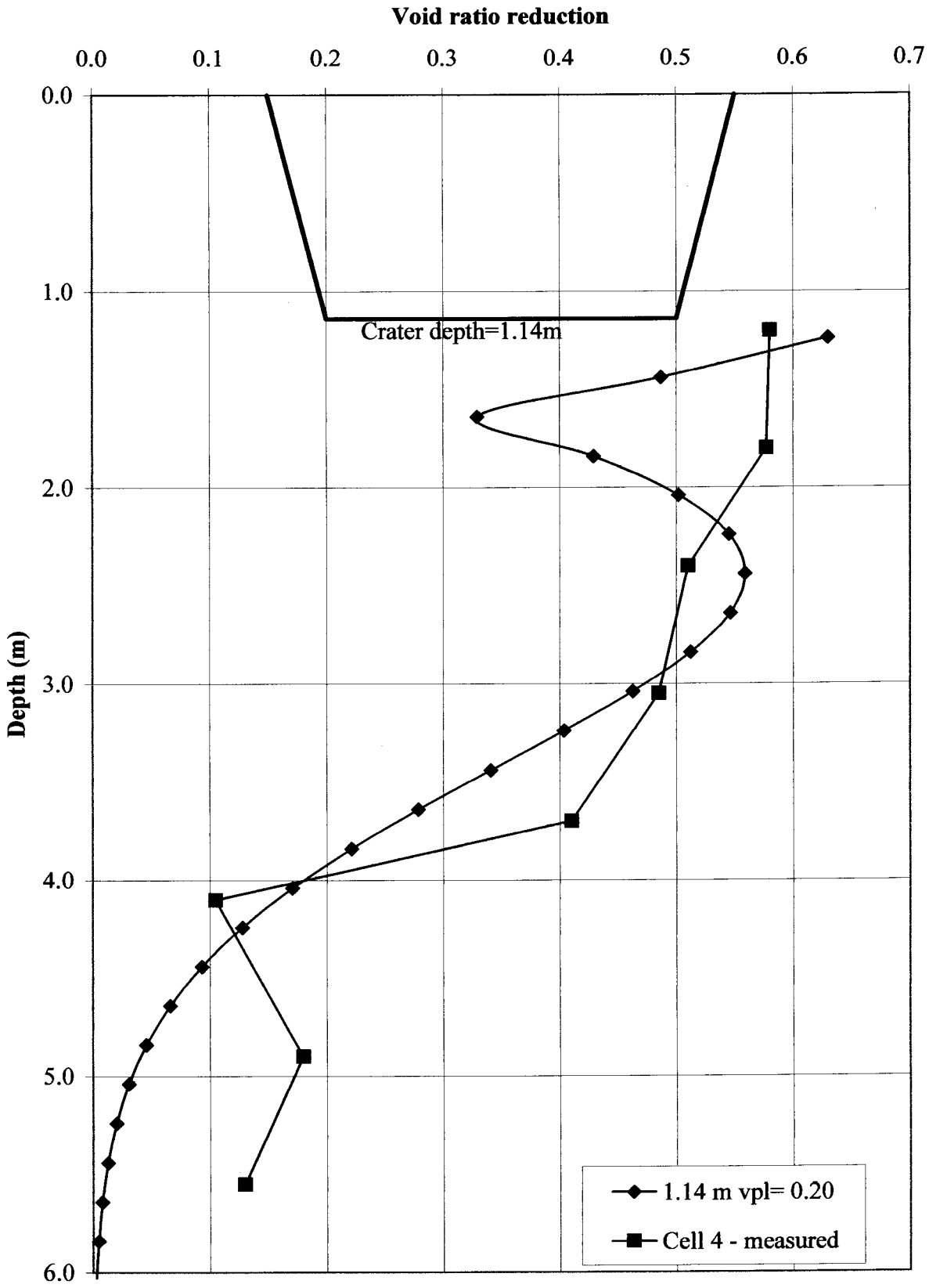

Figure 6.17 : Model verification [DC] - Cell4, Nefti, 1998

data after Rollins, 1998

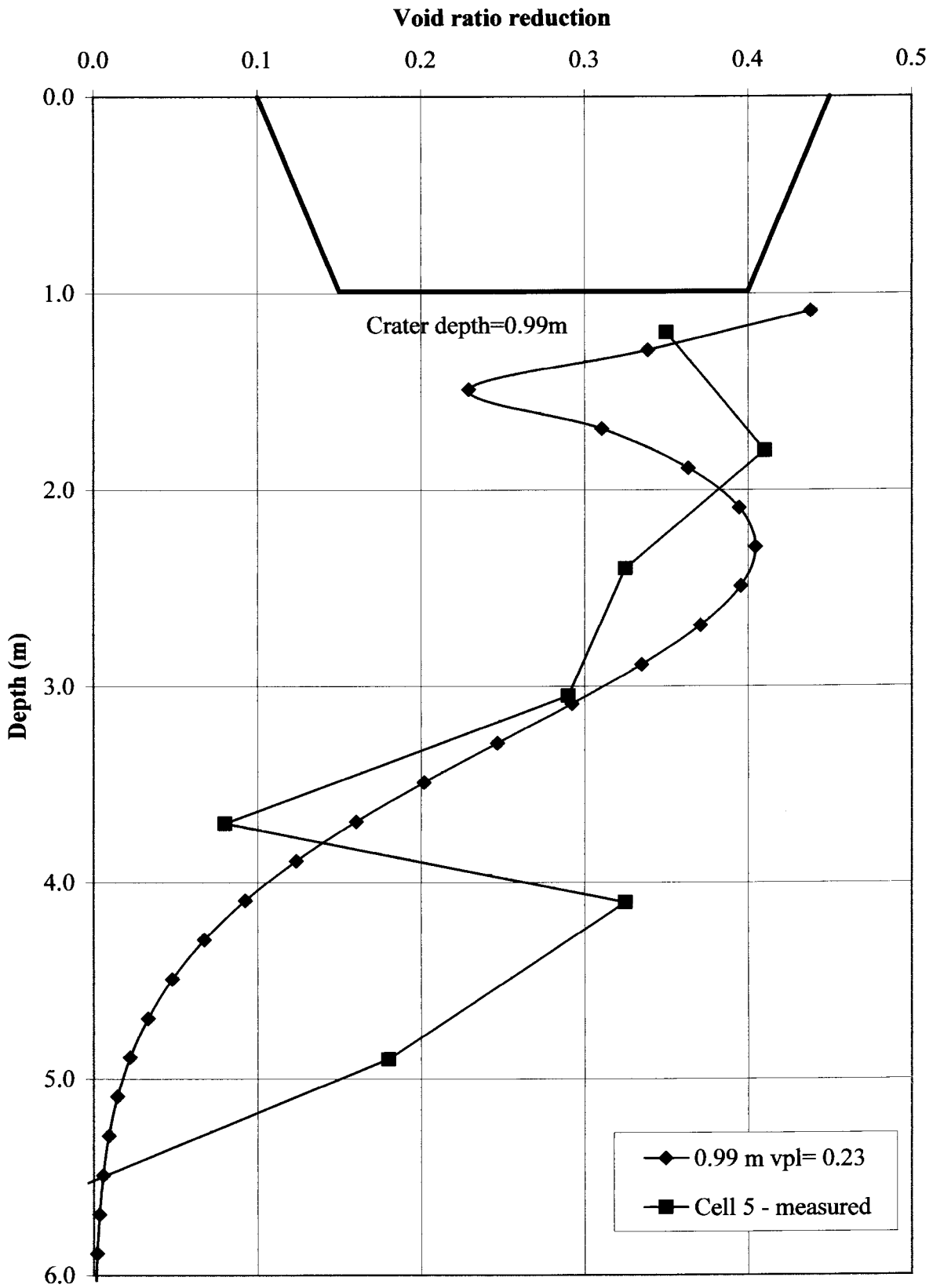

Figure 6.18 : Model verification [DC] - Cell5, Nefti, 1998

data after Rollins, 1998

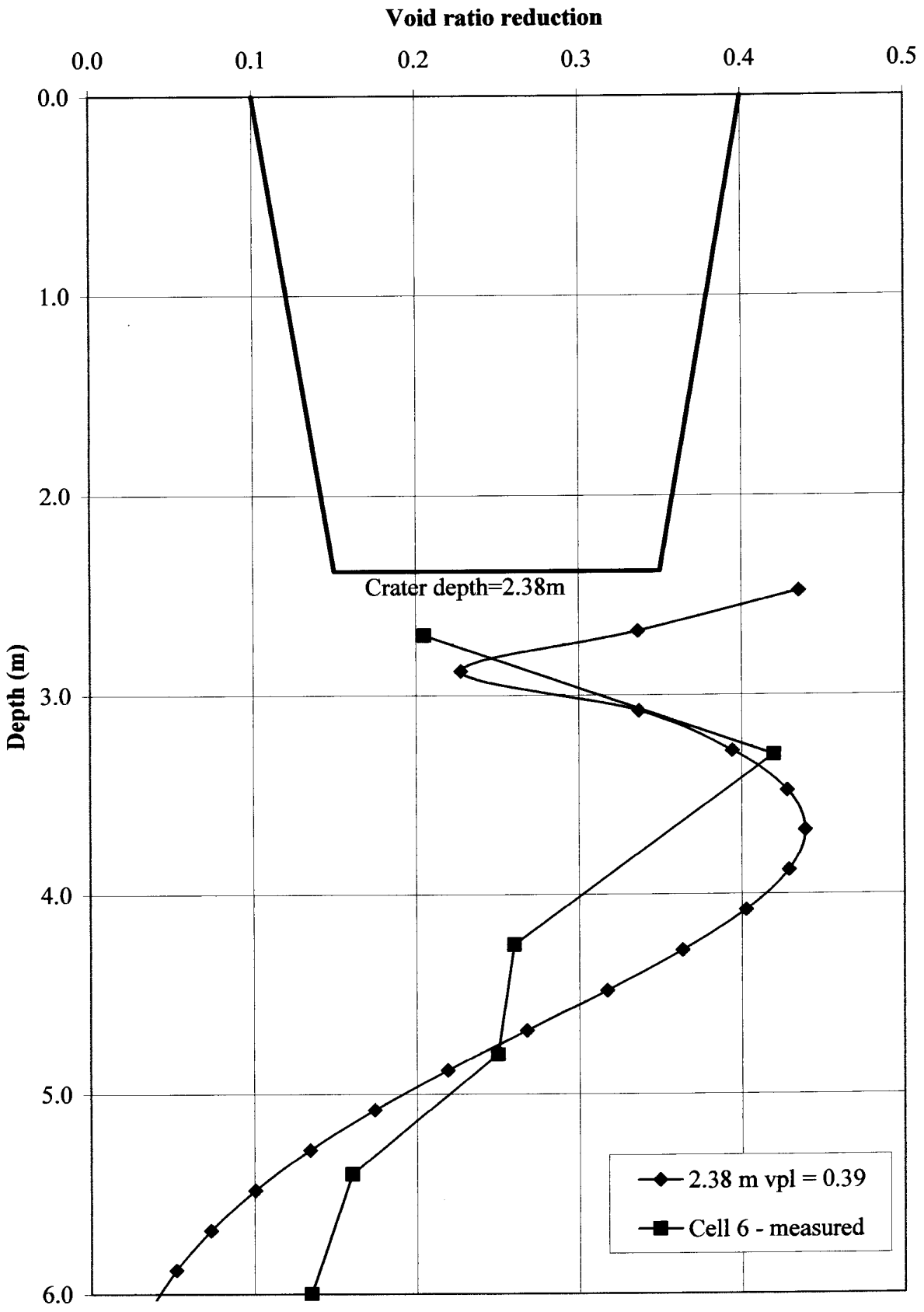

Figure 6.19 : Model verification [DC] - Cell 6, Nefti, 1998

data after Rollins, 1998

The results of the back-analysis of dynamic compaction data confirm that the patterns of improvement found for impact compactors have similarities to the improvement profile of dynamic compactor in un-saturated conditions.

The much higher dynamic forces generated by dynamic compactors further complicate the prediction of improvement, as a punching in quite often occurs when small diameter pounders are used. The initial predictions however, look promising.

6.5 APPLICATION OF MODEL TO CONVENTIONAL COMPACTION

At the International Conference on Compaction held in Paris in 1980, Forssblad presented a paper on the compactometer. In this paper results showing the density – settlement – compactometer accelerations were presented. The applicability of the use of surface settlement to conventional compaction density calculation is demonstrated using this data.

Table 6.3 : Vibratory compaction site used in model verification

Site No.	Name	Reference	No. of profiles	Void ratio from:
8	Compaction trial	Forssblad, 1980b	1	Sand replacement

The calculations for the back-calculation shown in Figure 6.20 and 6.21 are given in Appendix J.

The trial was conducted using a 300mm thick approximately subbase quality material, which was placed on top of a stiff rockfill layer. The strain distribution assumed was constant throughout the layer and assumed no strains in the underlying rock layer. If one-dimensional densification is assumed (1D calc), the surface settlements over-estimate the densification. However, if lateral strains are taken into account using the operative Poisson's ratio, a direct correlation can be achieved between settlement and density.

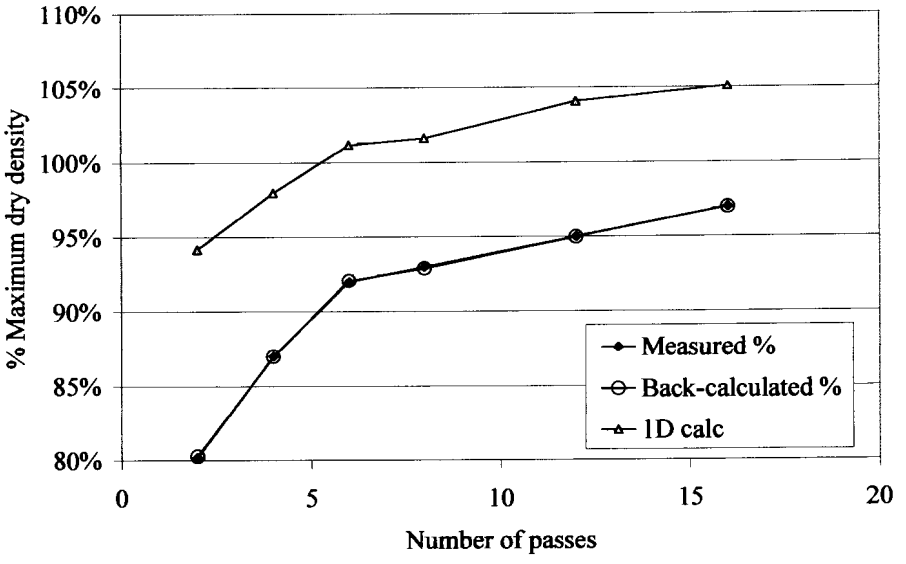

Figure 6.20 : Back-calculated change in densities

The required values of operative Poisson's ratio to achieve an exact correlation are shown in Figure 6.21.

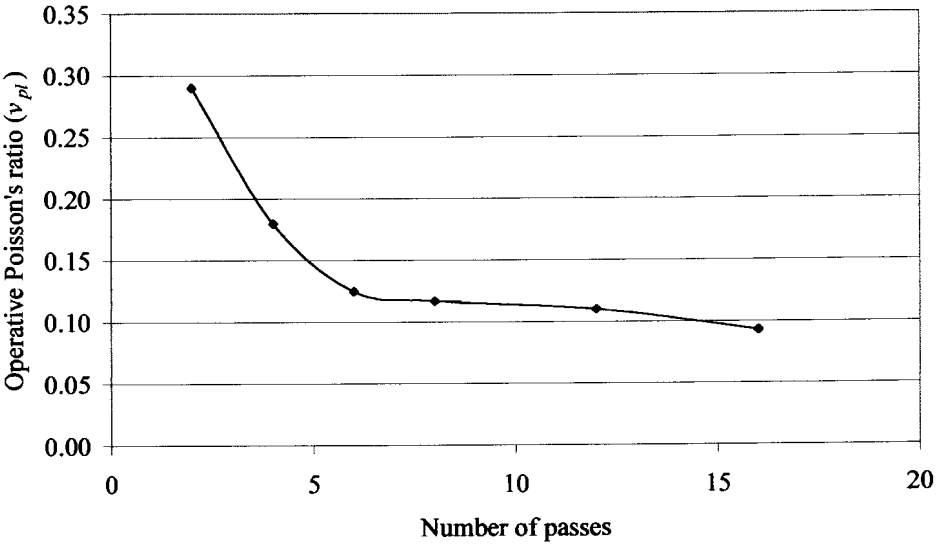

Figure 6.21 : Back-calculated operative Poisson's ratio

It is noteworthy that the back-calculated operative Poisson's ratio reduces from a value close to the typical elastic Poisson's ratio to a lower value during the compaction process. An intuitive explanation for this is that strain hardening is taking place and hence stiffening occurs in both the vertical and horizontal directions.

This warrants further investigation.

The use of surface settlement to estimate the densification during conventional compaction therefore also seems feasible if the operative Poisson's ratio is known.

6.6 VERIFICATION USING A 2 TON DROP MASS COMPACTOR

In order to simulate the compaction achieved by an impact compactor a 2 ton drop mass machine [DMM] was developed by Landpac with a view to simulation of the impact compaction process. The foot-plate of the compactor is of a similar size, while the energy could be varied up to a maximum of about 18kJ/blow. The details of this testing was reported by Berry (1999). A typical result of the soil improvement is shown in Figure 22. Reasonable agreement with the measured and back-calculated void ratio reduction is found, but a volumetric strain distribution that more closely follows the elastic volumetric strain profile would have been more appropriate. By decreasing the peak of the Rayleigh distribution, the depth of influence (DI) is decreased (DI=3.5σ, where σ=depth of the peak). A plot of this revised distribution is also shown in Figure 22 with the depth of the peak at 0.45m. The resulting distribution more closely fits the measured data. This seems to support the findings of the numerical analysis (see Figures 4.6 and 4.7), where materials with higher strength parameters such as the well-graded gravelly sands at the site, are less likely to dilate below the load. Below the Rayleigh peak the default strain distribution proposed yields reasonable results.

The volumetric strain influence profile appears to be a function the soil strength parameters, compactor geometry, mass and energy. Until a better understanding of the dynamic volumetric strain profile is obtained, a unique volumetric strain influence distribution, obtained form static analysis as proposed, appears adequate for initial estimates of improvement.

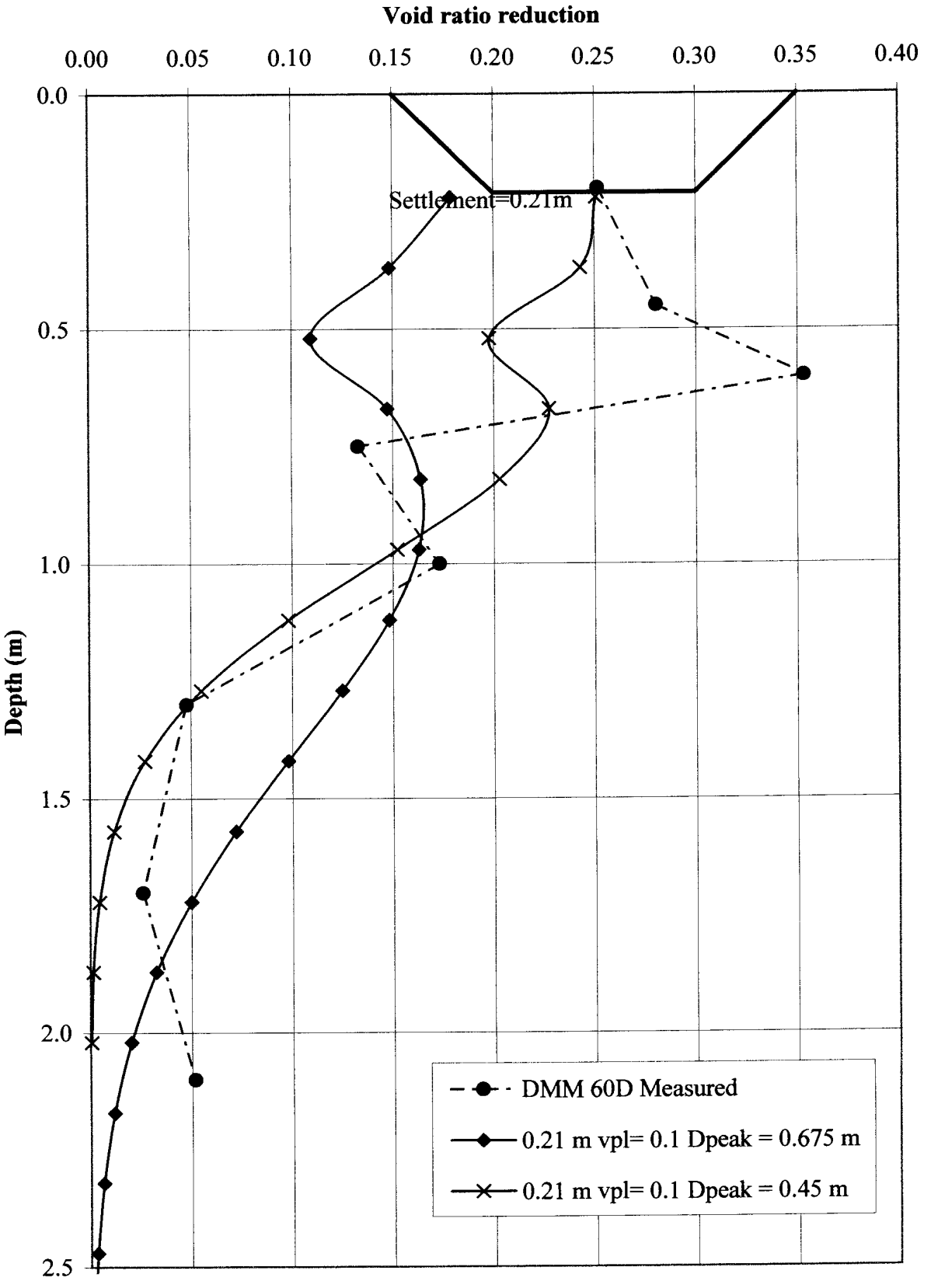

Figure 6.22 : Model verification [DMM-Midrand]

Report for Landpac, Berry (1999)

6.7 DISCUSSION

6.7.1 *Limitations of the proposed model*

6.7.1.1 *General*

The proposed void ratio reduction prediction model appears to be generally applicable to impact compaction, dynamic compaction and conventional compaction if the compactor contact dimensions are known and the surface settlement is measured. The model is not intended for use where the water table is present within the depth of influence of the compactive load (i.e marine conditions etc). Furthermore, a single volumetric strain influence distribution has been used throughout, with no allowance for layering of the soil, or changes in the soil strength parameters. These additional parameters could be built into a more comprehensive model. These limitations are common to most of the prediction models surveyed in the literature study. The factors that significantly affect the predictions of the proposed model are discussed below.

6.7.1.2 *Choice of volumetric strain influence diagram*

A limitation of the model is the selection of an representative volumetric strain influence diagram. This includes estimating the depth of influence at the end of compaction and an appropriate distribution of permanent volumetric strains. Static numerical analysis and field data confirmed a depth of influence of approximately 3 times the impact compactor contact width (B) gives a good estimate of the maximum depth of compaction. The proposed "S" shaped volumetric strain influence diagram appears to give a reasonable estimate of the average volumetric behaviour under the compactor. The current proposal that a single volumetric strain influence profile applies to all soil types and conditions, is clearly an over-simplification. Yet the model yielded acceptable results in most of the soil types encountered in this study (R^2=0.59 in Figure 6.23). The greatest deviations are often found over the top 0.75B meters below the compactor. Large variations in the volumetric strain profile were also found in this region in the numerical analysis in undertaken in chapter 4.

A model that accurately predicts the improvement close to the surface is therefore going to be difficult to achieve. In addition, verification testing at close vertical and horizontal intervals is not often undertaken, and changes in the soil improvement profile may therefore not be measured.

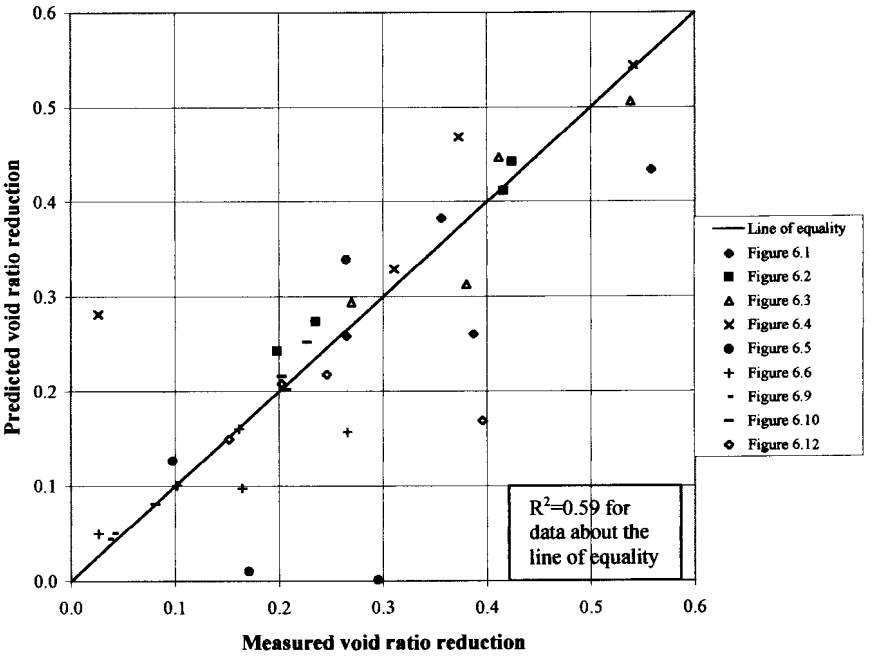

Figure 6.23 : Comparison of measured and predicted void ratio reduction for impact compaction

The use of the Rayleigh distribution limits the depth of influence of the compactive load to 3.5σ, where σ is the depth to the peak of the distribution. Possible alternative distributions can be used, but the proposed distribution is preferred as it highlights the complexity of the behaviour under the loaded area and, being continuous, allows for simple calculation in a spreadsheet.

To properly assess the permanent volumetric strains under a compactor, a dynamic analysis using the measured displacement-time plot as input is essential (Lourens, 2000). The soil constitutive model should allow for non-linear soil behaviour and preferably takes hysteresis into account.

Although a complex analysis may be preferable, Figure 6.24 shows that a good correlation was obtained when the model was applied to dynamic compaction.

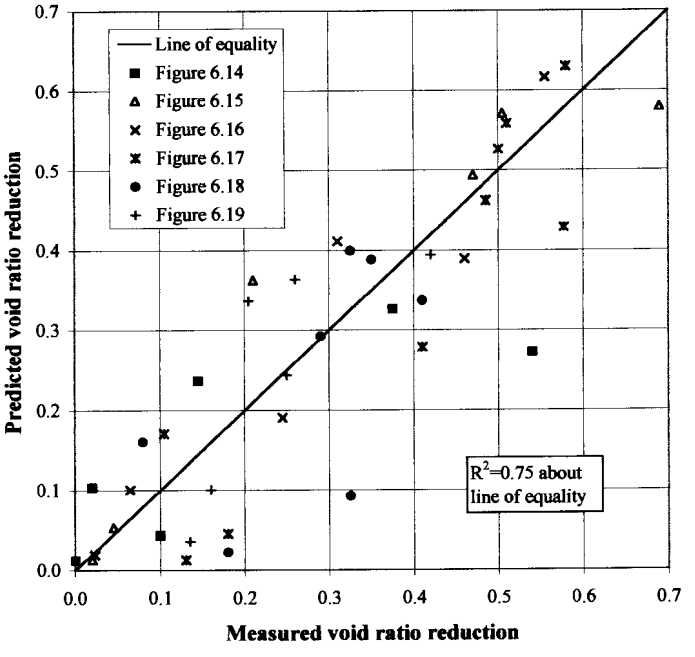

Figure 6.24 : Comparison between measured and predicted void ratio reduction for dynamic compaction

In addition to the good correlation obtained in Figure 6.24, the frequent presence of a peak in the improvement profile data appears to tie in with the presence of a peak in the residual horizontal stress profile.

The occurrence of residual horizontal stresses occurs because of elasto-plastic strains according to Smith and Yandell (1987). A plot of the residual horizontal stresses calculated in the FLAC numerical analysis is shown in Figure 6.25. The peak calculated by the intersection of the horizontal stresses and the passive pressure line (Kp=3.0) is slightly deeper than anticipated at 1,1m. However, if Kp>3.0, as noted is possible by Broms (1965), then the residual horizontal stress peak would increase to between 1.1m and 0.6m (Broms noted that Kp can vary between Kp and 3Kp for passive toe-in pressures for soldier-pile walls).

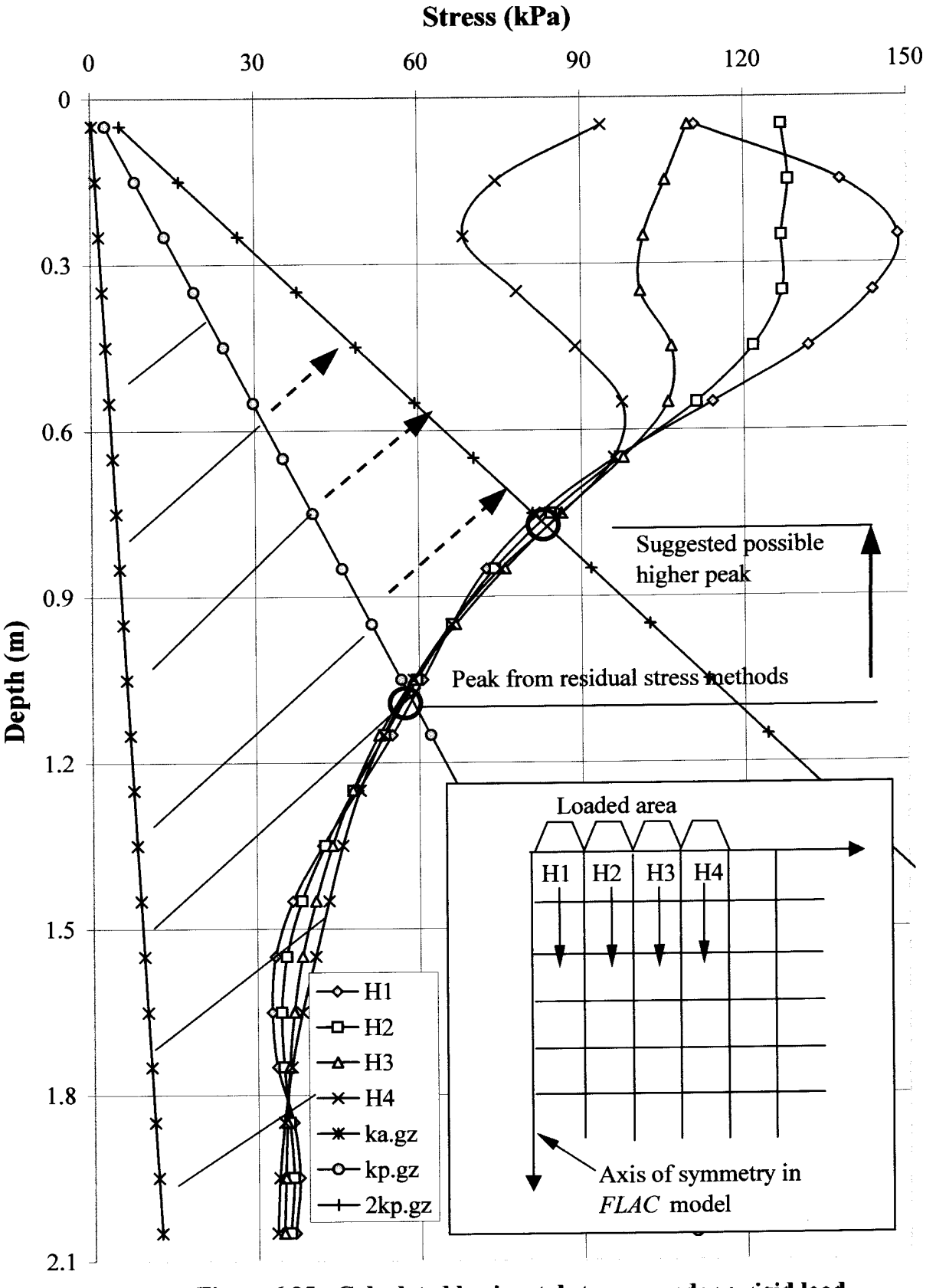

Figure 6.25 : Calculated horizontal stresses under a rigid load

Figure 6.25 shows the effect of an increase in the Kp line on the distribution of residual horizontal pressures. The common thread between the currently proposed volumetric strain influence profile and the residual compaction stress method appears to be the presence of permanent lateral strains and the presence of a peak in the improvement profile. Both these models are similar in principle to the patterns noted by Lukas (1986) and shown in Chapter 2, Figure 2.2. Patterns of improvement appear to be emerging using different approaches. Further research could therefore investigate these similarities further.

An empirical method is currently being investigated by the author, of estimating the improvement in stiffness of the soil after compaction, using the residual (locked in) horizontal stresses as a basis of the prediction.

What is interesting to note from Figure 6.25, it the variation in the horizontal stress profile immediately below the loaded area. Series H1 shows the stresses immediately adjacent the axis of symmetry in an axi-symmetric model, while H4 represents the stresses below the edge of the edge of the rigid loaded area. The elasto-plastic stress distributions do not necessarily follow the continuously decreasing profile of elastic theory. This behaviour could perhaps explain the pressure transducer measurements of Figure 6.7.

6.7.2 *Operative Poisson's ratio*

A further limitation of the model is in determining the value of the operative Poisson's ratio, ν_{pl}. The use of the operative Poisson's ratio is an attempt to correct the over-estimation in void ratio reduction initially found, when one-dimensional behaviour was assumed. The important effect of lateral strains in compaction was highlighted by Chow et al (1992).

The presence of permanent strains and the cumulative nature of these strains have been demonstrated by Wolff and Visser (1994). No literature can be cited where use is made of an operative Poisson's ratio to estimate permanent volumetric strains.

The hypothesis needs further verification and testing, but provides a simple tool for estimating permanent volumetric changes in the soil without the need for complex analyses. The approach is therefore pragmatic and semi-empirical as v_{pl} requires back-calculation to be quantified.

Initial indications are that the value of v_{pl} is about 0.15 at the end of the compaction process, as indicated in Table 6.4.

Table 6.4 : Summary of operative Poisson's ratios from back-calculation of impact compaction data

Figure No	v_{pl}	Type of compactor
6.1	0.075	23kJ IC
6.2	0.175	23kJ IC
6.3	0.175	23kJ IC
6.4	0.150	23kJ IC
6.5	0.250	25kJ IC
6.6	0.075	15kJ IC
6.9	0.100	23kJ IC
6.10	0.100	23kJ IC
6.11	0.200	23kJ IC
6.12	0.150	25kJ IC
6.13	0.075	23kJ IC
Average	*0.14*	*[Std dev=0.06]*

A summary of operative Poisson's ratios back-calculated in verifying the model for dynamic compaction, is given in Table 6.5. A value of approximately 0.25 appears an appropriate initial estimate for v_{pl} for dynamic compaction. As the database of back-calculated values increases, this initial estimate can be revised.

It is believed that the convention to compact on a grid (5.4m minimum spacing) leads to there being significant lateral strains during dynamic compaction, and larger values of v_{pl} are therefore hypothesised.

The argument for this is as follows: Current model impact compactors impact the ground between about 1.5m to 2.5m centres depending on the type of compactor.

Table 6.5 : Summary of operative Poisson's ratios from back-calculation of dynamic compaction data

Figure No	v_{pl}	m.c %	Type of compactor
6.14	0.15	7	DC
6.15	0.15	10	DC
6.16	0.25	15	DC
6.17	0.20	17	DC
6.18	0.23	18	DC
6.19	0.39	20	DC
Average	*0.23*	*Std. Dev.=0.09*	

With repeated passes of the compactor, the ground is usually compacted in different positions, resulting in a uniform distribution of compaction energy density (kJ/m^2) to the lane being compacted. In addition, split drum compactors compact in strips as shown below in Figure 6.26, alternating from one strip to the other in successive passes.

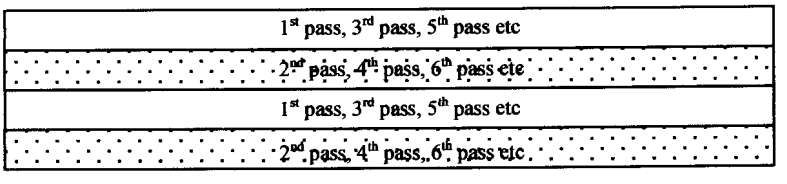

Figure 6.26 : Typical split drum impact compaction rolling procedure

The author believes that when compacting adjacent lanes, lateral strain hardening is occurring. This can be likened to bending a piece of wire, first in one direction and then back again. When compacting one lane lateral strains occur in the direction of the adjacent lane. When compacting the other lane, strains in the opposite direction occur, with an effect similar to bending back the wire. The close proximity of the compaction lanes, it is suggested, results in significant lateral stiffening. It is further suggested that this effect is not nearly as pronounced when the compaction blows are far

apart, as with dynamic compaction. A higher value of the operative Poisson's ratio is therefore hypothesised for increased compactor impact spacing. The effect of surface ironing after dynamic compaction does however, result in a more even application of applied energy. This should be investigated further.

From Figure 6.27, it appears possible that ν_{pl} increases with moisture content (Data from Figures 6.14-6.19).

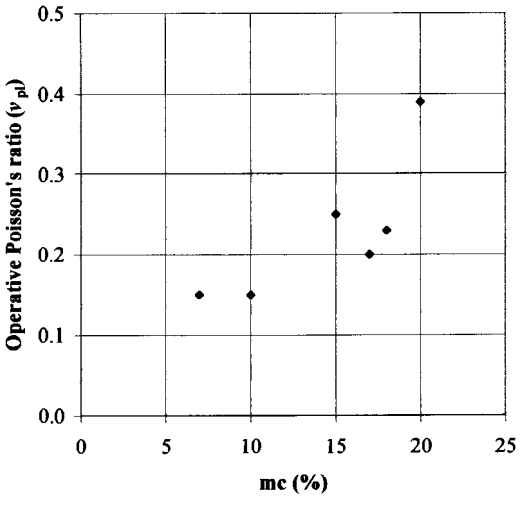

Figure 6.27 : Variation of ν_{pl} with moisture content at a dynamic compaction site

The saturation moisture content for the soils at the site was approximately 33%. The effect of moisture content on the plastic volumetric strains warrants further investigation.

In Figure 6.21 it was also demonstrated that the back-calculated ν_{pl} varied from about 0.3 at the beginning of compaction to 0.1 at the end of the compaction process, using an 11 ton vibratory compactor. This shows similarity in behaviour to the plasticity parameter, ε, proposed by Adam et al (2000), shown in Chapter 2, Figure 2.12. These authors noted that the soil becomes more elastic as compaction proceeds. The reduction in ν_{pl} from 0.3 to 0.1 can be explained by the build-up of residual horizontal stresses due to permanent lateral strains. In other words, a strain hardening appears to be

taking place as the horizontal stresses become "locked-in". It is suggested that further work in this regard be conducted, particularly with the aid of the Mechano-lattice software developed by Smith and Yandell (1987).

6.7.3 *Effect of layering*

The effect of a layering has not been included in the proposed model. A more comprehensive model could make allowance for changes in the soil's initial density and stiffness. It is proposed that if layering needs to be taken into account, the volumetric strain influence distribution be obtained from a numerical model. Stiff layers would show a reduced volumetric strain and softer layers an increased volumetric strain within each layer. In developing such a model, the effect of wave absorption and reflection would probable need to be considered. It is probable that layering only need be taken into account for sizeable projects, where the additional effort is warranted.

6.7.4 *Effect of the water table*

The current model is not applicable to compaction with the water table within the zone of influence of the compactor. A criticism levelled at most of the DC models currently available is that no clear differentiation is made between compaction with the water table absent or being present.

The presence of water completely changes the soils response to load and effective stresses and pore water and pore air pressures become significant.

The long-term volumetric effects in a saturated soil is complex, but from observation of field data where the water table is present, its appears that the Rayleigh distribution may be modified to include a longer tail. (see Appendix J). The explanation according to Varaksin (1981) is that the shock waves (Compression, shear and Rayleigh waves) are felt deeper due to the virtually incompressible water. If sufficiently permeable ($<10^{7}$m/s) the soil will consolidate in proportion to the permeability within the zone of increased pore water pressure. An example of the soil improvement profile with the water table near the surface is attached in Appendix J.

As impact compaction usually takes place unsaturated conditions, a model that considers saturated conditions is not essential.

6.7.5 *Suggested further research*

6.7.5.1 *Profile of work done on the soil*

In addition to the dynamic analysis suggested earlier, an investigation into the profile of work done in the soil under a dynamic load, taking hysteresis into account, is also suggested. It is suspected that there will be a correlation between the work done on the soil, once losses are taken into account and the improvement profile. This may then lead to a comparison between input energy of the pounder to the work done on the soil, highlighting where the energy losses occur. This could then result in more efficient compaction methods being proposed.

The dynamic analysis could also investigate the effect of compactor's impact load duration. It is commonly believed that a larger drop height (or total energy input) results in deeper and better compaction. The author suspects that above a certain contact stress, little if any benefit is gained as the energy is wasted in dilation of the soil near the surface.

6.7.5.2 *Investigation into the induced pore water and pore air pressure distributions*

It is believed that the distribution of pore air pressure, and possibly pore water pressures, increases in proportion to the volumetric strains induced during compaction. These effects should perhaps form part of a more comprehensive study.

6.7.5.3 *Prediction of surface settlement and energy requirements*

No attempt has been made to predict the energy requirements to achieve the surface settlement that is used as primary input into the proposed prediction model. This is a limitation to contractors, who have to estimate the energy requirements before making an offer. This limitation is usually overcome by undertaking a compaction trail once on site, from which both the surface settlement and energy requirements can be adjusted.

Never-the-less, the prediction of energy requirements for impact compaction is still based on experience. Many dynamic compaction models predict the energy requirements, but seldom settlement. It is unlikely that any model that does not consider the initial void ratio of the soil can predict the surface settlement after compaction. None of the dynamic compaction models are applicable to the prediction of impact compaction energy requirements and so further work in this area may be required.

6.8 CONCLUSIONS

A simplified volumetric strain influence model for predicting the profile of void ratio reduction for impact compaction has been proposed. The model was verified with reasonable success on 15 impact compact profiles. Further work is required to confirm the shape of the volumetric strain influence profile, particularly in the upper portions of the profile, but the proposed model appears adequate for initial estimation purposes, in unsaturated conditions.

The relative simplicity of the model is one of it's main limitations, but it is believed that this simplicity has highlighted patterns of behaviour that can serve as a starting point for further detailed research.

In addition, the principles of the model were also applied to both dynamic and conventional compaction with reasonable success.

CHAPTER 7

SUMMARY AND CONCLUSIONS

7.1 SUMMARY

The purpose of this dissertation was to show that the profile of improvement in the ground is predictable and proportional to the surface settlement of the compacted ground, provided lateral deformation is taken into account.

To accomplish this task, the pertinent literature was surveyed. No prediction model was found in compaction literature surveyed, which predicted the volumetric changes in the ground based on the surface settlement after compaction.

In order to estimate the volumetric changes in the ground using a numerical model, an estimate of the dynamic force of the compactor is required. This was achieved using an accelerometer attached to the tube axle of the compactor. Comparisons of measured and predicted decelerations were in good agreement and the dynamic force applied to a numerical model to estimate the volumetric strains in the ground. The numerical model highlighted the complexity of the strains. The average volumetric strain profile under the compactor was adopted for use in a simplified model.

Data from fifteen impact compaction profiles on six different sites was collected. In addition to this, measurement of the ground improvement using a two-ton drop mass compactor was undertaken. Data from dynamic compaction and vibratory compaction research was also used to demonstrate the principle of the model appears to be applicable to various types of compaction. Although actual predictions were not undertaken by virtue of the data being back-calculated, reasonable correlation of "predicted" against back-calculated data was achieved.

Some of the significant findings of this study were:

- Surface settlement can be used to estimate the void ratio reduction in the soil after impact compaction
- The proposed soil improvement model for impact compaction appears to be applicable to other forms of compaction
- The volume changes under dynamic loading are complex and a dynamic analysis is warranted to better understand the volumetric strain profile under impact loading. A more detailed analysis that can more accurately model the permanent strains should be used.
- The assumed volumetric strain influence diagram/distribution yields reasonable results considering the simplification of the complex problem at hand. Modification to the assumed volumetric strain influence distribution is likely as a better understanding of the factors affecting the distribution unfold.
- The simple numerical analysis performed in Chapter 4 indicated that the soil strength parameters have a major effect on the volume change characteristics of the soil, and could in future be built into a more rigorous model.
- Lateral strains appear to have a significant effect on the volume changes in the soil.
- Back-calculation is required to estimate operative Poisson's ratio, ν_{pl}, which is essentially a plastic soil volume change parameter. The model is therefore dependent of an accurate assessment of this parameter and therefore remains semi-empirical is nature. The soil volume changes are also very sensitive to the magnitude of ν_{pl}.
- Small settlements imply small void ratio reductions (little improvement achieved)
- Improvement of between 2 and 3 compactor diameters can typically be expected for an impact compactor, in unsaturated conditions
- Improvement of between 3 and 4 compactor diameters can typically be expected for dynamic compactors, in unsaturated conditions
- A peak in the improvement profile is often found at a depth of about 0.75B for impact compactors and 1.0B for dynamic compactors

7.2 CONCLUSIONS

A simplified volumetric strain influence ground improvement prediction model has been presented. Although in many respects, the model is over-simplified, initial indications are that the reduction is void ratio through-out the depth of influence of an impact compactor, can be estimated with a reasonable degree of confidence. The argument, that the plastic volumetric strains are proportional to the total volumetric strains produced by a compactive load, was (although possibly not proven beyond doubt) given substantial credibility. The proposal that the surface settlement is a direct measure of the improvement in the ground, provided lateral deformation is considered was confirmed. Of particular use to the practicing engineer, is the possibility of drawing contours of void ratio reduction profile possible with varying amounts of surface settlement. A predetermined minimum surface settlement could then be used as a quality control measure.

The model requires three input parameters: the volumetric strain distribution, the operative Poisson's ratio and the surface settlement. Initial proposals have been made for both the volumetric strain distribution and the operative Poisson's ratio. Only the surface settlement is unknown. As the surface settlement is dependent on the initial void ratio of the soil (amongst other parameters), it is recommended that a settlement trial be conducted to determine the magnitude of the settlement.

The study has unveiled patterns of improvement that appear to be predictable. It is recommended that the similarities between the proposed model improvement profile and the residual horizontal stress profile be further investigated, preferably with software capable of modelling dynamic effects as well as hysteresis in the soil constitutive model. The relationship between the void ratio reduction profile and the stiffness profile must also be researched, hopefully leading to a prediction of the stiffness improvement as an additional output to the model.

Similarities in the void ratio reduction profile and the stiffness profile were seen in some of the trials where stiffness was also measured (e.g Kriel, 1998). The relationship between the two is a challenging next step in the research started here.

In conclusion, it is hoped that some of the additional questions raised, will inspire further more detailed research.